UNIVERSITY OF SOUTHAMPTON

FACULTY OF MEDICINE

Functional characterisation and role of Tissue Transglutaminase during the progression of Colorectal Cancer

by

Doriana Cellura

Thesis for the degree of Doctor of Philosophy
September 2015

CANCER RESEARCH UK

ROTHSCHILD

UNIVERSITY OF SOUTHAMPTON

ABSTRACT

FACULTY OF MEDICINE

Academic unit Cancer Sciences

"Functional characterisation and role of Tissue Transglutaminase during the progression of Colorectal Cancer"

By Doriana Cellura

Colorectal cancer (CRC) is the 4th most lethal cancer worldwide. Currently available chemotherapy treatments used in combination with surgery have toxic effects which limit their prolonged usage. Thus, there is still great need for less toxic and more specific treatments, alongside better predictive and prognostic disease markers. Tissue Transglutaminase (TG2) is a multi-functional enzyme whose role in cancer can be either tumour-promoting or tumour-suppressing depending on cell type and intracellular localisation. There is a large body of literature dissecting TG2 tumour-promoting role, whereas very little is known about its tumour-suppressing functions. MicroRNAs are small RNA molecules with translation regulation functions. Their altered expression in cancer causes abnormal translation of their target mRNAs.

The aim of this work was to fully characterise TG2 in a unique *in vitro* model of CRC progression, to assess by which mechanisms it acts a tumour suppressor, and how TG2 expression is regulated.

The *in vitro* CRC model used consisted of two cell lines: SW480 (derived by the primary tumour site of a CRC patient and expressing very high TG2), and SW620 (derived by a lymph node metastasis of the same patient and expressing very little TG2).

Silencing of TG2 in SW480 directly promoted cell invasion on Transwell system, whereas transfecting TG2 in SW620 prevented it. Compared to SW620, in SW480 TG2 is found more SUMOylated at the leading edges of cells, and TG2 levels are positively

correlated with β-catenin levels, suggesting a role for TG2 in maintaining cell-cell junctions and regulating motility. Silencing TG2 in SW480 and transfecting TG2 in SW620 show that TG2 levels are positively correlated with expression of HLA-I; this effect may be linked to tumour immune evasion. To understand how TG2 expression is regulated, *in silico* and experimental analysis were performed which identified miR-19a as a regulator. Transfection of miR-19a in SW480 directly downregulated TG2 resulting in cell invasion.

Given that exogenous administration of TG2 would not represent a viable option due to its systemic expression and pleiotropic functions, these observations provide a rationale for sequestering miR-19a in primary CRC tumour in order to prevent downregulation of TG2 and thus metastasis.

List of contents

List of figures and tables

List of figures

List of tables

List of abbreviations

APCs	Antigen-presenting cells
ATP	Adenosine triphosphate
Bio-MDC	Biotin-Monodansylcadaverine
BSA	Bovine serum albumine
cDNA	Complementary deoxyribonucleic acid
CD	Coeliac disease
CF	Cystic fibrosis
CFTR	Cystic fibrosis transmembrane regulator
CMA	Chaperone-mediated autophagy
CRC	Colorectal cancer
DEPC	Diethylpyrocarbonated
DMEM	Dulbecco's modified Eagle medium
DNA	Deoxyribonucleic acid
ECL	Enhanced chemiluminescence
ECM	Extracellular matrix
EDTA	Ethylenediaminetetraacetic acid
EGF	Epidermal growth factor
EGFR	Epidermal growth factor receptor
EMT	Epithelial-to-mesenchimal transition
ER	Endoplasmic reticulum
ERAD	ER-associated degradation
FACS	Fluorescence-activated cell sorting
FAK	Focal adhesion kinase
FCS	Fetal calf serum
FITC	Fluoresceine-isothiocianate
FSC	Forward scatter
GTP	Guanosine triphosphate
HLA	Human leukocyte antigen
HCC	Hepatocellular Carcinoma
HMW	High molecular weight
HRP	Horseradish peroxidase
IBD	Inflammatory bowel disease
IEL	Intra-epithelial lymphocytes
IHC	Immunohistochemistry
IL-8	Interleukin 8
MDR	Multi-drug resistance
MFI	Mean fluorescence intensity
miRNA or miR	Micro RNA

MMPs	Matrix metalloproteinases
mTOR	Mammalian target of Rapamycin
NFkB	Nuclear factor kappa-light-chain-enhancer of activated B cells
NK	Natural killer
IkB	Inhibitor of the nuclear factor kappa-light-chain-enhancer of activated B cells
OIS	Oncogene-induced senescence
PBMCs	Peripheral blood mononuclear cells
PBS	Phosphate buffered saline
PCD	Programmed cell death
PCR	Polymerase chain reaction
PDI	Protein disulfide isomerase
PE	Phosphatydilethanolamine
PKB/AKT	Protein Kinase B/AKT
PKCδ	Protein kinase C-delta
PLA	Proximity ligation assay
PPAR-γ	Peroxisome proliferator-activated receptor-gamma
Pri-miRNA	Primary micro RNA
PtdIns3K	Phosphatidylinositol-3-kinase
PTEN	Phosphatase and Tensin Homologue
qPCR	Quantitative polymerase chain reaction
R.T.	Room temperature
RNA	Ribonucleic acid
RNAi	RNA interference
ROS	Reactive oxygen species
RPMI	Roswell Park memorial institute
RT	Reverse transcription
SDS	Sodium dodecyl sulphate
siRNA	silencing RNA
SSC	Side scatter
SUMO	Small Ubiquitin-like modifier
TBS-T	Tris-buffered saline plus Tween 20
TG2 or tTG	Tissue transglutaminase
Tgases	Transglutaminases
TGFβ	Transforming growth factor beta
TGFβR	Transforming growth factor beta receptor
Ub	Ubiquitin
Ubl	Ubiquitin-like
UPR	Unfolded protein response
UPS	Ubiquitin-Proteasome system
UTR	Untranslated

Academic Thesis: Declaration of authorship

I, DORIANA CELLURA, declare that this thesis and the work presented in it are my own and have been generated by me as the result of my own original research.

Functional characterisation and role of Tissue Transglutaminase during the progression of Colorectal Cancer

I confirm that:

1. This work was done wholly or mainly while in candidature for a research degree at this University;

2. Where any part of this thesis has previously been submitted for a degree or any other qualification at this University or any other institution, this has been clearly stated;

3. Where I have consulted the published work of others, this is always clearly attributed;

4. Where I have quoted from the work of others, the source is always given. With the exception of such quotations, this thesis is entirely my own work;

5. I have acknowledged all main sources of help;

6. Where the thesis is based on work done by myself jointly with others, I have made clear exactly what was done by others and what I have contributed myself;

7. Parts of this work have been published as:
   "MiR-19-mediated inhibition of Transglutaminase-2 leads to enhanced invasion and metastasis in colorectal cancer" Mol Can Res. 2015 Jul; 13(7) 1095-1105

Signed:

Date:

Acknowledgements

John 17:4 (NRSV) - "I glorified you on earth by finishing the work that you gave me to do"

Many people have crossed my academic and personal path since the start of my PhD… some have been put on my path to be genuinely helpful, some to be genuinely disruptive. It would take a whole volume to mention everybody, so I'd like to summarise by saying: THANK YOU ALL. If you are one of those who helped, thank you ever so much for what you did for me, and may life throw you an anchor any time you are in open rough waters. If you are one of those who have made my academic and personal life far more complicated than needed, thank you anyway, for the lessons I have learnt by facing such problems, for making me stronger, more patient, more resilient.

Axé!

1. Introduction

1.1 Cancer: a brief overview

Cancer is a very complex pathology that still causes numerous deaths worldwide. Statistics gathered in the United Kingdom during the last 30 years have shown that the overall incidence of cancer has increased among the population more than its death rate has decreased (source: Cancer Research UK). This suggests that, despite increasing knowledge acquired so far about the molecular mechanisms of cancer, new findings are yet to be contributed by scientists which will help to cure such pathology more efficiently.

Cancer is caused by hyperproliferation of cells within a tissue, which results from altered activity of cell cycle regulatory proteins. Physiologically, it is only stem cells that proliferate throughout life, whereas the proliferative potential of their daughter cells (non-stem cells) is more restricted[1]. Non-stem cells become progressively differentiated with each division, and proliferate for a definite number of generations, before entering G0 phase which allows for terminal differentiation and cell senescence. Such processes are normally kept under surveillance by tumour-suppressor proteins, negative regulators of the cell cycle, which also trigger mechanisms of programmed cell death (PCD)[2] if proliferative rate suddenly increases, or if genotoxic stress is sensed. Loss of function of tumour suppressors can promote oncogenic transformation. In contrast, proto-oncogenes are proteins that positively regulate the cell cycle, whose gain of function can promote oncogenic transformation[3]. Typically, three stages of cancer development can be recognised: initiation, promotion and progression[4]. However, some chemical and biological agents can function as "complete carcinogens" at sufficiently high dose or titer, causing an extent of alterations which are alone responsible for cancer onset[5].

Overall, cancer can be regarded as the result of an imbalance between proliferation, apoptosis and differentiation, caused by the aberrant activity of oncogenes and tumour-suppressors. Alterations in the abundance or functionality of these key proteins may be caused by direct environmental insult (UV rays, toxins, viruses, etc.), or be a consequence of

chronic exposure to inflammatory and oxidative stressors. In this regard, certain lifestyle and factors are known to be detrimental and have been associated with increased risk of developing cancer. For example, sun beds are a common source of UV-induced skin damage[6], cigarette smoke contains toxic oxidizing compounds[7,8] and Papilloma virus (a sexually-transmitted virus) promotes development of pre-cancerous lesions of the oral[9] and genital mucosa[10]. Importantly, most cancers result from the cumulative effects of multiple sequential alterations; such knowledge dates back to the Fifties, with the publication of the "multi-hit theory"[11].

Metastasis is the process by which cancer cells exit the primary tumour site and form colonies in adjacent as well as distant organs (described hereafter in section 1.1.1.)[12]. Gain of malignant potential is promoted by additional changes at the DNA or protein level[13].

Tumours usually express markers not previously known to the organism (such as gene rearrangement products), or "self" molecules whose temporal and tissue-pattern of expression have become altered[14]. As such, tumour markers may be recognised by the immune system and stimulate cytotoxic responses, therefore tumour cells try to escape immune system recognition by downregulating HLA-I molecules[15]. However, since a complete loss of HLA expression would lead to Natural Killer (NK) cell-mediated cytotoxicity[16], HLA-I expression is kept at a low level to simultaneously minimise recognition by CD8+ T and NK cells.

Many tumour-specific targeted therapies are now used in the clinic[17] however, for other tumours where such therapies are not available, broad-spectrum radio- and chemo-therapeutic treatments are used, often in combination with surgery. In the short-term, chemotherapeutics can be effective against a single, localized tumour, whereas a longer therapy is often needed to treat multiple, disseminated metastasis. A serious issue that can arise upon prolonged administration of chemotherapeutics is multi-drug resistance (MDR)[18]. Malignant MDR cells have acquired the ability to extrude or internally degrade drugs they have been exposed to extensively[19]. In such a scenario, clinicians must resort to

administering stronger treatments to patients, who will thus have to endure further unpleasant therapy-related side effects.

Several factors dictate progression from a primary to a metastatic multi-drug resistant tumour, including: the ability to diagnose a tumour before its clinical presentation, the intrinsic malignancy of the cells at clinical presentation, and the type of treatments administered. For these reasons, worldwide cancer research is focussed on discovering highly specific and sensitive tumour markers for aiding early diagnosis, along with setting up targeted non-toxic therapies.

1.1.1 Solid tumours and their microenvironment

Tumours are conventionally divided into two classes according to their macroscopic appearance: solid and hematological tumours. Solid tumours are so called because hyperproliferating cells grow in multiple overlapping layers, forming nodes surrounded by healthy tissue. Within a node it is possible to distinguish cancer cells, normal epithelial cells and stromal cells (i.e. fibroblasts, vascular cells, lymphocytes)[20]. These cell types, together with extracellular matrix molecules and soluble cell mediators, constitute the tumour microenvironment. Ultimately, establishment of a permissive or inhibitory microenvironment impacts on the ability of a tumour to expand and metastasise. However, it is not yet clear whether stromal cell behaviour (permissive or inhibitory) is pre-defined and unchangeable, or can be influenced by tumour aggressiveness[20].

Tumour growth and dissemination is usually accompanied by a variable degree of local inflammation, as first observed by Virchow more than a century ago[21]. It is now known that inflammation can both be a predisposing factor for cancer, and a consequence of it[22]. A pre-existing chronic inflammatory condition promotes continuous erosion of damaged tissue and deposition of scar tissue[23]. Such processes involve the constant activation of matrix-degrading enzymes, e.g. Matrix Metalloproteinases (MMPs) and Collagenases[24], and release of paracrine factors such as Epidermal Growth Factor (EGF)[25] and Transforming Growth

Factor-β (TGF-β)[26]. Overexpression of such enzymes and paracrine factors can lead to cell hyperproliferation while suppressing the anti-tumour immune response[27]. Most solid tumours promote inflammation. After the first mutation events that cause a cell to become cancerous, pro-inflammatory transcription factors become up-regulated which trigger the release of pro-inflammatory chemokines and cytokines[28].

Generally, the process of transformation from a normal tissue to an *in situ* (primary) neoplasm is accompanied by an increasing degree of identifiable cytological changes. Criteria for grading such changes were established by the American Joint Committee on Cancer and are based on markers of cellular differentiation (e.g. nucleus/cytoplasm ratio, overall shape and retention of cell functionality), and karyotype[29]. Accumulation of further morphological and chromosomal abnormalities leads to increased cell mobility and progression from *in situ* to invasive neoplasm[30]. Such morphological changes take place after any event of gene or protein modification has occurred.

In cancers of epithelial origin (carcinomas), a pre-requisite for the formation of distant metastasis involves cancer cells' transition from an epithelial phenotype to a mesenchymal one, a process which allows cells to detach from the basement membrane and enter the extracellular matrix (ECM), travelling via the connective tissues in order to reach other sites (Figure 1.1). Briefly, this process involves disruption of cell-cell junctions, loss of cell polarity, downregulation of epithelial cell-specific adhesion molecules (e.g. E-cadherin, ZO-1) and intermediate filaments (e.g. Keratins), and upregulation of stromal cell-specific adhesion molecules (e.g. N-cadherin) and intermediate filaments (e.g. Vimentin). Such process falls under the name of Epithelial-to-Mesenchymal Transition (EMT), and can be transient (EMT-like phenotype) or permanent (full EMT phenotype)[31]. Upon colonizing the new site, and having formed a metastasis, cancer cells may or may not revert to an epithelial phenotype through a process named Mesenchymal-to-Epithelial transition. However, some cells may retain the mesenchymal phenotype, thus maintaining the ability to migrate again to another site[32].

Ultimately, by identifying stage-specific markers of abnormality (at the protein or gene level) tumour progression can be predicted and arrested at an earlier stage, when the functionality of the organs affected is not yet compromised[33,34].

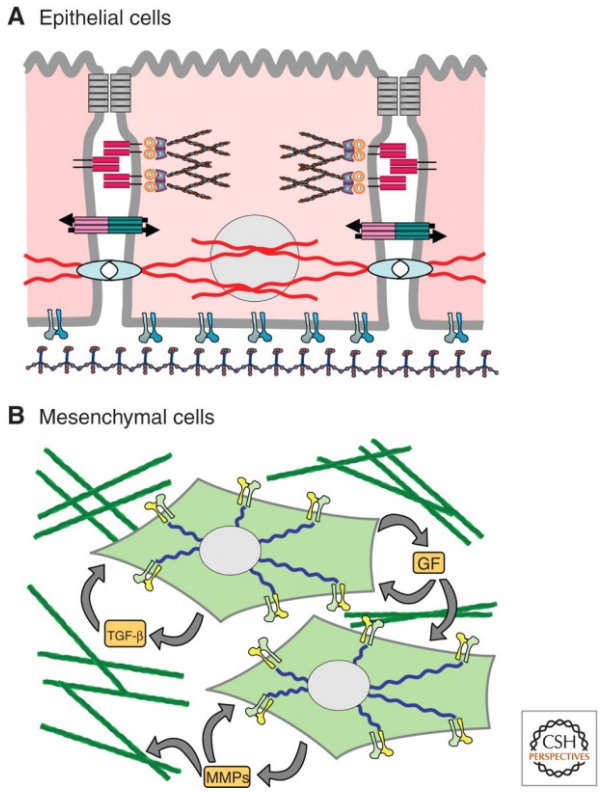

Figure 1.1 - (A) Epithelial cells interconnected through tight junctions (gray); E-cadherin-based junctions (red), which are connected to the actin cytoskeleton through b-Catenin (yellow); gap junctions (red/blue); hemidesmosomes (cyan), which are connected to cytokeratin-based intermediate filament. Epithelial cells also have specialized cell-ECM interactions for adhesion to the laminin-rich basement membrane. (B) Mesenchymal cells showing Vimentin-filaments (blue) and altered cell-ECM interactions optimized for adhesion to the collagen-rich environments. Mesenchymal cells also produce abundant TGFb, growth factors (GF), and matrix metalloproteinases (MMPs). Adapted from Nistico et al.[35]

1.1.2 Biology of Colorectal Cancer and Liver Cancer

The main two cancers that will be used as model for the experiments in this dissertation are Colorectal cancer and Liver cancer.

According to the Globocan 2012 database, Colorectal cancer is the 3rd type of cancer for incidence and the 4th for mortality on a worldwide scale. From the same source, Liver Cancer ranks 6th for incidence, and 2nd for mortality, with Hepatocellular Carcinoma (HCC) accounting for 75% of all liver cancers.

A milestone on the overall understanding of cancer biology was set by the 1990 Fearon and Vogelstein study on Colorectal carcinoma (CRC), which illustrated a multi-step genetic model of progression from normal epithelium to carcinoma and metastasis[13]. According to this study, each of the described mutations was associated with a specific phenotypical change, and all the described changes had to occur in the correct sequence for the tumour to develop. With the advances in the genetic field, and especially with the discovery of microsatellite repeats and of the existence of methylation patterns that regulate gene expression, the knowledge on the genotype of CRC has since expanded, and it is now widely accepted that there are: i) tumours carrying mutations due to Chromosomal Instability (CIN), ii) tumours carrying mutations due to Microsatellite Instability (MSI), iii) tumours carrying both CIN-related and MSI-related mutations, iv) tumours showing altered CpG islands methylation patterns (CIMP)[36]. Furthermore it has become apparent that the sequence of mutations that drive CRC progression is not mandatory even within neoplasias of the same etiology.

Virtually all CRC start from a polyp, which represents an intraluminal growth process; fortunately, though, not all polyps undergo neoplastic transformation and carry on growing underneath the colon mucosa. Chronic inflammatory diseases of the GI tract such as Celiac Disease (CD) and Inflammatory Bowel Disease (IBD), as well as all polyposis syndromes are predisposing factors for colon cancer[37]. Interestingly, according to the type of genetic mutations observed in the patient, it is now possible to predict the probability, location and histological features of the colon neoplasia, thanks to a series of retrospective studies[38] (see summarizing Figure 1.2).

Staging of CRC is based on the TNM international classification system, although it is not unusual to still find reports based on the old Dukes classification (see Appendix A).

Current screening procedures for CRC include: digital rectal exam, fecal blood test, endoscope-aided imaging, CT scan, X-ray scan, cytogenetic analysis, and serum measurement of a yet very limited numbers of oncological markers[38,39].

Current pharmacological treatments for CRC patients still include 5-Fluorouracil (first introduced in the 1960s), as well as the newer agents Oxaliplatin and Irinotecan (a Topisomerase I inhibitor), and the recently introduced Cetuximab (an EGFR inhibitor) and Bevacizumab (a VEGFR inhibitor). Although used in combination with surgery, these treatments are still not totally effective to induce disease remission and prevent recurrence; furthermore, side and toxic effects limit their prolonged use, hence there is still great need for less toxic agents, alongside better predictive and prognostic markers[39].

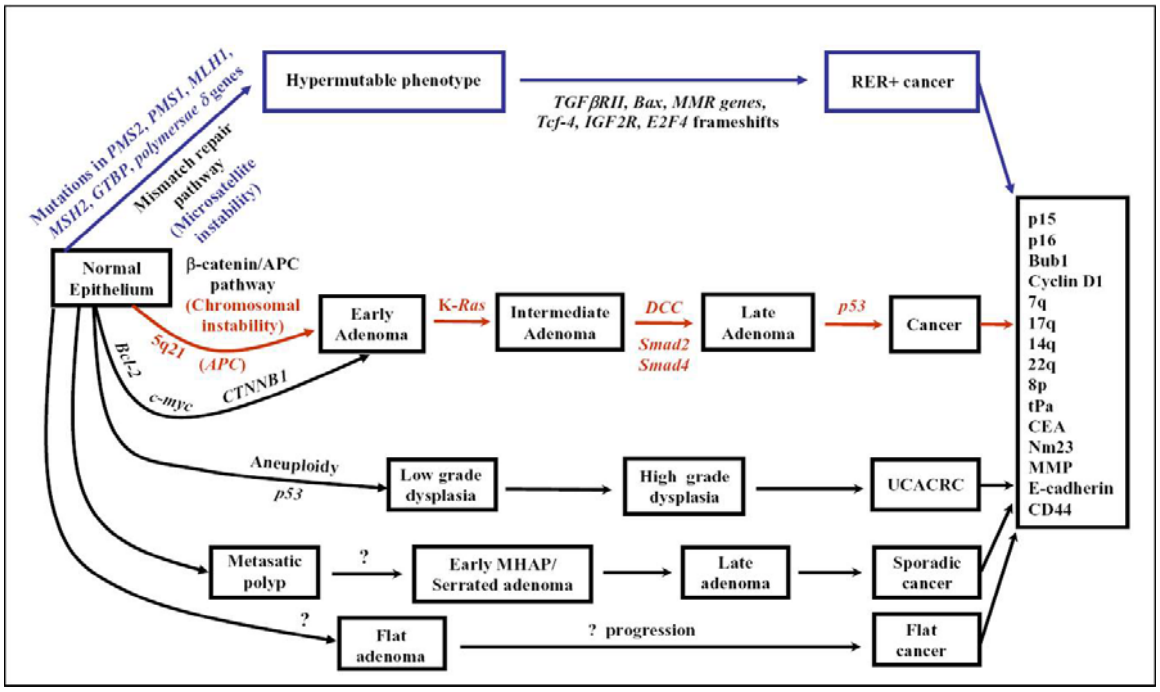

Figure 1.2 – Diagram depicting the alternative pathways that lead to formation and progression of colorectal cancer (from Narayan and Roy, 2003)[40]. CIN pathway shown in red (also known as Fearon and Vogelstein pathway), MSI pathway shown in blue. Alternative pathways due to a combination of CIN and MSI shown in black.

Liver cancer can develop from different cell types, most commonly from proper hepatocytes and from biliary duct epithelial cells. The first cell type is involved in the formation of Hepatocellular carcinoma (HCC) and Hepatoblastoma (only affecting children), whereas the second is involved in the formation of Cholangiocarcinoma. The commonest form, i.e. the HCC, usually develops from instances of chronic inflammation of the liver (cirrhosis), whose most common causes are Hepatitis B and C viruses, ethanol/drug abuse,

Aflatoxin B1 ingestion. Interestingly, Hepatocellular Adenoma (HCA) is a benign condition in liver and rarely progresses to Carcinoma[41]. Distinguishing between HCA and HCC can be difficult macroscopically, however observation of the tissue histology, cell morphology and cell proliferation marker are a useful tool to clear any doubts.

Current diagnostic tools for HCC include: ultrasound, MRI scan, CT scan, PET scan, biopsy with histological staining, and serum measurements of liver-produced enzymes (Transaminases, Gamma-GT) as well as oncological markers (Alfa-fetoprotein). None of these exams, though, gives conclusive results alone; furthermore each of them presents limitations of usability. Current treatments for HCC include: liver resection, transplantation, treatment with chemotherapeutic drugs Doxorubicin, Cisplatin, and Mitomycin C, radio-frequency tumour ablation, kinase-receptor inhibitors. It is important to note that not all patients are eligible for invasive or minimally invasive surgical procedures, along with the issue that not all patients tolerate the side effects of chemotherapeutic drugs. For this reason there is constant need for improvement of the administration routes of current drugs, as well as a need for safer treatments[42].

1.1.3 Cellular mechanisms of degradation and their involvement in cancer and chronic inflammatory diseases

In Chapter 3 of this dissertation I will be assessing the propensity to degradation of a specific protein, therefore here I will briefly detail two such mechanisms of intracellular protein degradation: Autophagy and Ubiquitylation

- Autophagy

Autophagy is a highly dynamic and inducible mechanism by which cells degrade large amounts of long-lived or misfolded proteins, and even whole organelles[43]. The most potent stimuli for the activation of autophagy are: starvation, oxidative stress, endoplasmic reticulum (ER) stress, the unfolded protein response (UPR), and damaged organelles. In

each of these circumstances, cells face the need of breaking down large amounts of protein either for metabolic purposes (*i.e.* to counteract starvation), or to avoid intracellular toxicity generated by the presence of protein adducts and stress-related by-products[44]. Other circumstances where autophagy activity is found to be increased are within the context of immune responses and chronic inflammatory diseases.

The formation of functional autophagosomes starts with a protein-mediated assembly of a phagopore. The phagophore serves as a nucleation centre for the future autophagosome, whose formation is catalysed by a Type III phosphatidylinositol-3 kinase complex (PtdIns3K) comprising Vps34-p150-Atg14-Beclin-1 proteins. This complex, in turn, recruits another enzymatic complex that mediates addition of phosphatidylethanolamine (PE) to a protein named LC3, on the autophagosomal membrane, in a reaction that is considered crucial for the expansion of the autophagosome. Later, the autophagosome fuses with a lysosome in order for its cargo to be degraded by lysosomal enzymes[45] (Figure 1.3). Currently, it is believed that upon completion of the degradation processes, the autophagosomal membranes and proteins are recycled, although such pathways are yet to be fully elucidated[46].

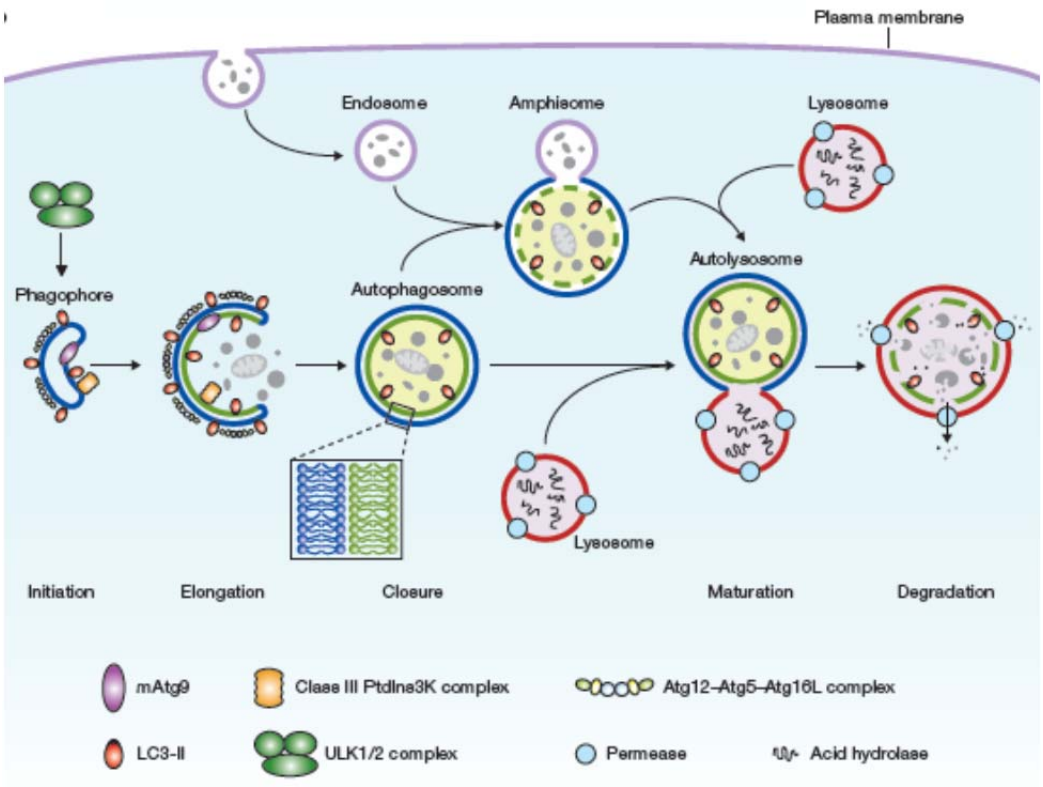

Figure 1.3 – Diagram of the autophagy pathway (from Yang, Klionsky)[47]

The main switch regulator for autophagy is the mammalian Target of Rapamycin (mTOR) protein kinase. Pathways activated following the internalisation of amino acids and glucose, lead to activation of mTOR, which in turn prevents autophagy[47]. As a consequence, starvation blocks such pathways and leads to autophagy by inhibiting the activation of mTOR[48]. Other conditions such as ER stress, UPR, hypoxia and anoikis (detachment from ECM)[49] activate autophagy via mTOR-independent pathways[50].

Early studies linking autophagy to cancer showed that mice with heterozygous loss of the *Beclin-1* gene[49], had increased propensity to develop spontaneous tumours. Such findings placed autophagy as a general tumour suppressive mechanism, which was later shown to occur via elimination of the p62/SQSTM1 Ubiquitin-binding protein (hereafter referred to as p62)[51] and via oncogene-induced senescence (OIS)[52]. Conversely, further studies revealed that autophagy is also activated in tumour cells, during anoikis, starvation and hypoxia, and acts to promote their metastatic progression[53]. Autophagy during

tumorigenesis may thus play differential roles: it may act as a tumour suppressor, by clearing stress by-products and protein aggregates which could permanently damage the cell and induce its oncogenic transformation; and it may act to promote metastasis, by helping tumour cells survive starvation, hypoxia and anoikis, which are likely to occur within a fast-growing tumour mass[54] (Figure 1.4).

A study conducted in pancreatic cancer cell lines showed that the Tissue Transglutaminase (TG2) protein downregulates autophagy[69]; furthermore, given the known role of TG2 in promoting metastasis and acquisition of MDR phenotype in pancreatic cancer[55], the authors implied (but did not demonstrate) that autophagy is responsible for preventing metastasis and MDR.

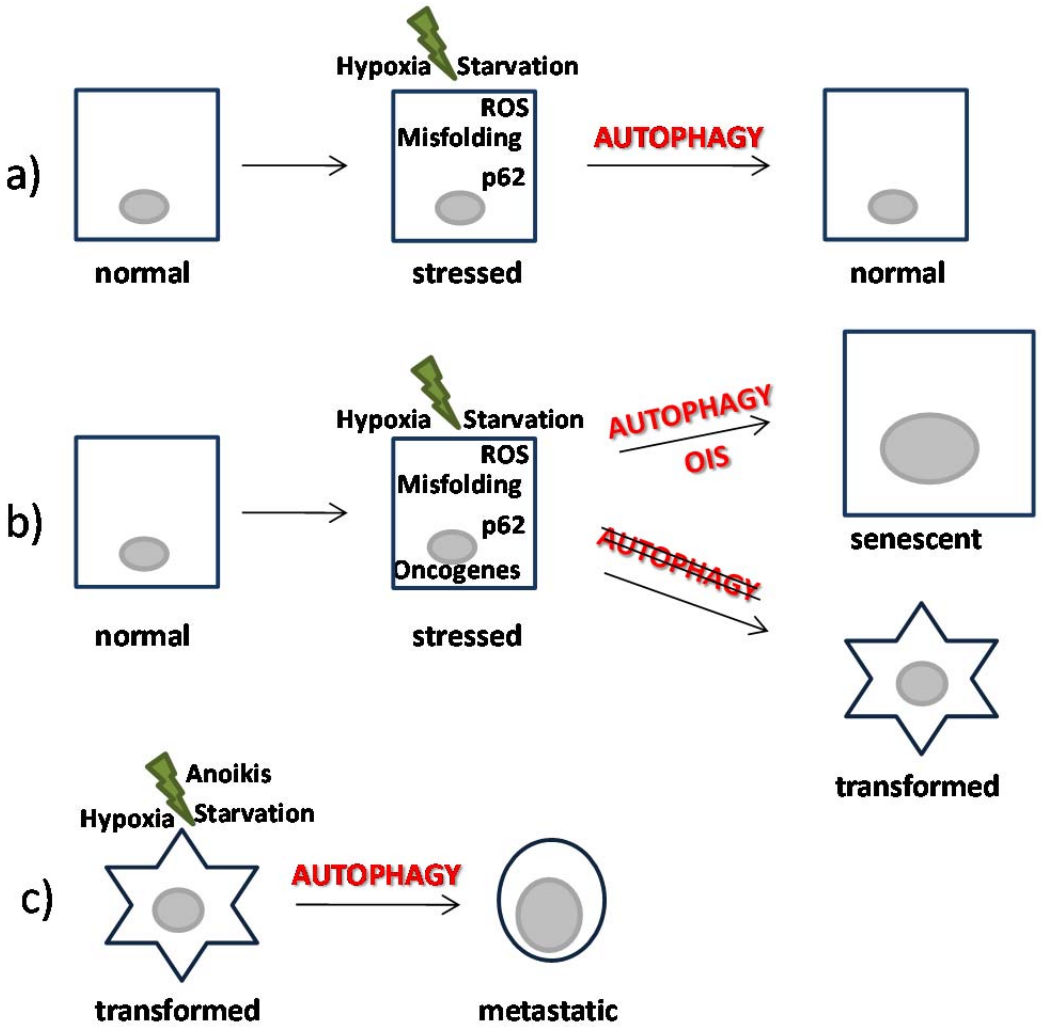

Figure 1.4 – Effects of autophagy activation in: a) stressed cells, b) stressed and/or oncogene-induced senescent(OIS) cells, and c) transformed cells.

An important role for autophagy within the context of the immune response has been defined following unexpected discovery of further processes of intracellular degradation where autophagy is involved. Specifically, it has been found that autophagy helps clearance of intracellular pathogens[55,56], and increases MHC class I and II-mediated antigen presentation, probably by providing them with peptides generated during autolysosomal degradation[57]. Such functions exerted by autophagy in the context of immunity raised the possibility that impairment of autophagy may lead to autoimmune responses, however, definitive associations are yet to be made[58].

Autophagy also plays a critical role in chronic inflammatory diseases, such as Crohn's disease and Cystic Fibrosis (CF). Crohn's disease is one type of inflammatory bowel disease (IBD), which is characterised by a massive infiltration of leukocytes within the mucosa, and is associated with an increased risk of small intestine, colon and colorectal cancer[59]. The development of Crohn's disease is commonly regarded to be the result of the interaction between genetic predisposition, environmental factors (cigarette smoke, hormones, diet), and defects in the immune response (which may be due to genetic or environmental factors)[60]. Among the associated susceptibility genes, it is worth to mention *Atg16L* (coding for the aforementioned Atg16 autophagy protein), *NOD2* (coding for a protein which recognises microbial molecular patterns and can induce autophagy)[61], and *XBP1* (coding for a protein upregulated during ER stress and UPR)[62]. These genetic alterations contribute to the impaired microbial clearance and chronic mucosal inflammation found in Crohn's disease.

Cystic Fibrosis is a chronic inflammatory condition affecting bicarbonate and chlorine secreting exocrine glands and epithelia (lungs, pancreas, gallbladder, intestine, cervico-uterin tract, sweat glands). It is caused by autosomal recessive mutations on the gene coding for the Cystic Fibrosis Transmembrane Regulator (CFTR) protein, which cause its loss of function. The most common CFTR mutation is the deletion of a Phenylalanine in position 508 (ΔF508) which causes the misfolded protein to be retained within the ER at

the physiological temperature of 37°C[63]. Defective CFTR function impacts on the correct electrolyte composition and viscosity of bronchial mucus, pancreatic juice, bile salts, cervical mucus, and sweat[64]. In the lungs, the viscous mucus serves as an adhesive surface for pathogens, which stimulates a strong neutrophil-mediated inflammatory response[65]. Recently it has been shown both *in vivo* and *in vitro* that autophagy is ultimately responsible for the inflammatory phenotype shown by CF epithelial cells[68]. In particular, it was demonstrated that production of ROS (caused by the accumulation of misfolded CFTR within the ER) promotes TG2-mediated cross-linking and inactivation of the anti-inflammatory transcription factor PPARγ and of Beclin-1. Consequently, activity of the NF-kB proinflammatory transcription factor in promoting production of IL-8 (and other inflammatory mediators) is unrestricted. Furthermore, defective autophagy prevents clearance of oxidative stress caused by intracellular accumulation of misfolded CFTR protein[66]. Hence, autophagy mediates chronic inflammation of the airways in individuals affected by CF.

- Ubiquitylation and SUMOylation

Ubiquitylation is defined as the conjugation of a substrate to molecules of Ubiquitin. Different from the degradation "in bulk" carried out by autophagy, Ubiquitylation mediates the degradation of smaller amounts of protein within the context of the so-called Ubiquitin-Proteasome System (UPS)[67]. Similarly to autophagy, impaired function of the UPS is involved in inflammation[68] and cancer[69].

Ubiquitin (Ub) is a small molecule (76aa., 8.5kDa) characterised by a distinctive Glycine-Glycine C-terminus (residues G75 and G76), and by seven Lysine (residues K6, K11, K27, K29, K33, K48, K63) in its sequence; all of these residues being necessary for the conjugation of Ub to its substrates, which occurs via formation of amino-carboxyl isopeptide bonds[70]. According to which and how many of the Ubiquitin Lysine residues are involved in the Ubiquitylation of a substrate, different types of isopeptide bonds can be

formed (e.g. homotypic, heterotypic, branched, and multiple monoubiquitylation) which target the protein for different types of degradation (e.g. Proteosomal, Lysosomal, etc.)[71,72].

In order to maintain a balance between protein degradation and synthesis, Ubiquitylation is regulated by multiple enzymes which catalyse three sequential processes: 1) ATP-dependent "activation" of a molecule of Ub, catalysed by an E1 Ubiquitin-activating enzyme; 2) transfer of the activated Ubiquitin to an E2 Ubiquitin-conjugating enzyme; 3) recruitment of a substrate and its conjugation to Ubiquitin mediated by an E3 Ubiquitin-ligase enzyme[67] (Figure 1.5).

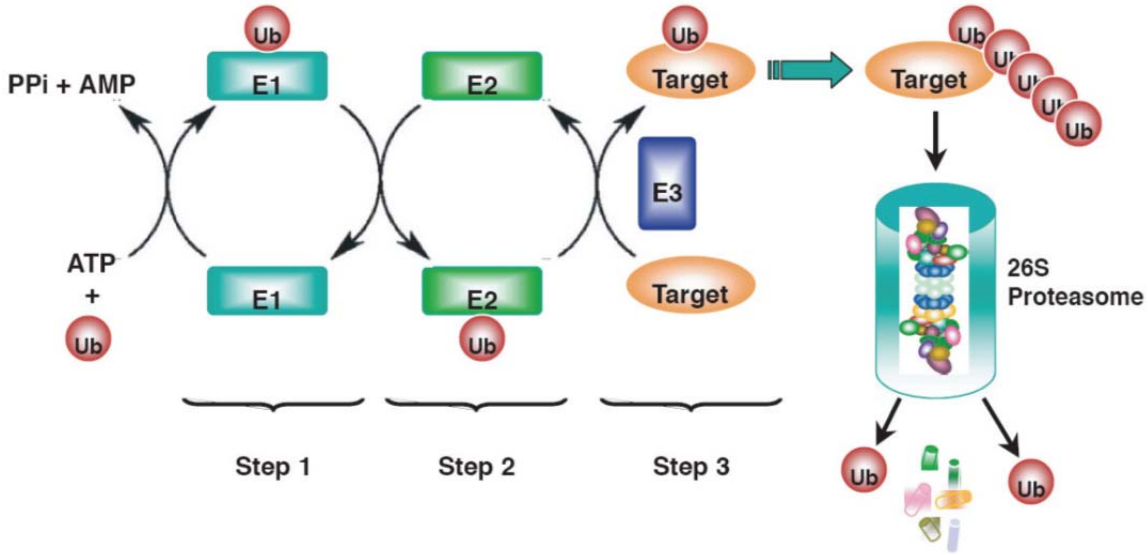

Figure 1.5 – Diagram of the steps required for Ubiquitylation of a target substrate (from Wang[68])

The Proteasome is a multimeric complex that carries out proteolysis of Ubiquitin-tagged proteins. It is composed of a central barrel-shaped catalytic core, and of two regulatory protein complexes, one capping each end of the catalytic core. Ubiquitylated proteins enter the upper regulatory complex where de-Ubiquitylation and unfolding occur; later proteins proceed towards the catalytic core where enzymatic degradation occur, followed by release of peptide fragments into the cytoplasm[68].

Ubiquitylation of target proteins not only can be reversed, but also physically prevented. The main mechanism which prevents Ubiquitin-mediated protein degradation is SUMOylation. Small Ubiquitin-like modifiers (SUMO) are small proteins (101aa., 11kDa)

belonging to the Ubiquitin-like protein (Ubl) family[73]. In mammals, three different isoforms of SUMO have been identified, including SUMO-1, SUMO-2, SUMO-3; however because SUMO-2 and SUMO-3 cannot be functionally distinguished *in vitro*, they are collectively addressed as SUMO-2/3. It is accepted that targets bind with high specificity to either SUMO-1 or SUMO 2/3[74].

The process of SUMOylation is similar to that of Ubiquitylation in that it is regulated by the sequential activation of three SUMO-specific E1, E2 and E3 enzymes. The process starts with the ATP-dependent activation of a SUMO molecule catalysed by an E1 SUMO-activating enzymatic complex. Next, the activated SUMO molecule forms a trans-thiol bond with another subunit of the same E1 enzymatic complex. Successively, SUMO is transferred to an E2 SUMO-conjugating enzyme which makes contact with a substrate. Finally, through an E3 SUMO-ligase enzyme, an isopeptide bond is formed between SUMO and the substrate[75]. Since Ubiquitin and SUMO share the same recognition sites on a given substrate (ΨKxE, where Ψ= any hydrophobic residue, K=Lysine, E=Glutamic acid, and x=any amino acid), it was thought that no substrate could be Ubiquitylated if it was already SUMOylated, and vice versa; however, the aforementioned heterotypic Ubiquitin bond has recently been demonstrated to occur between a Ub and a Ub-like molecule (such as SUMO)[74]. Therefore, SUMOylation is regarded as a process that decreases turn-over of a protein (by temporarily preventing its Ubiquitin-mediated proteasome degradation) but does not completely abrogate it[75].

Accumulation of misfolded proteins within the ER is sensed as stress and activates a series of rescue mechanisms which, collectively, constitute the Unfolded Protein Response (UPR). If the overload of misfolded proteins cannot be cleared due to the formation of high molecular weight aggregates, or if the ER itself undergoes damage, autophagy (via interaction of Beclin-1 with the Vps34-p150-Atg14 complex) program is initiated. However, if stress is prolonged, cell death pathways may become activated via a poorly understood cross-talk between the autophagic and the apoptotic machinery[76].

Interestingly, autophagy and Ubiquitin-mediated degradation do not always occur independently from each other; in fact, the specificity of Ubiquitin-mediated degradation and the non-specificity of autophagic mass degradation can converge in a process named "selective autophagy". The bridging factor in such context is represented by the p62 protein, which binds to ubiquitylated protein aggregates and targets them to autophagic vacuoles; such vacuoles will then fuse to a lysosome in order for the aggresomes to be degraded[77].

The Ubiquitin-proteasome system can exert a pathogenic role in cancer, as well as in inflammatory and autoimmune diseases. In cancer, ideal pharmacological targets have been identified among those E3 ligase enzymes that regulate ubiquitylation of p53 protein (the "guardian of the genome") and Inhibitor of Apoptosis (IAP) proteins[78]. Drugs against E2 and E3 enzymes have already been developed and their efficacy is currently being tested in clinical trials[79]. Conversely, in the field of inflammatory diseases, ideal pharmacological targets have been identified among those E3 ligase enzymes responsible for hyperactivation of the NF-kB proinflammatory transcription factor (due to degradation of its inhibitor IkB), for T cell proliferation (due to degradation of the p27 cell cycle inhibitor), and for T cell anergy (by degradation of proteins involved in T cell activation pathways)[80].

A drug that reversibly blocks the Proteasome (known as Bortezomib or Velcade®) was approved by the US Food and Drug Administration in 2003. Despite blockade of the Proteasome being a non-cell-specific treatment, it is successfully used to treat mantle cell lymphoma and chronic lymphocytic leukaemia[81]; however, it has also neuropathic side effects that are considered "tolerable" given the success of the therapy.

1.2 Tissue transglutaminase in cancer and inflammatory diseases

Transglutaminases (TGases E.C. 2.3.2.13) are a family of enzymes able to catalyse the formation of isopeptide bonds within or between substrate proteins. The isopeptide bond is

an amide bond that can be formed through transamidation of the γ-carboxamide group of a Glutamine residue, and the ε-amino group of a Lysine residue or a small primary amine[82]. Formation of the first isopeptide bond often increases the chance of further reactions occurring, which facilitates the generation of highly cross-linked, high molecular weight (HMW) proteins[83]. To date, nine proteins have been included in the TGases family, which show wide tissue distribution. Functionally, they all show multi-enzymatic capability; however, functions performed by TGases can be broadly divided in protein structure modification and signal transduction[84].

Tissue transglutaminase (tTG or TG2) is a member of the TGase family with ubiquitous tissue distribution, and found both intra- and extracellularly. It is known that TG2 can be internalised from the extracellular environment to undergo lysosomal degradation[85]; however, it is not yet known how it can be externalised.

The cross-linking activity of TG2 is exerted by the catalytic triad Cys277-His335-Asp358 and is Ca^{++}-dependent[86]. Mutations of Cys277 render TG2 unable to bind substrate and form thioester intermediates, thus resulting in complete loss of cross-linking activity[87]. TG2 is also able to hydrolise Guanosine triphosphate (GTP) and Adenosine triphosphate (ATP) in the presence of Mg^{++}[88], however only binding of GTP causes a conformational change that inhibits Ca^{++} binding. Hydrolysis of GTP reportedly permits TG2 to function as Gα subunit of the G_h transducing protein, modulating activation of the α1-adrenergic receptor in liver cells[89]. Another function ascribed to TG2 is the Protein-disulfide isomerase (PDI) in mitochondria, where it contributes to the correct assembly of respiratory chain complexes[90]. TG2 can also function as a molecular adaptor, binding to integrin β1 and β3 subunits and mediating their interaction with fibronectin at the cell surface[91]. Additionally, recent evidence has shown that TG2 also has serine/threonine kinase activity and, thus, has the potential to phosphorylate proteins[92]. The structure and functions of TG2 are schematically summarised in Figure 1.6, however it is important to note that each of the

above mentioned activities of TG2 takes preferentially place in a specific cellular compartment (depicted in Figure 1.7).

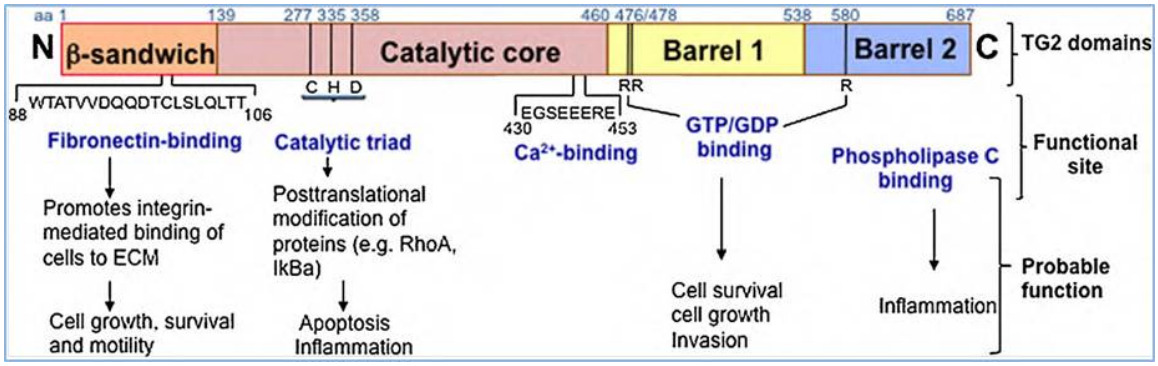

Figure 1.6 –Diagram of the structure and main functions of TG2 (from Mehta K. et al, 2010)[93]

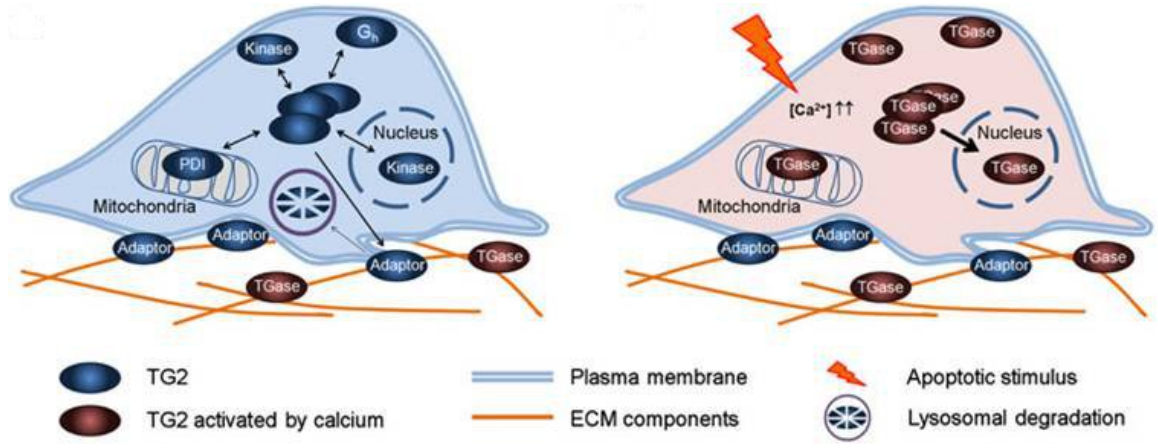

Figure 1.7 –Cartoon depicting the cellular compartments where TG2 enzymatic activities preferentially take place (from Park D. et al, 2010)[94]

In a study published by Zirvi et al.[95] colon cancer cell lines were screened for TG2 activity, and surprising results showed the presence of TG2 protein with variable heat sensitivity in those cell lines. Consequently, authors raised the possibility that different variants of TG2 could exist in some cell lines. Such an assumption was later confirmed by Fraij et al. who identified a shorter TG2 mRNA, deriving from alternative splicing of the main variant and lacking the original 3'UTR[96]. It was later recognised that the shorter variant of TG2 lacked also the GTP-binding domain, and different functional studies agreed

that this variant was capable of inducing differentiation (in neurons)[97] or trigger apoptosis (in mouse embryo fibroblasts)[98]. To date, a total of 5 protein variants of TG2 have been identified which are transcribed from five different alternative transcripts; these are summarized in the table below.

Variant name	**Protein**	**Accession nr.**
TGM2_v1 (TG2-FL)	77 kDa (687 aa) main variant	NM_004613.2 NP_004604.2
TGM2_v4a	77 kDa (687 aa, but different C-term)	XM_011529029.1 XP_011527331.1
TGM2_v4b	77 kDa (687 aa, but different C-term)	XM_011529028.1 XP_011527330.1
TGM2_v2 (TG2 E10)	55 kDa (548 aa, lacks last 139aa)	NM_198951.1 NP_945189.1
TGM2_v3	38 kDa (349 aa, lacks last 338aa)	S81734.1

Table 1.1 – List of known TG2 variants

Given the many different roles of TG2, it is probably unsurprising that the ratio TGM2_v1/other variants is not as linear in cancer lines as it is in normal tissues. In fact, in a study carried out by Phatak et al., it is demonstrated that TGM2_v1 represents on average ~84% of all variants in normal tissues; however, in cancer tissues this value drops to an average ~57% and is accompanied by an increased expression of all other variants, particularly so in some breast cancer and melanoma cell lines[99].

1.2.1 Pro-tumoral and EMT-promoting activity of TG2

In the context of cancer, TG2 can exert two opposing functions: pro-tumoral and anti-tumoral[100]. The key to understanding how TG2 is able to have such opposing roles lies in its ability to bind to a wide variety of targets, affecting both their stability and function. A number of studies have associated TG2 levels with tumour cell survival, migration, invasion and onset of drug resistance, although not all of them also provide mechanistic explanation. For example, in the MCF7/DOX drug resistant breast cancer cell model, TG2 physically

interacts with Integrin β1 and β5 subunits and facilitates binding to Fibronectin-coated surfaces; this leads to a significant increase in cell survival when compared to the same cells grown on Bovine serum albumin (BSA)-coated surfaces, or when compared to a cell line which does not express TG2[101]. Furthermore, studies carried out in a pancreatic adenocarcinoma cell line show that TG2 also associates with an important mediator of the Integrin-Fibronectin signalling pathway, Focal Adhesion Kinase (FAK)[102]. Authors show a positive correlation between TG2 and levels of phosphorylated (activated) FAK, which persists even upon hyperexpression of the cross-linking defective form of TG2 (C277S mutant)[103]. Therefore, they conclude that the relationship between TG2 and phosphorylated FAK does not depend on TG2 cross-linking activity; however, they fail to address whether TG2 is directly responsible for FAK phosphorylation. So far, FAK has been linked to drug resistance only indirectly, i.e. through its ability to activate the Phosphoinositide-3-Kinase (PI3K)-Protein Kinase B/AKT (PKB/AKT) pathway[104,105]. Therefore, it is only based on indirect evidence that authors suggest the use of TG2 inhibitors as a therapeutic approach for MDR pancreatic cancer[103].

Involvement of TG2 in cell migration has been further demonstrated by various studies from Antonyak et al. conducted in *in vitro* models of breast cancer. This group consistently demonstrates not only that recruitment and activation of TG2 occurs as a downstream event of the EGFR/RAS signalling pathway, but also that its recruitment occurs at the "leading edges" of the cells, where it assists with cell migration[106,107].

The PKB/AKT pathway is also important in transmitting cell survival signals. Consequently, its deregulation can lead a normal cell to hyperproliferate, and a tumour cell to become malignant. Evidence suggests that modulation of the PKB/AKT pathway is one way in which TG2 affects cell survival. In a glioblastoma cell line, Yuan et al. found that TG2 inhibition caused cell death by reducing levels of phosphorylated (pro-survival) PKB/AKT, and other key anti-apoptotic proteins downstream of PKB/AKT[108]. An important inhibitor of the PKB/AKT pathway is the Phosphatase and Tensin Homolog (PTEN)[109,110], whose

activity in preventing metastasis is demonstrated by two studies carried out in human endometrial carcinoma tissue sections[111] and in a mouse melanoma cell line[112]. Interestingly, in a pancreatic cancer cell line, high levels of TG2 are associated with ubiquitination and decreased expression of PTEN; however the authors did not provide a mechanism by which TG2 may affect PTEN stability and function[113].

In human pancreatic cancer cell lines, the anti-inflammatory Peroxisome proliferator-activated receptor-γ (PPAR-γ) acts as a transcriptional factor promoting transcription of PTEN[114]. PTEN is a phosphatase (responsible for dampening the proliferative PKB/AKT pathway) whose levels have been inversely correlated with TG2[113]. Interestingly, PPAR-γ functionality can be limited by TG2-mediated cross-linking and subsequent degradation, as shown in CF cell lines[115]. The transcription factor NF-kB naturally prevents transcription of the anti-inflammatory PPAR-γ. In this context it is known that TG2 can activate NF-kB by cross-linking and inactivation of its inhibitor IkB[116], thus tilting cellular balance towards an overall pro-inflammatory phenotype.

Another way by which TG2 is involved in survival is by impairing autophagy. When impaired, autophagy fails to protect normal cells from oncogenic transformation but, at the same time, fails to sustain metastasis of tumour cells (reviewed in Section 1.1.3). A study in Cystic Fibrosis first showed that TG2 causes impairment of autophagy via cross-linking and inactivation of its initiator protein Beclin-1[117]. A slight different mechanism is proposed by the study from Akar et al. carried out in a model of pancreatic adenocarcinoma. In this model, authors demonstrate that TG2-mediated inhibition of autophagy occurs by Protein Kinase C-delta (PKCδ)-mediated upregulation of TG2[118].

An important event that characterises gain of malignancy in carcinomas is represented by EMT[119]. A recent study from Shao et al.[120] shows that TG2 can indirectly activate the *Zeb1* gene in ovarian carcinoma cells. The Zeb family of transcription factor is known to be upregulated by the NF-kB pathway during EMT[121]; additionally, it is known that TG2 can activate NF-kB by cross-linking and inactivation of its inhibitor IkB[122]. Hence, authors

conclude that TG2 promotes EMT in ovarian carcinoma cells via NF-kB-mediated activation of the *Zeb1* gene which, in turns, leads to E-Cadherin repression.

One study carried out on A549 cell model of lung cancer, shows that TG2 promotes the E-Cadherin-to-N-Cadherin switch upon treatment with TGFβ-1 ligand via decrease of PP2A which in turn leads to hyperactivation of JNK[123]. In addition, Kumar et al. show that in breast cancer cells lacking TG2, TGFβ-mediated EMT fails to initiate[124].

Another interesting study carried out in epidermal cancer stem cells shows not only that TG2 is necessary for downregulation of E-Cadherin and consequent upregulation of mesenchymal cell markers, but that this is due to TG2 GTP-ase activity as opposed to its transamidase activity[125].

A further way by which TG2 promotes metastasis is described in a study from Satpathy et al., showing that TG2 can promote transcription of MMP-2. This is the downstream effect of the TG2-mediated cross-linking and inactivation of the PP2A phosphatase. Inactivation of PP2A leads to the inability of dephosphorilating and inactivating the CREB transcription factor. This way, CREB remains bound to the promoter of MMP-2 and sustains its trascription[126].

Tumours usually express markers not previously known to the organism (such as gene rearrangement products), or "self" molecules whose temporal and tissue-pattern of expression becomes altered[14]. As such, tumour markers may be recognised by the immune system and stimulate cytotoxic responses[15]. Tumour cells commonly escape immune system recognition by downregulating HLA-I molecules[15]. However, since a complete loss of HLA expression would lead to Natural Killer (NK) cell-mediated cytotoxicity[16], HLA-I expression is kept at a low level to simultaneously minimise recognition by CD8+ T and NK cells. A study from 1981 reports that, in peripheral blood mononuclear cells (PBMC), exogenously administered TG2 is able to cross-link and cause intracellular aggregation of β2-microglobulin protein into HMW polymers[127]. β2-microglobulin plays an essential role in the assembly and cell surface expression of HLA-I molecules[128]. The 1981 study was

carried out following the discovery of many Glutamine residues in the primary amino acid structure of β2-microglobulin, a structure that made it a likely candidate for TG2-mediated cross-linking. Notably, to date, no relationship between intracellular levels of TG2 (protein and activity) and β2-microglobulin has been established.

The notion of TG2 can act as a tumour enhancer renders it a potential therapeutic target that has been exploited in some *in vivo* studies. For example, in a mouse model of glioblastoma, treatment with the KCA075 TG2 inhibitor plus a chemotherapeutic agent effectively reduced tumour mass, and increased sensitivity of tumour cells to the chemotherapeutic agent[108]. Similarly, in a mouse model of pancreatic adenoncarcinoma, administration of lipo-soluble TG2 small interfering RNA in combination with a chemotherapeutic drug effectively reduced tumour proliferative rate and volume, as well as intra-tumour neoangiogenesis[129]. None of these studies has currently been followed by human clinical trials.

1.2.2 Anti-tumoral activity of TG2

A large body of evidence now supports the concept that TG2 can have anti-tumoral effects. It is known that TG2 can promote local aggregation of ECM proteins either via their direct cross linking[130] or via activation of TGFβ1 (which enhances deposition of ECM components)[131], therefore Jones et al. carried out experiments to ascertain whether these features could impact on tumour progression. Interestingly, they discovered that intra-tumoral injection of TG2 enzyme caused matrix changes which decreased tumour growth rate in mice implanted subcutaneously with CT26 cancer cells[132]. Moreover, in the same study, it was shown that the injection of B16 tumour cells in $TG2^{+/+}$ mice caused a significant decrease in tumour growth and viability, compared to $TG2^{-/-}$ mice receiving the same treatment. Interestingly, in both studies, TG2 was mainly found localised in the ECM of the tumour-surrounding stroma. In a rat model of mammary adenocarcinoma, Haroon et al. administered TG2 subcutaneously at the primary tumour site. End-staged tumours were

removed and sections obtained, which were stained for TG2 and isopeptide bonds by immunohistochemistry (IHC). As in the previous studies, TG2 was detected in abundance in the ECM of the tumour-surrounding stroma[133]. Altogether, these results indicate that extracellular hyperexpression of TG2 enhances the deposition of peritumoral scar tissue via extensive cross-linking of ECM proteins, which acts as a barrier physically limiting tumour expansion.

Less well characterised is the anti-tumoral role played by intracellular TG2. In an experiment carried out in the rat, Hand et al. found that chemical induction of liver carcinogenesis was associated with decreased intracellular TG2 protein and activity compared to healthy liver, whereas no difference in levels of membrane-bound TG2 was observed[134]. A more complex experiment was carried out by Johnson et al.[135], which involved transfecting a TG2-encoding plasmid into hamster fibrosarcoma cells, and implanting these cells into a recipient hamster. The resulting tumours were harvested and cell lysates obtained whereupon TG2 activity was measured. Results showed that a higher level of TG2 expression and activity in hamster fibrosarcoma is negatively correlated with tumour incidence. Interestingly, authors also observed that when a tumour did manage to develop in a hamster treated with TG2-transfected fibrosarcoma cells, the lag-time between the injection and the appearance of the tumour was longer than in control hosts; however, once the tumour was visible, its growth rate was similar to that observed in hosts treated with non-TG2-transfected fibrosarcoma cells. The authors concluded that, in this model, TG2 is essential for suppressing cancer onset, but that this is independent of cell proliferation rate. An interesting descriptive study published in 1991 by Zirvi et al.[95] showed for the first time that TG2 activity (measured on total cellular protein extract) was inversely correlated with metastatic potential in four human colon carcinoma cell lines. However, no further work was conducted to address the underlying molecular mechanisms supporting the role of TG2 as a metastasis inhibitor in colon cancer.

A study by Ahn et al.[136] shows that, in a breast adenocarcinoma cell line, TG2 can cause transcriptional downregulation of MMP-9; however, the mechanisms that lead to such downregulation were not elucidated. The authors concluded that in this model TG2 behaves as a metastasis-suppressor through downregulation of MMP-9.

TG2 is target of translational repression driven by N-Myc and mediated by Histone Deacetilase 1 (HDAC1) in neuroblastoma; hence, Liu et al.[137] aimed at restoring the differentiation-promoter role of TG2 in a mouse model of neuroblastoma, by administering an HDAC inhibitor. Such treatment resulted in an effective decrease in tumour volume.

Protein cross-linking does not normally occur intracellularly, due to the low concentration of Ca^{++} (an essential enzymatic co-factor) and the high concentration of GTP as compared with the extracellular environment[138]. However, any event disrupting the intracellular homeostasis of Ca^{++} (e.g. apoptosis, oxidative stress)[139] can induce TG2 cross-linking activity. Upregulation of TG2 cross-linking activity at the onset of programmed cell death facilitates the formation of apoptotic bodies, which prevents leakage of intracellular proteins and triggering of unwanted inflammatory reactions[140]. Furthermore, analysis of TG2 protein domains has identified it as a new member of the proapoptotic BH3-only protein family[141]. A further way in which TG2 promotes cell death is via cross-linking of Retinoblastoma protein (pRb) in the nucleus, leading to initiation of the apoptotic programme[142], or via cross-linking and inactivation of the Sp1 transcription factor, which leads to decreased EGFR expression[143].

All of this evidence demonstrates that tumour-expressed intracellular TG2 can decrease the tumour's proliferative rate, and delay or impair acquisition of metastatic properties via promotion of apoptosis, differentiation, and via other less known pathways that interfere with cell migration and invasion. Extracellular (stromal) and surface TG2 can also interfere with cell migration and invasion, via TG2-mediated stabilisation of ECM components[91]. Notably, whilst tumour-expressed TG2 can exert the described functions by

many of its enzymatic and non-enzymatic activities, extracellular and surface TG2 exerts its functions solely via its cross-linking activity.

In light of such facts, it has been suggested that the behaviour of TG2 in the context of cancer may depend not only upon the tumour type, but also upon the histological localisation (tumour or stroma), and the intra-tumoral subcellular localisation (inner plasma membrane, cell surface, cytoplasm, nucleus, mitochondria)[144].

1.2.3 TG2 in inflammatory diseases

The first disease where TG2 was shown to play a pathogenic role was Coeliac disease (CD), in 1997[145]. In the context of CD TG2 catalyses the deamidation of glutamine residues within gluten proteins[146], which increases the affinity of gluten-derived peptides for DQ2 and DQ8 HLA-II (Human Leukocyte Antigen class II) molecules expressed by antigen presenting cells (APCs) in the intestinal lamina propria[147]. These "toxic" gluten-derived peptides also activate innate immune cells such as APCs and intra-epithelial lymphocytes (IEL), which mount an inflammatory response[148]. Altogether, these events lead to a strong cytotoxic T-Helper 1- and IEL-mediated immune response, with production of TG2-specific and gluten-specific autoantibodies[149]. If gluten is not withdrawn from the patient's diet, the chronic inflammatory and immune response can lead to complete destruction ("flattening") of the intestinal mucosa[149]. Administration of TG2 inhibitors has been successfully tested *in vitro* or *ex vivo*, however their employment *in vivo* is still matter of debate, given the potential risks of: i) targeting TG2 in all body tissues, and ii) targeting other members of the transglutaminase family, among which is the indispensable coagulation factor XIII[150].

More recently, TG2 was shown to mediate most of the events that lead to sustained inflammation in Cystic Fibrosis. In the context of CF, increased production of reactive oxygen species (ROS) mediates upregulation of TG2, which in turn cross-links the anti-inflammatory transcription factor PPAR-γ and targets it for degradation[115]. Interestingly, cross-linked PPARγ is found within large intracellular aggregates (termed "aggresomes") in

association with molecules of HDAC6 and Ubiquitin that mediate its degradation. In this way, balance between the proinflammatory transcription factor NF-kB and the anti-inflammatory PPAR-γ is lost, and enhanced transcription of proinflammatory mediators (IL-8, TNF-α) occurs[66]. A follow-up study reported that administration of the generic TG2 inhibitor Cystamine in a mouse model of CF, resulted in a decrease of the above mentioned proinflammatory mediators[151]. Therefore, authors suggested that targeting TG2 in CF patients could ameliorate the phenotype of their disease; however, there are currently no ongoing studies testing the suitability of a TG2 inhibitor for clinical use.

Protein aggresomes are also a distinctive feature of neurodegenerative diseases such as Huntington's, Parkinson's, and Alzheimer's disease. Each of these diseases is characterised by neuronal cytotoxicity caused by the formation of insoluble aggregates of one or more specific proteins: huntingtin in Huntington's, α-synuclein in Parkinson's, tau and β-amiloid in Alzheimer's. The presence of high levels of TG2 (protein and cross-linking activity) in the brains of people affected by these diseases, suggested the hypotheis, later confirmed, that this enzyme might be responsible for the formation of highly cross-linked protein aggregates[152,153]. The most promising TG2 inhibitor for human clinical use seems to be the KCC009 inhibitor, due to its short half-life in the plasma[154]; however, the above mentioned caveats on the use of TG2 inhibitors are still hurdles to overcome.

1.3 MicroRNAs, and their role in cancer

MicroRNAs (miRNAs) are a class of small (21-23 nucleotides), non-coding, single-stranded RNAs produced by the eukaryotic cell[155]. The presence of small RNAs with a transcription-inhibiting function was first discovered in 1993[156,157], however it was only recently that the name miRNA was introduced, together with the discovery of their mechanisms of generation within the eukaryotic cell (here reported in Figure 1.8)[158]. Briefly, the generation of mature miRNAs starts with the production of a long primary

transcript (pri-miRNA) by RNA polymerase II, in the nucleus. The single-stranded pri-miRNA folds into a 60-70-nt hairpin-shaped molecule and is cleaved at its unpaired 5' and 3' extremities by the RNAse III enzyme Drosha and the ancillary protein DGCR8, to become a pre-miRNA. Through binding to the molecular chaperones Exportin 5 and RAN-GTP[159], the pre-miRNA is transported into the cytoplasm where a complex consisting of the RNAse III enzyme Dicer and the ancillary protein TRBP, cleaves the hairpin loop to generate a 21-23nt miRNA. This miRNA associate with an Argonaute superfamily protein and enters the multi-enzymatic RNA-induced silencing complex (RISC), within which separation of the two strands occurs. The least stable of the two strands is selected as the mature miRNA which will bind to a sequence at the 3'UTR of the target mRNA to prevent its translation or mediate its degradation[160].

One further class of small RNA, called short-interfering RNA (siRNA) is also endogenously produced via the RISC complex, however differently from miRNA their precursor is represented by dsRNA instead of ssRNA; furthermore siRNA are conventionally linked to mRNA degradation rather than translation repression.

In fact, the fate of the target mRNA, whether translational repression or degradation, has conventionally been attributed to a looser or stricter sequence matching, respectively[161]. However at the present date this knowledge is being challenged, with many studies reporting miRNA-mediated total mRNA degradation even in the presence of base mismatches, as well as lack of siRNA-mediated total degradation in the presence of a total sequence match[162]. Current trends in molecular biology suggest that the final outcome from the miRNA/siRNA binding to its target mRNA, may depend on which isoform of the Argonaute protein is present within the RISC complex[163].

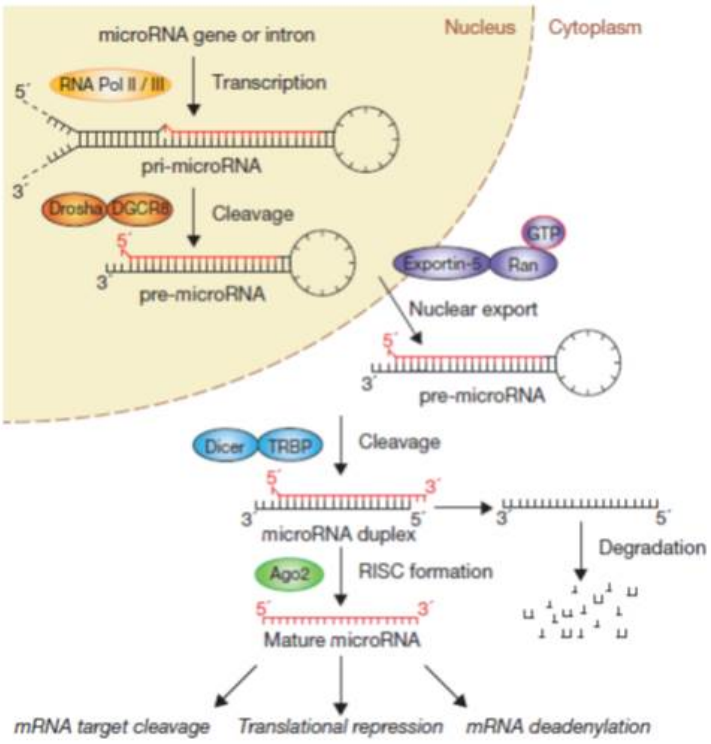

Figure 1.8 – Biogenesis of miRNA (from Diederichs[160])

Owing to such ability of interfering with mRNA translation in a time-specific and cell-specific fashion, miRNAs are now recognised as essential mediators of many physiological and pathological process in the cell biology of animals[158] and plants[164].

Among the various clusters of miRNA characterised so far, the miR 17-92 cluster (also known as *Oncomir*-1) seems to play an important role in all of the most common solid and haematological tumours[165]. Despite its first functional characterisation as a tumour promoter (hence the name "oncomir"), further studies have established that the miRNAs belonging to this cluster can have both oncogenic and anti-oncogenic properties, and are found at varying levels in different tumours[166].

The human *miR17HG* primary transcript for this cluster is a polycistronic mRNA that gives rise to 7 mature miRNA, miR-17-5p, miR-17-3p, miR-18a, miR-19a, miR-19b, miR-20a, miR-92-1 and is situated on chromosome 13q31-32. This region is often target of genetic alterations associated with cancer; for example, it is found amplified in some solid and haematological tumours (colorectal, lung, stomach, bladder, head/neck cancer and mantle

cell lymphoma)[167,168], whereas it is lost in other tumours (melanoma, hepatocellular carcinoma, ovarian and breast cancer)[169,170].

A vast number of targets of miR17-92 cluster have been predicted through a bioinformatics approach, and the results are now available in online databases; however, screening and identification for targets with key roles in cancer must have proven difficult, thus resulting in the current paucity of studies correlating miR17-92 with established cancer pathways. A review summarising such few known functional roles of miR17-92, reports that this cluster might interfere with the TGF-β-mediated cell cycle arrest and apoptosis pathways. Such interference is supposed to take place via miR17-92-mediated downregulation of two downstream targets of TGF-β signalling, namely the p21 and BIM proteins. This way, tumours might escape TGF-β-mediated cell cycle arrest and apoptosis[171].

1.4 Rationale

Cancer is a complex phenomenon in which cell proliferation becomes deregulated[4]. In this context, TG2 has opposing functions: either favouring or interfering with tumour progression[97]. Current literature suggests that the precise role played by TG2 may be dependent upon tumour type, cell type and subcellular localisation[93]. Thus far, researchers have identified some pathways through which intracellular TG2 may influence primary tumour expansion, metastasis formation and acquisition of an MDR phenotype[172–174]. However, very little data is available regarding the mechanisms through which intracellular tumour-expressed TG2 can suppress tumour expansion and the subsequent acquisition of invasive and metastatic properties.

Tumour growth and metastatic progression essentially depend upon the following key processes: hyperproliferation, genetic alterations, immortalization, immune evasion, EMT, migration, invasion and metastasis (Figure 1.9); a large body of work carried out across

several tumour types has established that TG2 plays a role in each of these processes. However, no comprehensive data are available on an *in vitro* model of primary-to-metastatic cancer where intracellular TG2 levels are inversely correlated with tumour stage.

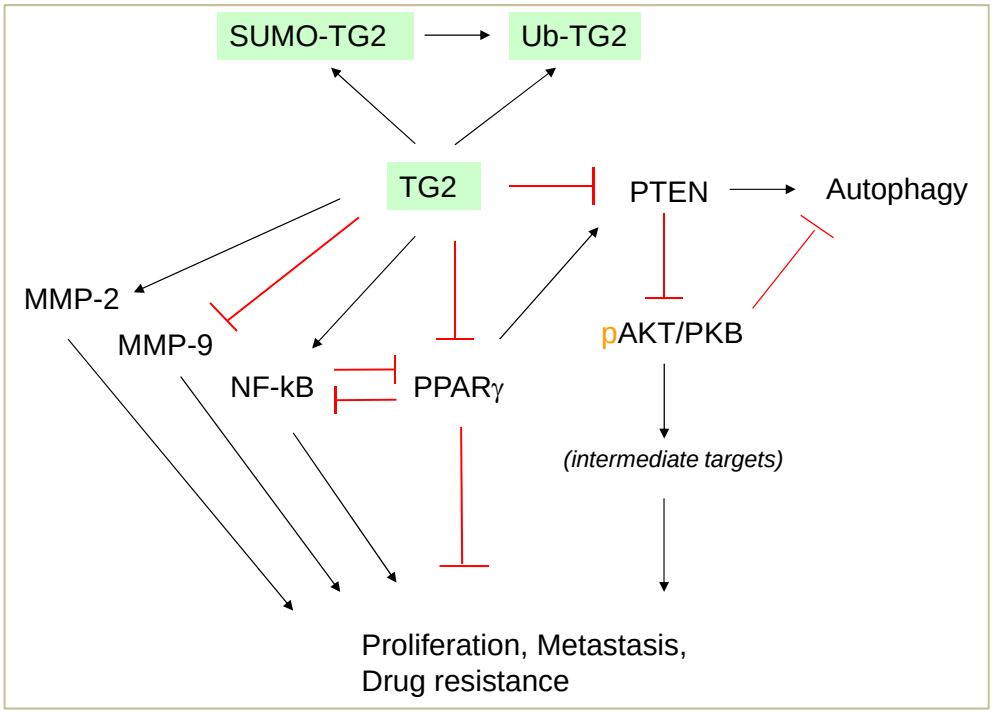

Figure 1.9 – Schematic drawing of the interactions between TG2 and key proteins involved in proliferation, survival, metastasis, drug resistance.

The aim of my project is to study the role of intracellular, tumour-expressed TG2 in an *in vitro* model of cancer progression, where levels of TG2 are inversely correlated to malignancy, i.e. where high TG2 levels are found in the primary tumour, and low TG2 levels found in the metastases.

I therefore plan to test the following hypotheses:

i) that TG2 presence may be inversely correlated with EMT, expression of MMPs, and cell invasion *in vitro*, and inversely correlated with tumour progression *ex vivo*;

ii) that TG2 presence may be inversely correlated with activation of autophagy;

iii) that TG2 expression may be correlated with surface expression of HLA-I, thus affecting tumour immune evasion;

iv) that the intracellular accumulation of TG2 may not just be due to increased genic expression and protein translation, but also to an increased SUMOylation or decreased Ubiquitylation;

v) that stability of TG2 transcripts and their translation may be regulated by miRNA;

vi) that the EGFR and TGF-β pathway, frequently altered in various cancers, may affect TG2 expression and hence all TG2-driven intracellular alterations.

In order to carry out these investigations, I will first select an appropriate model by characterising TG2 protein in a panel of solid and haematological cancer cell lines; next, I will carry out extensive characterisation of the selected model by assessing levels of TG2 mRNA, TG2 cross-linking activity, and the extent of post-translational modifications that can affect molecular half-life (i.e. SUMOylation and Ubiquitylation). Following this initial characterisation, I will optimise methods for modulating TG2 in the selected model using DNA transfection, siRNA- and miRNA-mediated RNAi. When such optimisations are completed, I plan to use the optimised protocols to assess how TG2 exerts its tumour-suppressive function, i.e. by targeting which biological functions essential for tumour growth and metastasis. Along with *in vitro* studies, antigenic localization of TG2 on tissue sections obtained from cancer patients and healthy controls will be carried out in collaboration with pathologists.

2. Materials and Methods

2.1 Cell lines

The following human-derived cell lines were used to carry out the experiments reported within this dissertation

Cell line	Type
IB3-1	Cystic Fibrosis (ΔF508) bronchial epithelial
C38	Isogenic line derived from IB3-1 by stable transfection of w.t. CFTR
SKMEL31	Dermal malignant melanoma
SKMEL28	Dermal malignant melanoma
Raji	Burkitt's lymphoma
Ramos Rx3	Burkitt's lymphoblastoid lymphoma, lacking BCR
Ramos	Burkitt's lymphoblastoid lymphoma
Davoli	B cell lymphoma
DOHH2	B cell lymphoma
SW480	Dukes type B colorectal adenocarcinoma
SW620	Dukes type C lymph node metastasis of colorectal adenocarcinoma
HCT116	Colorectal carcinoma
Colo205	Dukes type D ascite metastasis of colorectal adenocarcinoma
MES-SA/Dx5	Multidrug resistant uterine sarcoma
MES-SA	Uterine sarcoma
G361	Malignant melanoma
A549	Epithelial lung adenocarcinoma
Colo-205	Dukes type D ascite metastasis of colorectal adenocarcinoma
MCC-287	Merkel Cell carcinoma
Granta-519	Leukemic transformation of mantle cell B-lymphoma, stage IV
H441	Epithelial lung adenocarcinoma
HBL1	Diffuse large B-cell lymphoma
MM200	Primary melanoma
A20 super hi	B-cell lymphoma
SU	B-cell lymphoma
RL	Diffuse large B-cell lymphoma
MCF7	Breast adenocarcinoma
MCF7/DOX	Multidrug resistant breast adenocarcinoma
SNU475	Hepatocellular carcinoma
SKHEP1	Endothelial line of liver adenocarcinoma
PLC/PRF/5 (PLC)	Hepatoma
HUH7	Hepatocellular carcinoma

Table 2.1 – List of cell lines used

Only SW480, SW620, Colo205, HCT116, HUH7, PLC, SNU475, SKHEP-1 cell lines were cultured for in vitro experiments. All other cell lines were received in the form of cryopreserved total cell lysates or total RNA as a gift from internal collaborators. The above

mentioned eight CRC and HCC cell lines were grown in Dulbecco's modified Eagle medium (DMEM) containing 4.5 g/L Glucose (Lonza) and supplemented with: 10% Foetal calf serum, 1% L-Glutamine, 1% Non-Essential Amino Acid, 1% Sodium Pyruvate

Unless otherwise stated, cells were cultured at 37°C 5% CO_2 in flasks or multiwell plates (Greiner Bio-One) depending on the requirements of the experiment. During routine culture, confluent cells were split using standard methods. In brief, medium was removed by aspiration and cells washed 1X with Phosphate buffered saline (PBS). Next, PBS was removed, Trypsin-Versene (Lonza) was added to the monolayer, and cells were returned to the incubator for 20 min. Trypsinised cells were then pipetted into a Falcon tube (BD) and centrifuged at 400g for 4 min. After centrifugation, supernatant was discarded and the cell pellet resuspended in the desired amount of fresh medium, for subcultivation or experiment set up purposes.

All work was carried out in sterile conditions under a biological hood, using sterile solutions.

2.2 Cell counting

Cell counting was performed using the Trypan blue exclusion assay, unless otherwise stated. To perform the assay, 5 μL of resuspened cell pellet was added to 45 μL Trypan Blue 0.4% solution (Sigma. UK), and mixed well. Next, a glass coverslip was placed over the grid of a Neubauer's chamber (Figure 2.1), and 25 μL of the Trypan blue cell mixture was pipetted along one edge of the coverslip, allowing it to spread out between the coverslip and the chamber by capillarity. Cells with white appearance (i.e. live cells, able to extrude Trypan blue dye) were counted in each of the 4 large corner squares (A-D), and the average number per square obtained. This number was then multiplied by the dilution factor used (10), the volume of the chamber (0.1 mm^3 or 0.1 μL), and the correction factor 10,000 in order to obtain the amount of cells/mL.

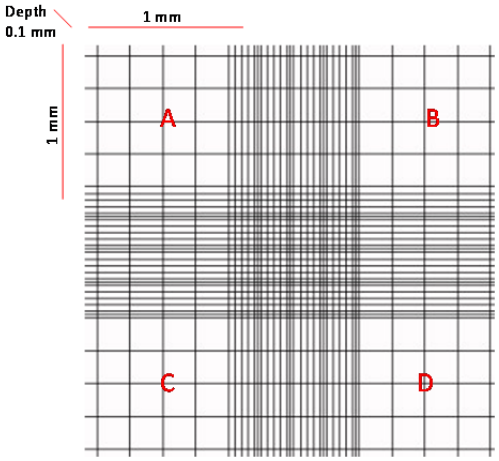

Figure 2.1 - Schematic representation of a Neubauer's chamber

2.3 Invasion assay

Matrigel (BD Biosciences, Basement membrane matrix) was thawed on ice before use, accounting 24 µL per well. When thawed, the Matrigel was diluted 1:3 in the appropriate serum-free cold medium. Transwell inserts (8.0 µm pore size, Corning) were placed in the wells of a 24-well plate, then 70 µL of the diluted Matrigel solution carefully pipetted into each insert. The plate was then incubated at 37°C 5% CO_2 for 2 h to allow the Matrigel to polymerise. At the end of this incubation, each insert was briefly lifted in order to fill the lower chamber with 650 µL complete growth medium, and then put back in place.

Cells were harvested and counted as described in sections 2.1 and 2.2. Next, 200 µL of cell suspension (at 2.5 x 10^5 live cells/mL) was pipetted dropwise into each well over the polymerised Matrigel layer (upper chamber). Plates were then placed in the incubator for 24h to allow migration of cells through the inserts, chemically attracted by the serum-containing medium in the lower chamber (see Figure 2.2).

At the end of the assay, the number of cells that migrated into the lower chamber was counted using a CASY® TTC counter (Roche Innovatis AG) following the manufacturer's instructions. In brief, inserts were removed and all 650 µL of medium from the lower chamber of each well was aspirated and added to tubes containing 9 mL CASY®ton buffer, in

order to recover migrated cells that had not attached to the bottom of the well. To recover adherent cells, 350 µL Trypsin was added to the lower chamber of each well, and the plate returned to the incubator for 20 min. Trypsin was then aspirated and added to the tubes already containing medium and CASY®ton buffer, to reach a total volume of 10 mL. Tubes were read at the CASY® TTC counter, and an average of three reading per sample was automatically taken by the machine.

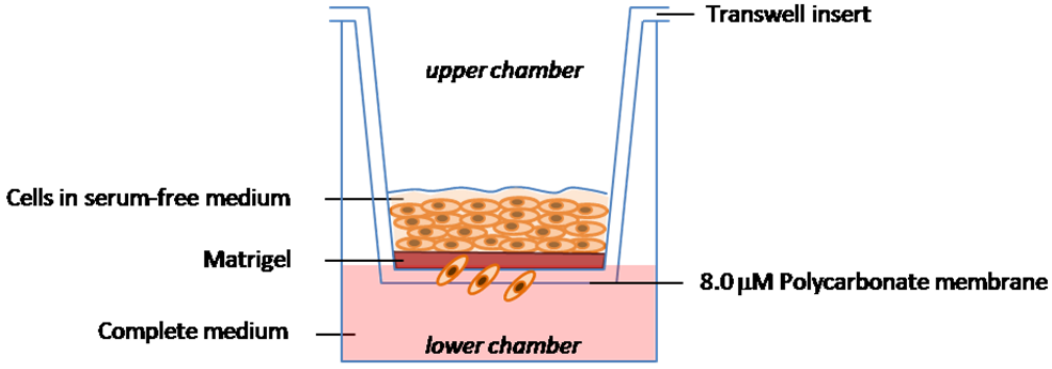

Figure 2.2 - Schematic setup of an invasion assay using the Transwell system

2.4 Indirect immunofluorescent staining

Before seeding the cells, a round coverslip (VWR) was placed at the bottom of each well of a 24-well plate and 200 µL Poly-L-Lysine (Sigma, UK) applied on its surface for 20 min. At the end, each coverslip was washed 3X with PBS. Cells were seeded at a suitable concentration in order to have 80% confluence on the day of the assay. Before starting the IF protocol, medium was removed and cells washed 3X with PBS. Next, cells were fixed with 4% Paraformaldehyde (in PBS) for 5 min and permeabilised with 0.1% Triton X-100 (in PBS) for 15 min. Subsequently, cells were incubated with primary antibody (diluted in 1% BSA/PBS) for 90 min at room temperature (R.T.). Afterwards, cells were incubated with a fluorophore-conjugated secondary antibody (diluted in 1% BSA/PBS) for 1h at R.T. in the dark. Finally, to counterstain nuclei, cells were incubated with 1 µg/mL DAPI for 10 min at

R.T. in the dark. Three washes were performed between each of these steps, except after the permeabilisation and the secondary antibody step when five washes were preferred. By means of sterile forceps, coverslips were retrieved from the bottom of each well and placed cell-side down onto microscope slides where a drop of ProLong Gold anti-fade mounting medium (Molecular Probes, UK) had been placed. Slides were visualised at a Zeiss Axioskop2 MOT equipped for epifluorescence; images were acquired through Zeiss Axiocam and processed by Zeiss KS 400 3.0 software (Zeiss). Three-dimension (3D) images were taken by using the Leica TCS SP5 confocal microscope and processed by using Leica LAS AF software (Leica).

Where needed, quantitation of fluorescence (expressed in Gray values/Area) was performed by using Leica LAS AF software (Leica). Briefly, a suitably shaped area was drawn and pasted into at least four representative fields of each image. The mean Gray value for each image was determined, and statistical analysis of the means was performed by using SPSS software (SPSS Inc.). Data were then plotted by using Prism software (ver.4, GraphPad).

2.5 *In situ* proximity ligation assay (PLA)

PLA is a technology that allows detection of protein homodimers and heterodimers, and protein modifications (such as phosphorylation). Duolink II (Olink Bioscience) is a kit based on the detection of PLA events by immunofluorescence[175].

Cells were seeded as described in section 2.4 and staining was performed as suggested by the manufacturer, with all steps being carried out in an incubator at 37°C and 5% CO_2. Briefly, after the fixation and permeabilisation steps (carried out as of section 2.4), cells were treated with the provided blocking solution for 30 min, before being incubated for 90 min with two primary antibodies (raised in different host) against the two proteins or features of interest. The primary antibodies were used at concentrations stated in Appendix B (page B). Next, cells were incubated with the two (provided) unlabelled host-specific

secondary antibodies (PLA probes), which are conjugated to reciprocally complementary short oligonucleotides, hence if the two features of interest are in close proximity, annealing of the complementary oligonucleotides and formation of a circular DNA molecule occurs. Subsequently, the provided DNA polymerase was added for 1 h 40 min (which performs rolling-circle amplification of the circular DNA molecule). Finally, the provided fluorescent detection probe was added for 30 min which specifically binds to the newly synthesised DNA. Slides were then mounted with the provided DAPI-containing mounting medium, and images acquired using a Leica TCS SP5 confocal microscope. Quantitation of the PLA events was performed by counting (by eye) the number of positive signals on the acquired images.

2.6 TG2 activity assay

In order to obtain a visual representation of intracellular TG2 activity, an IF-based assay was carried out. Cells were seeded in 24-well plates at a suitable concentration in order to have 80% confluence on the day of the assay (as explained in detail in section 2.4). Before starting the assay, medium was removed, and cells washed 3X with PBS. Cells in each well were then pre-treated with 990 μL reaction buffer (965 μL of 100 mM Tris-HCL pH 7.4 + 25 μL of 200 mM $CaCl_2$) for 15 min at R.T. At the end of this incubation, the reaction buffer was removed, and the complete reaction mix was pipetted in each well which was made up of 990 μL of reaction buffer (as above) + 10 μL of 10 mM biotin-MonodansylCadaverine (bio-MDC, Cambridge Bioscience, UK) TG2 substrate. The Ca^{++}-dependent cross-linking activity catalysed by TG2 was allowed to take place by returning cells to the incubator for 1 h. The reaction was stopped by pipetting 50 μL of 0.5 M EDTA (a Ca^{++} chelator) into each well and incubating the plate at R.T. for 5 min. Afterwards, fixation and permeabilisation steps were carried out as of section 2.4. Staining was performed using a directly conjugated antibody Streptavidin-FITC IgG (BD Pharmingen), and incubating the plate for 1 h at R.T. in the dark. Nuclear counterstain was performed with 1 μg/mL DAPI for

10 min at R.T. in the dark. Slides were visualised by epifluorescence microscopy, and images taken and analysed as described in section 2.4 .

2.7 Production of cell lysates and protein quantitation

For Western blot experiments, cells were grown in 6-well plates, 2 mL medium per well. At approximately 90% confluence (assessed by eye under light microscope), medium was removed by aspiration. Cells were lysed by adding, to each well, 150 μL per well of a solution made of 1% SDS in distilled water + 1X protease inhibitor cocktail (Merck, UK). Lysis was encouraged by repeated suction-and-expulsion with the micropipette. The resulting viscous solution was quickly transferred into a 1.5 mL Eppendorf tube, whereupon it was either kept on ice for immediate quantification or stored at -20°C for later quantification. Lysates were quantified by microBCA Assay Kit (Pierce, UK) against a BSA standard series (0.5-200 μg/mL), following the manufacturer's instructions. Briefly, in a 96-well microplate, 100 μL per well of each standard and pre-diluted sample (1:100 in distilled water) were added to 100 μL per well of the detection reagent provided by the kit, in duplicate wells. The microplate was then incubated at 37°C 5% CO_2 for 90 min, during which time coloration developed proportionally to the protein content in each well. At the end of the incubation period, absorbance in each well was read at 570 nm using a Bio-Rad 680 microplate reader (Bio-Rad Laboratories, Inc.). Averaged background OD value was subtracted from all measurements; then, a best-fit standard curve was built and unknown values interpolated using Prism software (ver.4, GraphPad). Final protein concentration was then determined by adjusting the interpolated values for the dilution factor.

2.8 SDS-PAGE

The desired amount of total protein lysate was mixed with 4X reducing sample buffer (40% Glycerol, 240 mM Tris-HCl pH 6.8, 8% SDS, 0.04% bromophenol blue, 5% beta-mercaptoethanol) up to the desired final volume to load in the wells of the Polyacrylamide

gel. The lysates mixtures were boiled for 5 mins in a thermal block at 90°C, cooled to R.T. for 5 min, then centrifuged for 2 min at 13,000 rpm.

Depending upon the molecular weights of species to separate, an 8% or 10% Polyacrylamide loading gel was prepared (according to Sambrook & Russell's "Molecular cloning manual") from a solution of 30% Acrylamide/Bis-acrylamide (Sigma, UK). The loading gel solution was poured into a 1mm thick disposable cassette (Invitrogen UK, #NC2010), overlaid by 200 μL of Isopropanol, and left to polymerise for 45 min. When the loading gel had set, the Isopropanol overlay was poured off and the excess absorbed into blotting paper. Next, a 4% Polyacrylamide stacking gel was prepared (according to Sambrook & Russell's "Molecular cloning manual") from the same Acrylamide/Bis-acrylamide solution used for the loading gel. The stacking gel solution was poured on top of the loading gel, whereupon a comb was immediately inserted. The stacking gel was left to polymerise for 30 min. When the Polyacrylamide gel was set, the comb was carefully removed and the cassette placed into an electrophoresis chamber (XCell SureLock, Invitrogen UK), which was later filled with SDS running buffer (25 nM Tris, 250 mM Glycine pH 8.3, 0.1% w/v SDS). Samples were the, loaded in the stacking gel and run for 90 min at 120V.

2.9 Western blotting

At the end of the run, the gel was freed from its cassette and briefly immersed in Methanol transfer buffer (24 mM Tris base, 192 mM Glycine, 20% Methanol). Blotting was set up as shown in Figure 2.3 below. Proteins were blotted onto Hybond C Extra nitrocellulose membrane (GE Healthcare, UK). Transfer was carried out in a blotting chamber (XCell II blot module, Invitrogen UK) for 90 min at 400 mA, with the apparatus surrounded by ice.

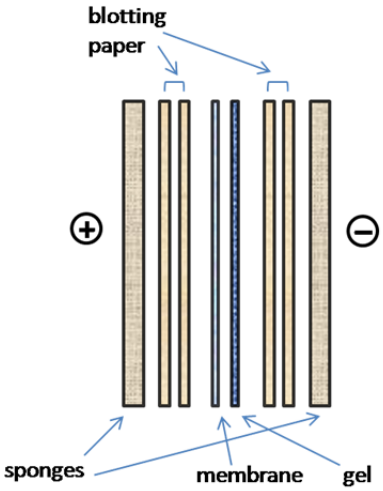

Figure 2.3 - Schematic diagram of a blotting "sandwich"

At the end of the blotting time, the membrane was immersed for at least 30 min at 4°C in a blocking solution of 5% non-fat milk/0.1% TBS-Tween (TBS-T). The membrane was then incubated overnight at 4°C with primary antibody diluted in 5% non-fat dry milk/0.1% TBS-T on a rotating plate. Afterwards, the membrane was washed 3X with 0.1% TBS-T and incubated with horseradish peroxidase (HRP)-conjugated secondary antibody diluted in 5% non-fat dry milk/0.1% TBS-T, for 3 h at 4°C on a rotating plate. At the end of the incubation, the membrane was washed 3X, and specific binding was revealed with an enhanced chemiluminescence (ECL)-based system (Super Signal West Dura Kit, Thermo Scientific, UK). Briefly, in the presence of hydrogen peroxide, horseradish peroxidise is able to oxidise luminol to 3-aminophtalate, resulting in a concurrent weak emission of light; in the presence of an enhancer, such emission can be amplified up to 1000-fold.

Images were acquired either using a Bio-Rad Fluor-S MAX Multimager (Bio-Rad) and the associated Quantity One Analysis software (Bio-Rad), or using a Xograph X4 photographic film processor (Xograph Healthcare Ltd).

2.10 RNA extraction and Reverse-Transcription Polymerase Chain Reaction (RT-PCR)

Total RNA was extracted from mammalian cells using TRI reagent (Ambion, UK), following the manufacturer's protocol. Total RNA concentration and purity was determined using a NanoDrop 2000 spectrophotometer (Thermo Scientific). In order to obtain PolyA-enriched cDNA from total RNA, a mix for each sample was prepared as follows: 4 μL of MMLV-RT 5X buffer (Promega, UK), 1 μL of 0.5 mg/mL OligodT primer (Promega, UK), 2.5 μL of 10 mM PCR Nucleotide Mix, 40 U of RNAsin enzyme (Promega, UK), 200 U of MMLV-RT enzyme (Promega, UK), 5 μL RNA (up to total 1.5 μg), and enough Diethylpyrocarbonate-treated H_2O (DEPC-H_2O, Ambion, UK) to reach a final volume of 20 μL. This mix was prepared in a 1.5 mL Eppendorf tube, which was then sealed with Parafilm and incubated in a water bath at 37°C for 90mins. At the end of the reaction, enzymes were inactivated by placing the tube in thermal block for 4 min at 72°C. Concentration and purity of the resulting cDNA was determined using the NanoDrop 2000.

2.11 PCR and Quantitative PCR in real-time (qPCR)

All primers and probe sequences were designed by using GeneTool Lite software (ver 1.0, BioTool Inc.), and target-specificity assessed by using BLAST query service (www.pubmed.gov). A list of all sequences used throughout this study is provided in Appendix C (page C). PCR reactions were carried out in 0.2 mL PCR tubes (Eppendof). For each reaction, the following reagents were used: 10 μL 5X GoTaq Buffer (Promega, UK), 4 μL of 25 mM $MgCl_2$, 1 μL of 10 mM PCR Nucleotide Mix (Promega, UK), 1μL of 25 μM forward primer, 1 μL of 25 μM reverse primer, 1 U of GoTaq Flexi DNA Polymerase (Promega, UK), 5 μL DNA (up to total 1 μg), and enough DEPC-H_2O to reach a total volume of 50 μL. Each new set of primers was initially used for a test amplification run, according to this standard amplification protocol:

Initial denaturation step	3:00 min at 95°C	
Denaturation	0:45 min at 95°C	x 34 cycles
Annealing	0:45 min at 60°C	
Extension	0:45 min at 72°C	
Final extension step	5:00 min at 72°C	
End	hold at 4°C	

At the end of the amplification reaction, 5 μL of the PCR product were run on a 1.2% agarose gel containing 0.2 μg/mL Ethidium Bromide (Sigma, UK) for 30 min at 50V. At the end of the run, the DNA bands were visualised by illuminating the gel with a UV light, and images acquired by UVP VisionWork LS software. (UVP Ltd). If the results were satisfactory no further optimisations of the amplification protocol were carried out.

qPCR reactions were performed using the probe hydrolysis method, in 96-well plates (MicroAmp plates, Applied Biosystems, UK). For each reaction, the following reagents were used: 12.5 μL 2X qPCR Master mix (Eurogentec UK), 0.4 μL 25 mM forward primer, 0.4 μL 25 mM reverse primer, 0.025 μL probe, 5 μL DNA (up to total 0.2 μg), 7.275 μL DEPC-H_2O, for a total volume of 25 μL. Each reaction was prepared in duplicate wells, to account for technical and biological variability. The plate was sealed with an adhesive cover (MicroAmp adhesive films, Applied Biosystems, UK) and spun at 1300 rpm for 10 sec at 4°C. Finally, the plate was run on a 7500 Real-Time PCR system (Applied Biosystems, UK).

2.12 DNA plasmid transfection

Lipofectamine LTX with PLUS reagent (Invitrogen UK, # 15338) was used to transfect plasmid constructs into adherent mammalian cells. Transfection conditions were first optimised by creating a matrix of reagent:DNA conditions, in order to identify the condition that achieved the highest transfection efficiency and the lowest toxicity, to be used in functional assays. Cells were usually seeded in 24-well plate in a total volume of 500 μL of their complete growth medium, at a density that allowed 70% confluence to be reached the

following day. Transfection mix was prepared in one well of a round-bottomed 96-well plate, and steps performed according to Invitrogen's protocol. Briefly, DNA was first diluted in a total of 100 μL of Opti-MEM I basal medium, then PLUS reagent was added, and the plate was vortexed for 2 sec and incubated for 5 min at R.T. Next, Lipofectamine LTX was added and the plate vortexed for 2 sec, then incubated for 30 min at R.T. Finally, mix was pipetted drop-wise onto the cells, which were subsequently returned to incubator for 48 h. After 48 h, cell lysates were collected (as of section 2.7) and Western blotting performed (as of section 2.8 and 2.9). Alternatively, RNA was extracted (as of section 2.10) and amplification of cDNA performed (as of section 2.11). For stable transfections of cell lines, cells were grown in antibiotics-enriched media according to the resistance genes present in the elective plasmid. Where GFP-tagged plasmids were transfected, cells were periodically monitored for their levels of fluorescence under the microscope, and if necessary the GFP+ population was enriched by sorting with a FACS Aria (BD) cell sorter.

2.13 siRNA-mediated RNAi

A set of three TG2-specific 25 bp RNA duplexes (siRNA) was purchased from Invitrogen, along with a high-GC control duplex (Invitrogen, UK). Transfection conditions were first optimised by creating a matrix of reagent:siRNA conditions, in order to identify the condition that achieved the highest mRNA knockdown and the lowest toxicity, later to be used in functional assays. Cells were usually seeded in 24-well plate in a total volume of 500 μL of their complete growth medium, at a density that allowed 40% confluence to be reached the following day. Transfection mix was prepared in one well of a round-bottomed 96-well plate, and steps performed according to Qiagen's protocol. The three TG2-specific siRNA were all together diluted in a total of 100 μL of Opti-MEM I basal medium (Gibco, UK). Immediately after, Hiperfect reagent (Qiagen, UK) was added to the mix, and the plate was vortexed for 3 sec and then incubated for 10 min at R.T. Next, the mix was added drop-wise to the cells which were immediately returned to the incubator for 48 h. After 48 h, cell

lysates were collected (as of section 2.7) and Western blotting performed (as of section 2.8 and 2.9) to assess the levels of protein knock-down achieved. Alternatively, RNA was extracted (as of section 2.10) and amplification of cDNA performed (as of section 2.11) to assess the levels of mRNA knock-down achieved.

2.14 miRNA-mediated RNAi

PLASMID METHOD. Pre-MiR-19a expression plasmid (Genecoepia, Rockville MD) and a corresponding scrambled plasmid control (SCC) were transfected into SW480 cells using Lipofectamine LTX (Life Technologies UK) according to the manufacturer's instructions. Stable transfection was achieved by selecting resistant clones (named SW480/miR19A, and SW480/SCC) using puromycin (2μg/mL), and cell sorting by FACS for the IRES-driven GFP reporter, and after expansion used only for a few passages (<10). 24h prior to functional experiments, cells were also transfected with a miRNA-19a-3p mimic or corresponding scramble control (Qiagen) using Hyperfect (Qiagen, UK) according to manufacturer's instructions.

Anti-miR-19a containing GFP plasmid (MiRZip, System Biosciences) was transiently transfected into SW620 cells following manufacturer's instructions for a minimum of 24h to a maximum of 72h, including any functional assay performed after the initial transfection.

OLIGO METHOD. A set of oligos precursors and inhibitors of miR-19a and miR-19b was purchased along with a scramble miRNA negative control (all reagents from Dharmacon, UK). Transfection was performed by using a protocol of "fast forward transfection" which consists in dispensing the transfection mix immediately after seeding the cells. On the day of transfection, cells were counted (as described in section 2.2) immediately before preparing the transfection mix, and kept in suspension in tubes until mix was ready. Transfection mix was prepared in one well of a round-bottomed 96-well plate, and steps performed according to each reagent's protocol (more details on section 4.2). After the formation of miRNA:reagent complexes in Opti-MEM I, mix was dispensed on the cells that

had just been seeded in 24-well plate in a total volume of 500 μL of their complete growth medium, and transfection mix added immediately on top. Cells were subsequently placed into incubator for 48 h. After 48 h, RNA was extracted (as of section 2.10) and quantitative PCR of cDNA was performed (as of section 2.11) to assess the levels of mRNA overexpression or downregulation of the target genes achieved.

2.15 Immunolabelling and flow cytometry

For flow cytometry experiments, between 1 x 10^5 and 1 x 10^6 cells were harvested in Trypsin (as described in section 2.1), transferred to polystyrene tubes (BD), and centrifuged at 400g for 4 min at 4°C. After removal of Trypsin, cells were washed once in ice-cold PBS and centrifuged again. Next, cells were resuspended in 1 mL of cold wash solution (1X PBS, 1% FCS, 0.05% Sodium azide), filtered through a 70 μm cell strainer (BD), centrifuged at 1300 rpm for 4 min at 4°C, and supernatant discarded.

For detection of surface antigens, immunolabelling was performed by diluting each antibody (at a concentration suggested by the manufacturer) in 200 μL of cells resuspended in wash solution, and incubated for 20 min on ice in the dark. For intracellular antigens, prior to immunolabelling, in-tube cell fixation and permeabilisation steps were performed by using eBiosciences reagents (Fix-Perm concentrate, and Perm buffer) following the manufacturer's protocol. At the end of both immunolabelling protocols, cells were centrifuged and resuspended in 400 μL wash solution, prior to being run on a Canto flow cytometer (BD). For each sample, 50,000-100,000 events were acquired using FACSDiva software (BD, ver 6.1.2). Analysis was performed by first creating a Forward scatter (FSC) vs Side scatter (SSC) plot which represented the physical characteristics of the cells. Debris and dead cells in the bottom left corner of such plot were gated out, and another gate created around the main population of live cells. Negative control and secondary only control samples, visualised on a FITC vs SSC histogram plots, were used to identify autofluorescent cells and non-specific staining.

2.16 Immunohistochemical staining from CRC tissue sections.

Immunohistochemical staining was performed on formalin-fixed specimens from patients undergoing resections for CRC at the University Hospital Southampton as part of an NIHR portfolio study (UK CRN ID6067). Tumour specimens were snap-frozen in liquid nitrogen within 10 minutes of surgery and stored in a designated UK Human Tissue Act-approved tumour bank. Samples were selected from three clinically distinct groups; a) colonic tissue from early stage disease (stage I/II), b) colonic tissue from late stage disease (lymph node involvement, stage III/IV), c) liver tissue from CRC metastatic disease (stage IV). The whole staining procedure was carried out by technicians at the Pathology department of Southampton University Hospital Trust, following an internal Standard Operating Procedure. Specifically, for this analysis, antigen retrieval was performed by microwave citrate method, and staining using the antibody clone CUB7402 (AbCam, 1:800). Semi-quantitative scoring of TG2 levels on whole tissue sections was performed independently and in a blinded manner by a specialist pathologist and a further investigator. A modified 3-point scoring method was used; 1) low/negative staining <10% positivity, 2) focal/patchy staining 10-50% positivity, 3) strong diffuse staining >50% positive. All patients provided informed consent in accordance with the Helsinki protocol and the study was approved by the regional research ethics committee.

2.17 Measuring of intracellular Calcium (Ca^{++})

Intracellular Ca++ concentration was measured by the incorporation of a fluorescent calcium-sensitive probe, detected by a fluorescence plate reader. Briefly, 24 hours before the experiment 100,000 cells were seeded in duplicate on a flat-bottomed 96-well plate in their complete growth medium. On the experiment day, cells were permeabilised for 45 min by replacing growth medium with 100 μL of 0.1% Digitonin (Dako) in 1X Locke's

buffer. At the end of the permeabilisation, 1 μL of 0.5M Fluo4-AM (Molecular Probes) was added to the same wells and the plate was incubated for 40 min in the dark. During this period the chemical indicator Fluo-4AM is internalised, de-esterified, and upon binding to free Ca++ its emission spectra will shift to 488nm. At the end of the assay, the plate was read using the Varioskan fluorometric reader (Thermo scientific), and results interpolated by comparison to a standard curve of Ca++ created by adding CaCl2 in concentrations 0.1-10 μM to wells containing 1 μL of 0.5M Fluo4-AM in 1X Locke's buffer.

2.18 Endoglycosidase H (EndoH) assay

The Endoglycosidase H removes glycans from proteins within the E.R. EndoH-sensitive proteins will be unable to proceed to the Golgi apparatus and then be expressed on the cell membrane. Endo-H resistant proteins, instead, will carry on their maturation and will reach the cell membrane. The purpose of this assay is to test the existence of blocks during the maturation of a given protein that causes its cell surface expression to be low. Reactions were setup as follows: 40 μg cell lysate, 2 μL 10X G5 buffer (50mN Sodium Citrate at pH 5.5, NEB), 2 μL EndoHf (NEB) enzyme, water to 20 μL. Reactions were incubated o.n. at R.T. afterwards 5X denaturing Laemli buffer was added to each sample and Western blot analysis performed as described in sections 2.8 and 2.9.

2.19 Statistics and plots

Statistical analyses were performed by using SPSS software (ver.17, SPSS Inc.).

Comparisons were carried out either by the use of Student's *t*-test or by ANOVA followed by Bonferroni post-hoc correction, according to the number of categories to be compared. Significance levels were indicated by the following symbols: * (one asterisk) for

$p \leq 0.05$, ** (two asterisks) for $p \leq 0.005$, *** (three asterisks) for $p \leq 0.001$, **** (four asterisks) for $p \leq 0.0001$.

Data were plotted by using either Prism software (ver.4, GraphPad) or Microsoft Office Excel (Microsoft).

3. Characterisation of TG2 in colorectal carcinoma

3.1 Introduction

In mammals, TG2 is a ubiquitously expressed enzyme capable of different functions both intra- and extracellularly. Intracellular functions include those occurring in the cytoplasm (cross-linking activity), in the mitochondria (PDI), in the nucleus (kinase), and at the inner plasma membrane (Gα subunit of Gh transducing protein). Cell surface-associated and extracellular TG2 can act as bridging molecules that stabilises interactions between Fibronectin and Integrin, or mediate cross-linking of ECM proteins. The cross-linking activity is the most well studied and the most relevant function of TG2 in a range of physiological and pathologic cellular conditions. In both healthy and neoplastic cells, cross-linking activity is mainly useful for i) inactivating cellular or extracellular proteins and target them for degradation, ii) forming apoptotic bodies, and iii) creating stabilising isopeptide bonds between two proteins or macromolecules[93]. In the context of neoplastic cells, TG2 can have opposite functions, namely favour or interfere with tumour progression. The incidence of either of these functions varies according to the type of tumour, the histological localisation of TG2 (tumoral or stromal), and its function at the different subcellular localisations (inner plasma membrane, cell surface, cytoplasm, nucleus, mitochondria).

In cancer, TG2 is able to function as either a promoter or an inhibitor of tumour progression[97]. However, whilst all studies on the pro-tumoral role of TG2 (reviewed in section 1.4.1.) have agreed that this role is exerted by intracellular TG2, studies of its anti-tumoral role (reviewed in section 1.4.2) have failed to reach such a consensus, with some studies concluding a role for intracellular TG2 and others a role for extracellular TG2. For example, in *in vivo* models of melanoma[176] and mammary adenocarcinoma[133], TG2 was found to act as a tumour inhibitor when it accumulated in the ECM of the tumour-surrounding stroma. Only one *in vivo* study, conducted in a model of hamster fibrosarcoma, found that high levels of intracellular TG2 caused delayed tumour onset in the recipient

hamster; however, the role of intracellular TG2 in this model was not investigated further[135]. An *in vitro* study, investigating four colon cancer cell lines (where each cell line represented an increasingly aggressive metastatic stage) showed that levels of TG2 cross-linking activity (measured on total cell lysates) were inversely correlated with the intrinsic metastatic potential of the cell lines analysed, but no further characterisation or mechanistic explanation was provided[95].

The contrasting role of intracellular TG2 in tumour progression across the models studied, is interesting because it suggests that pharmacological treatments aimed at altering TG2 levels may be suitable for certain types of tumours, but not others. Hence, within a given tumour, it is essential to ascertain how the pattern, level of expression, and activity of TG2 relate to tumoral progression and formation of metastasis.

The aim of this chapter is to screen a series of solid and haematological tumour cell lines for levels of TG2, and to identify an interesting model for further characterisation and use in subsequent chapters. Characterisation carried out in this chapter include measurement of the abundance of TG2 protein, mRNA, cross-linking activity, intracellular vs. cell surface expression, and post translational modifications mediated by SUMO and Ubiquitin (affecting protein turnover). Furthermore, TG2 expression will be measured in tissue sections from five CRC patients.

3.2 Materials and methods

Cell lysates were prepared as in section 2.7. SDS-PAGE and Western blot were performed as in sections 2.8 and 2.9. Concentrations of antibodies used for Western blots are summarised in Appendix B (page B).

RNA extraction and cDNA synthesis were performed as in section 2.10. PCR for TG2 (697 bp) and Actin (550 bp) was performed as in section 2.11, using the primer pairs listed in Appendix C (page C).

Flow cytometry analysis for intracellular and surface TG2 was performed as in section 2.15. Primary anti-TG2 antibody clone CUB7402 (Abcam) was used for both intracellular and surface. A secondary FITC-conjugated goat anti-mouse IgG antibody (Sigma) was used following staining with the TG2-specific primary antibodies. Concentration of each of the above mentioned antibodies is summarised in Appendix B (page B). Flow cytometry was performed using a FACS Canto cytometer (BD), and data collected and analysed using FACS Diva software (BD).

TG2 activity assay was carried out in SW480 and SW620 cells as described in section 2.6. Cells were seeded on coverslips pre-coated with Poly-L-Lysine, which were placed at the bottom of wells in a 24-well plate. Cells were seeded in a total volume of 500 μL/well of complete DMEM, SW480 at 6.0 x 10^5 cells/mL, SW620 at 8.0 x 10^5 cells/mL. The activity assay was conducted the day after seeding. Revelation of the incorporation of the TG2 substrate bio-MDC was visualised by immunofluorescence as described in section 2.6.

In situ PLA assay was carried out in SW480 and SW620 cells using the Duolink II system (section 2.5), in order to detected SUMOylated and Ubiquitylated TG2. Cells were seeded on coverslips pre-coated with Poly-L-Lysine, which were placed at the bottom of wells in a 24-well plate. Cells were seeded in a total volume of 500 μL/well of complete DMEM, SW480 at 6.0 x 10^5 cells/mL, SW620 at 8.0 x 10^5 cells/mL. The PLA assay was conducted the day after seeding. For this assay, the primary rabbit anti-human TG2 clone H237 was used in combination with either the mouse anti-human SUMO-1 clone D11 or the mouse anti-human Ubiquitin clone P4D1 (concentration stated in Appendix B, page B). A mouse-specific and a rabbit-specific PLA probes (conjugated to reciprocally complementary oligonucleotides) were used to bind to the primary rabbit anti-human TG2 antibody and either the primary mouse anti-human SUMO-1 or the primary mouse anti-human Ubiquitin. If TG2 and SUMO-1 or TG2 and Ubiquitin were in close proximity, annealing of the complementary oligonucleotides and formation of a circular DNA molecule occurred, the

presence of which was revealed by the fluorescent detection system (section 2.5). The number of PLA events occurring in two fields per slide were counted.

Immunohistochemical analysis was performed as of section 2.16.

Gene expression of cytokines and MMPs was evaluated by qPCR (section 2.11).

3.3 Results

3.3.1 TG2 protein

Expression of TG2 protein by Western blot was assessed in two panels of tumour and non-tumour cell lines. Results in Figure 3.1 show high TG2 levels in IB3-1, SW480, G361, A549, MCC-287, H441, and MM200 cells (panel **a**), and in SW480, BxPC3, IB3-1 (panel, **b**); moderate levels of TG2 in C38, SKMEL31, SW620 (panel **a**), and in SW620, MCF7, MCF7/DOX (panel **b**); whereas TG2 expression was absent in all other cell lines. We also observed that the levels of the two TG2 variants (full-length at 77kDa, E10 splice variant at 55kDa) did not correlate to one another.

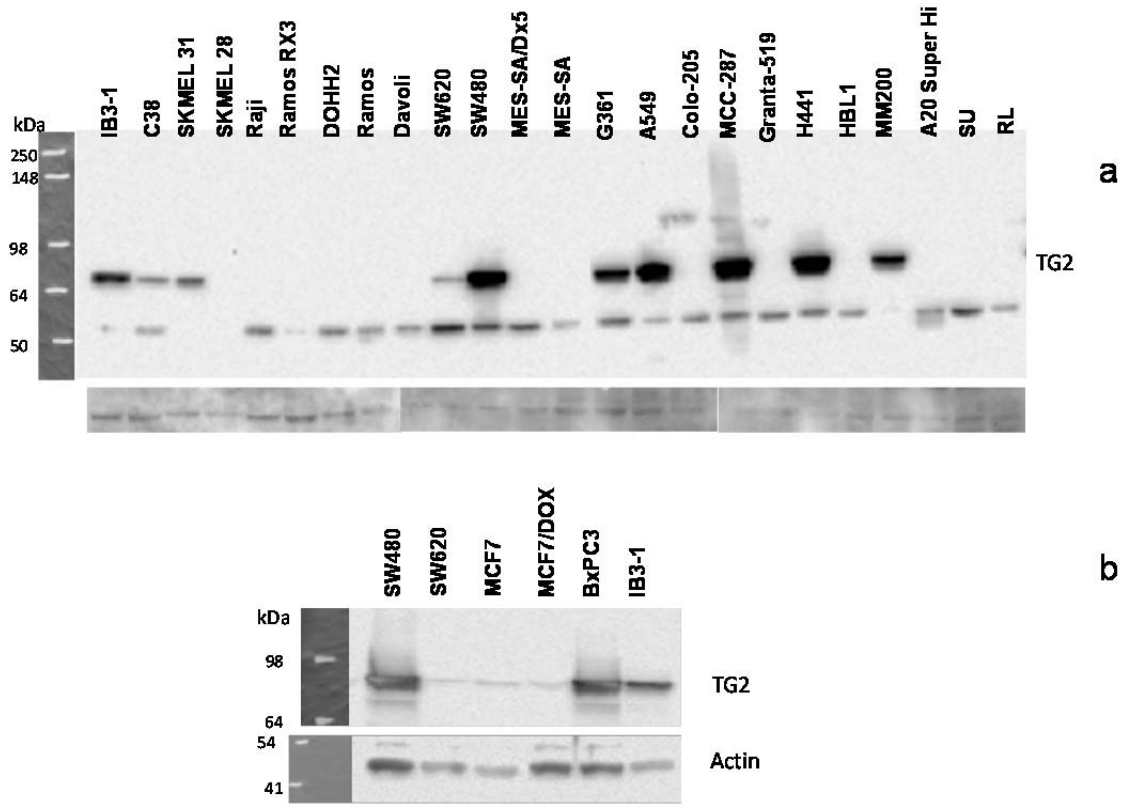

Figure 3.1 - Western blot analysis of TG2 protein (full length at 77kDa, smaller variant at 55kDa) in two panels of cell lines. 20 μg cell lysate loaded. For panel (a), Abcam anti-TG2 CUB7402 antibody was used; for panel (b) Santa Cruz anti-TG2 clone H237 antibody was used.

3.3.2 TG2 mRNA

To assess the expression of the full-length and the variant TG2 mRNA, standard or real-time PCR from cDNA was carried out on selected cell lines (SW480, SW620, MCF7, MCF7/DOX, BxPC3, A549, IB3-1). The results in Figure 3.2 panel **b** show that TG2 mRNA was abundant in A549 and SW480 cells (~80% of their β-Actin mRNA content); was less abundant in BxPC3, IB3-1 and SW620 (10-20% of their β-Actin mRNA content); and was least abundant in MCF7 and MCF7/DOX (<5% of their β-Actin mRNA content). The results in figure 3.2 panel **c** show that all TG2 transcript variants are expressed at higher levels in SW480 compared to SW620, however the TGM2_v2 variant shows a considerably lower expression compared to all others.

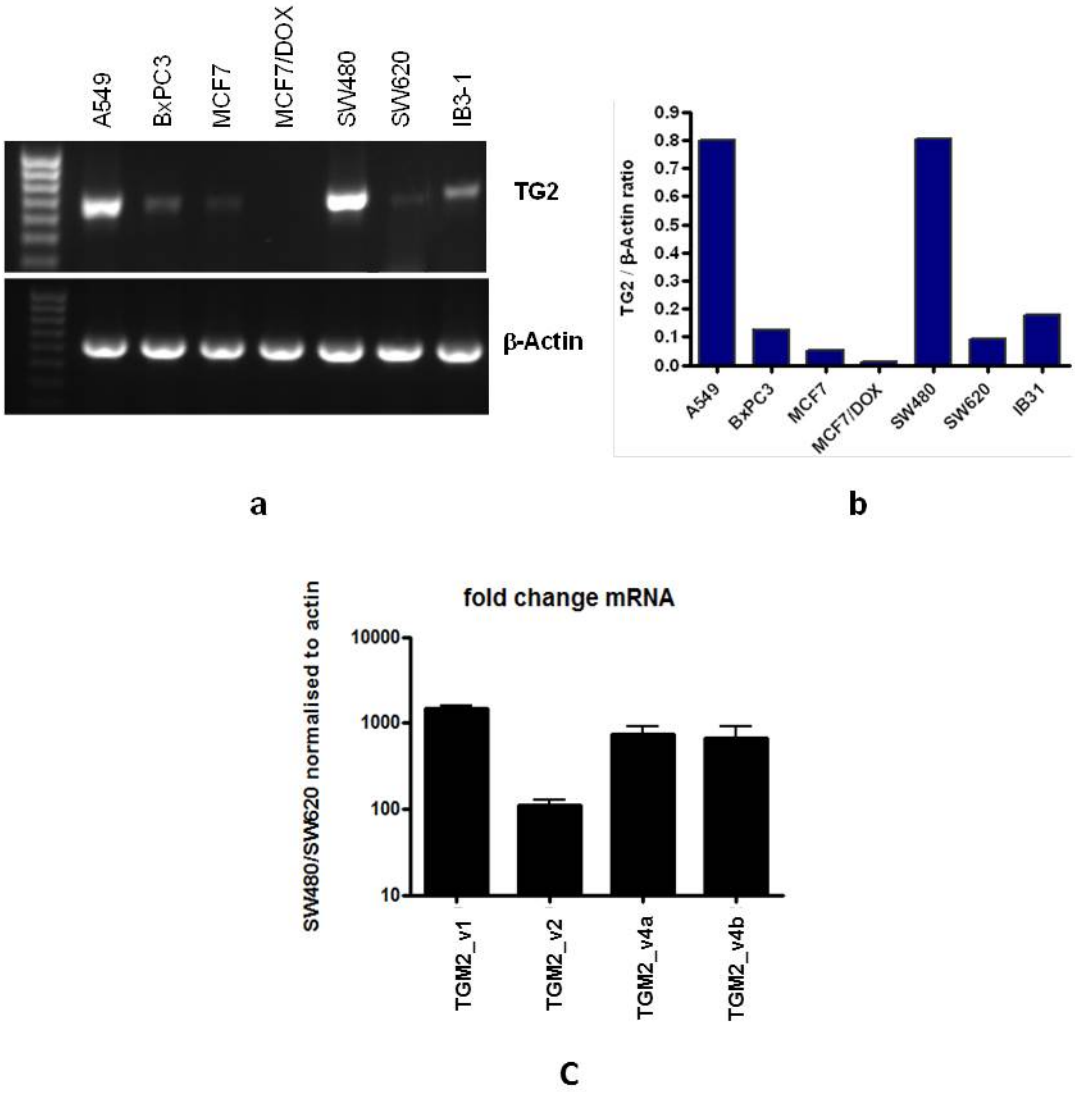

Figure 3.2 - PCR for full length TG2 and b-Actin (a), densitometric analysis of TG2 mRNA content normalised to % of b-Actin (b), real-time PCR of TG2 transcript variants in SW480 and SW620 cell lines (c)

3.3.3 Flow cytometry analysis of TG2

From the protein and cDNA analyses thus far performed, the most interesting pattern was shown by SW480 and SW620. SW480 is a primary colon adenocarcinoma cell line derived from a biopsy taken from a human patient; SW620 is the patient-matched metastatic liver adenocarcinoma cell line. SW480 expresses very high levels of TG2, compared to SW620, hence this represents an ideal model for further investigating the role of TG2 as a metastasis suppressor.

In order to assess whether Western blot and PCR results were mostly representative of intracellular or membrane-associated TG2, flow cytometry was performed in SW480 (high TG2-expressing) and SW620 (low TG2-expressing).

Figure 3.3 displays the results from intracellular TG2 staining. The FSC vs SSC plots (panels **a** and **d**) show that the SW480 population had an overall greater proportion of large cells, compared to SW620. In fact, whilst SW480 (panel **a**) show 37% large (pink) and 63% of small (blue) cells, SW620 (panel **d**) show 6% large (pink) cells and 94% small (blue) cells. Figure 3.3 panels **b** and **e** show unstained control samples for SW480 and SW620, respectively. Histogram plots of stained SW480 (panel **c**) and SW620 (panel **f**) show that ≥ 99% of cells expressed intracellular TG2, and that the mean fluorescence intensity (MFI) of SW480 cells was higher than SW620, indicating that the average amount of intracellular TG2/cell was larger in SW480 than SW620. Furthermore, this was independent of cell size, as the same pattern was seen when cells of the same size were compared across the two cell lines (e.g. small SW480 vs. small SW620, Figure 3.4). Figure 3.4 summarises the results of the intracellular TG2 staining, and shows that the MFI (and therefore intracellular TG2 expression) of SW480 cells was ~3.5-fold greater than SW620, independent of cell size. Figure 3.5 shows the microscope appearance of SW480 (panels a-b) and SW620 (panels c-d), confirming the presence of smaller and larger cells within the main cell populations.

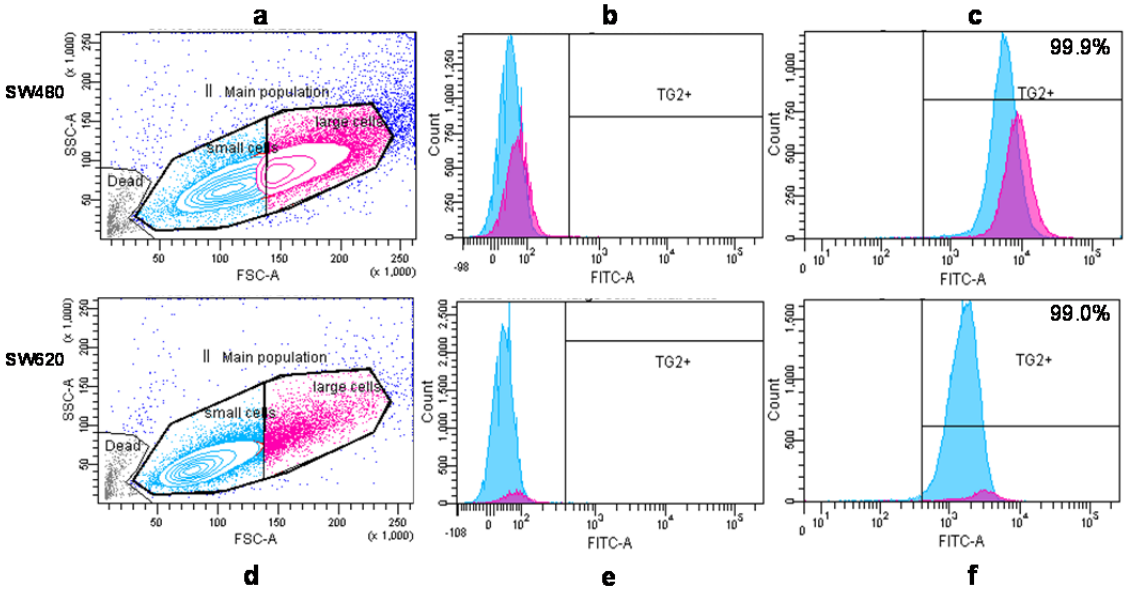

Figure 3.3 - Flow cytometry analysis of intracellular TG2. Panel (a) and (d) show size (FSC) and granularity (SSC) of SW480 and SW620, respectively. Panels (b) and (e) show unstained SW480 and SW620 controls, respectively. Panels (c) and (f) show anti-TG2 stained SW480 and SW620, respectively. Data are representative of 1 out of 2 experiments performed

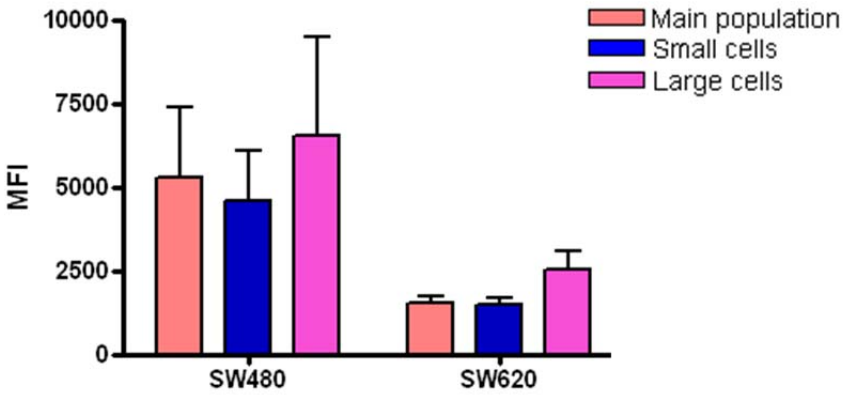

Figure 3.4 – MFI values of TG2-stained SW480 and SW620 analysed by flow cytometry. Values represent mean MFI + SEM, n=2.

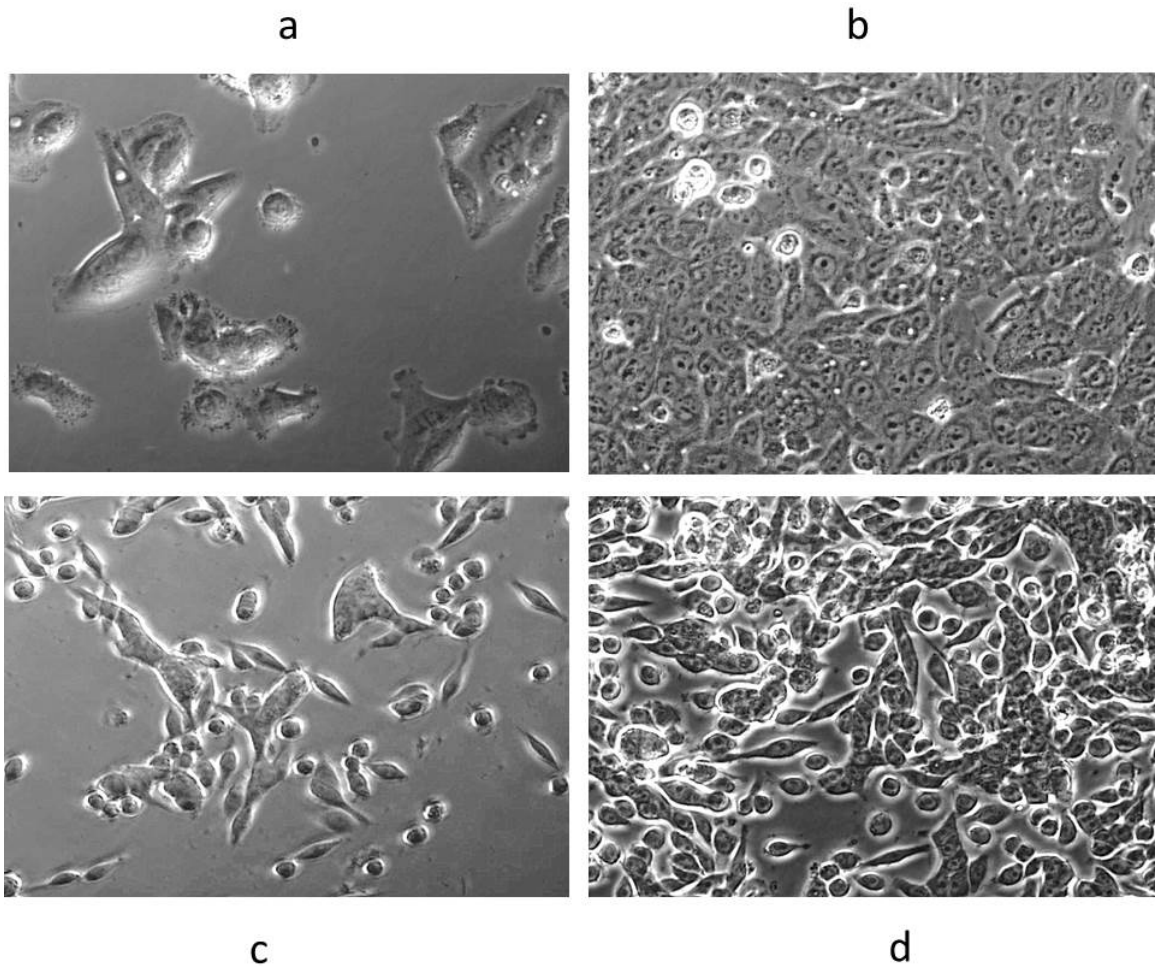

Figure 3.5 – Microscope appearance of SW480 at low (a) and high densitiy (b), and SW620 at low (c) and high (d) density showing the presence of smaller and larger cells within the main populations.

Figure 3.6 displays the results from surface TG2 staining. The main population of SW480 and SW620 live cells was gated as shown in panel **a** (SW480) and panel **d** (SW620). Panel **c** shows that, 1% of the main population of SW480 cells expressed TG2 on their surface. Panel **f** shows that 0.2% of the main population of SW620 cells expressed TG2 on their surface. Cumulative data from 3 experiments performed indicate that 0.75% of SW480 vs. 0.35% of SW620 cells expressed surface TG2, and that this difference was significant. Furthermore, cumulative MFI data show that the amount of TG2 expressed on the surface of positive cells was higher in SW480 and SW620, although this difference was not significant.

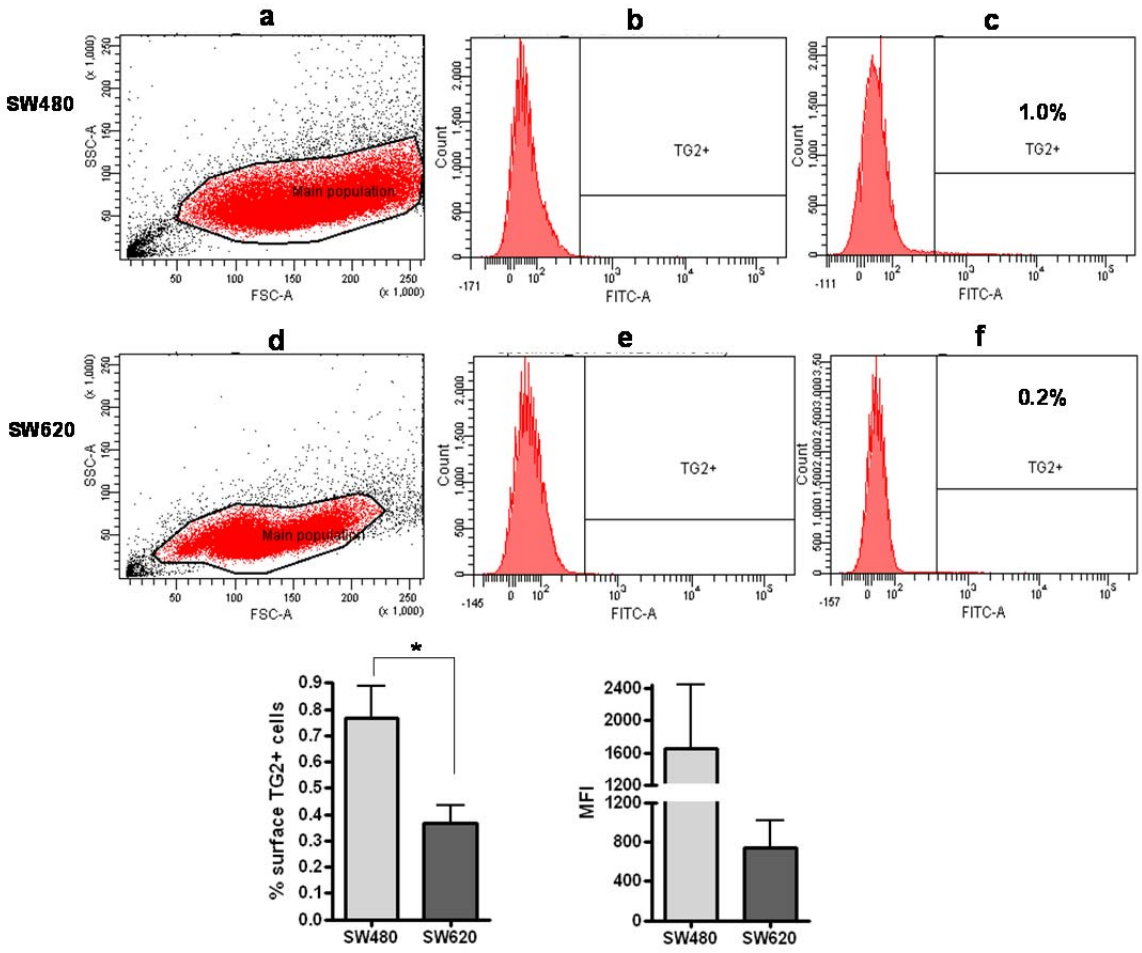

Figure 3.6 – Flow cytometry for surface TG2. Panels (a) and (d) show size and granularity of SW480 and SW620, respectively; panels (b) and (e) show unstained SW480 and SW620 controls, respectively; panels (c) and (f) show anti-TG2 stained SW480 and SW620, respectively. Percentages on panels (c) and (f) indicate the proportion of surface TG2 positive cells in SW480 and SW620 compared to their respective controls. FACS plots are representative of 1 out of 3 experiments performed. Bar chart shows mean + SEM, n=3. * = $p<0.05$ calculated by *t*-test

3.3.4 TG2 Activity

The ability of TG2 to form conjugates with a polyamine substrate (bio-MDC) was assessed as a measure of its cross-linking activity in SW480 and SW620 colon cancer cell lines. Results in Figure 3.7 show that TG2 activity in SW480 was very intense (panel **a**, green fluorescence), and that its distribution partially co-localised with the distribution of TG2 protein (panel **b**, red fluorescence). Approximately half of the SW480 cells stained only for TG2 protein, whilst the other half stained for both protein and activity (as visible in panel **c**). Moreover, whilst panel **a** shows that TG2 activity might be present in the nuclei of

SW480, panel **b** clearly shows that TG2 did not localise in the nuclei of these cells. In SW620, both TG2 activity and protein were extremely low compared to SW480 (panels **d** and **e**).

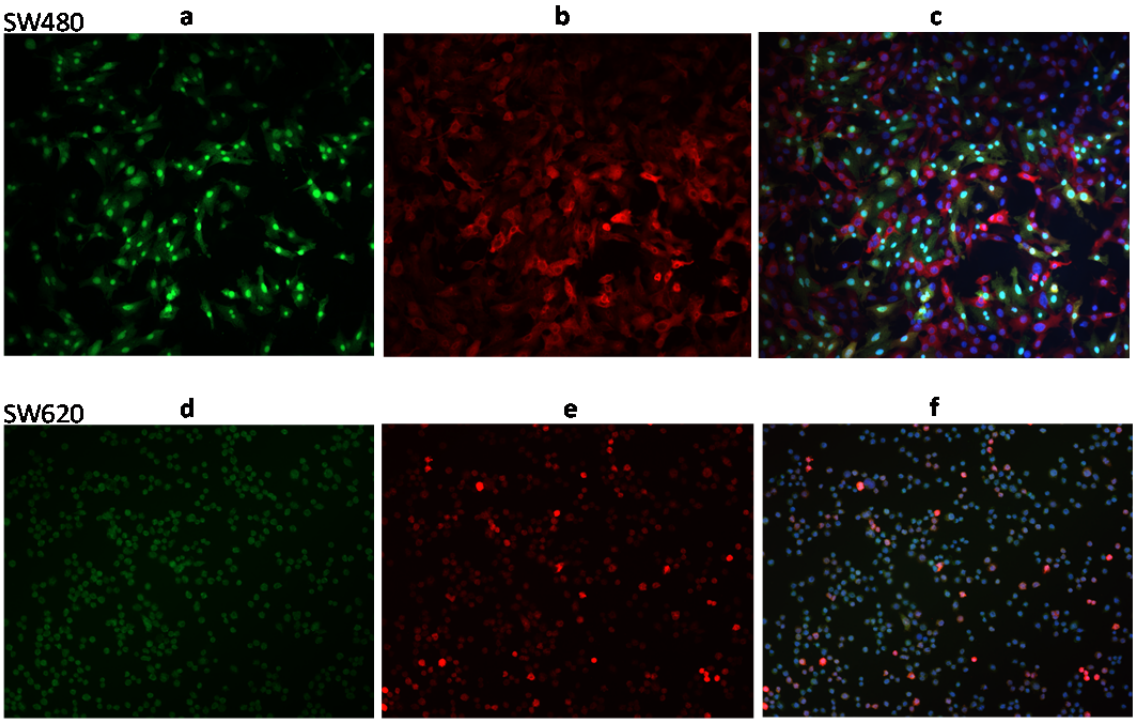

Figure 3.7 – Staining for TG2 activity (green) and protein (red) of SW480 (panels a to c) and SW620 (panels d to f). Panels a and d show TG2 activity only. Panels b and e show TG2 protein only. Panels c and f show merging of TG2 activity and protein, and include a nuclear counterstain (blue). All images were taken at 20X magnification. Images in panels d-f (SW620) were taken with a 20-fold higher exposure time than images a-c (SW480), for clarity purposes.

3.3.5 Intracellular Ca^{++} measurement and SUMOylation/Ubiquitylation pattern in SW480 and SW620

Results from the previous section raised the question as to whether the levels of TG2 activity were correlated to the intracellular content of Ca^{++}, and whether the levels of TG2 protein showed a normal SUMOylation/Ubiquitylation ratio.

Intracellular Ca^{++} was measured on SW480 and SW620 cells as described in section 2.17. Results shown in Figure 3.8 below show that the content of free cytosolic Ca^{++} is greatly higher in SW480 compared to SW620 (p <0.0001).

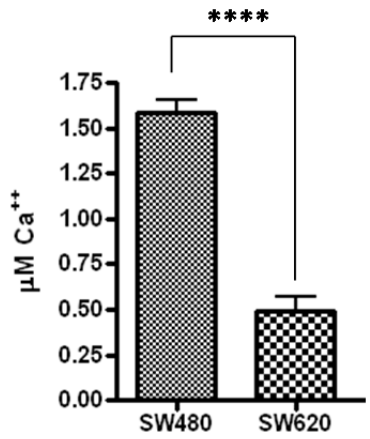

Figure 3.8 – Free cytosolic Ca^{++} concentration expressed in µM. Plot shows average ± SEM. n=3. ****=p<0.0001

The physical interaction between TG2 and SUMO-1 or TG2 and Ubiquitin was assessed in SW480 and SW620 colon cancer cell lines using the Duolink system, as described in section 2.5. Results in Figure 3.9 (panels **a** and **b**) show that in SW480 TG2/Ub interaction events occurred with a frequency of 0.08 events/cell, whereas TG2/SUMO-1 interaction events occurred with a frequency of 0.76 events/cell; hence, in SW480 Ubiquitylation of TG2 occurred less often than its SUMOylation (p<0.001). Figure 3.9 (panels **c** and **d**) shows that in SW620 TG2/Ub interaction events occurred with a frequency of 0.82 events/cell, whereas TG2/SUMO-1 interaction events occurred with a frequency of 0.61 events/cell; hence in SW620 Ubiquitylation of TG2 occurred more often than its SUMOylation, although this difference was not statistically significant. Furthermore, comparison of TG2/Ub interaction events occurring between cell lines shows that Ubiquitylation of TG2 occurred more often in SW620 than in SW480 (p<0.01).

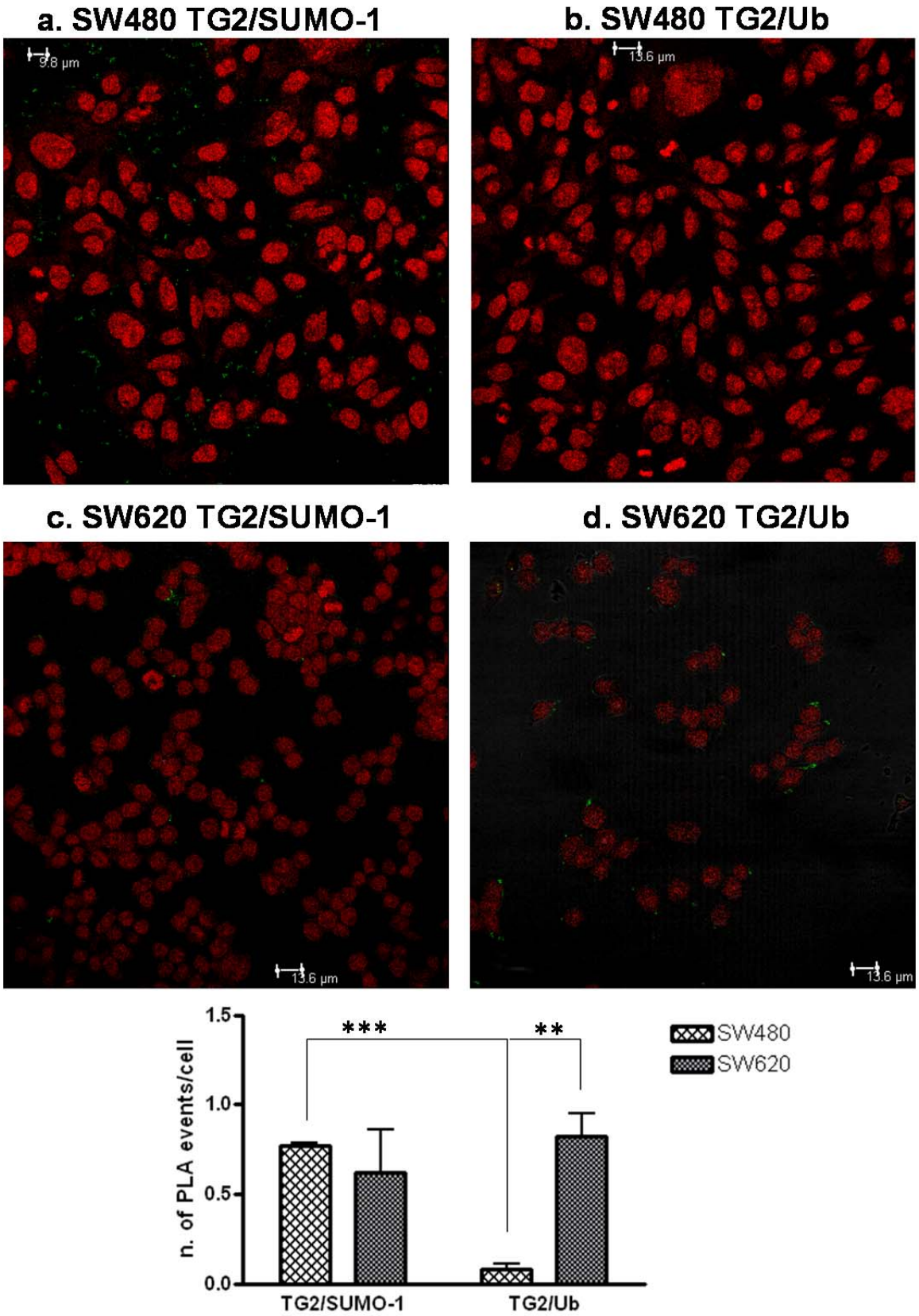

Figure 3.9 – Assessment of the extent of TG2 SUMOylation and Ubiquitylation occurring in SW480 and SW620 cells. Confocal images show PLA events (green) overlaid on the nuclear counterstain (red). All images takena t 40X magnification. Images are representative of 1 out of 3 experiments. PLA events were counted by eye (2 fields/slide) and plotted. Plot shows average ± SEM. n= 3. **=p<0.01; *** =p<0.001

3.4 Expression of TG2 in tissue sections from CRC patients

To complement the *in vitro* data about TG2 expression in colorectal cancer, tissue sections from 5 patients were stained for TG2 during the progressive stages of their disease.

Panel A of figure 3.10 shows a section of healthy colon mucosa where no TG2 staining can be detected. Panel B shows a section of primary tumour, where TG2 staining (red) can be seen more intense within the tumoral area ("t"), and at the tumoral frontline (middle of the picture), compared to the normal area ("n"). Panel C shows a section of liver metastasis from the same patient, where TG2 staining is virtually absent within the tumour parenchyma ("t"), and only present in the stroma ("s") instead.

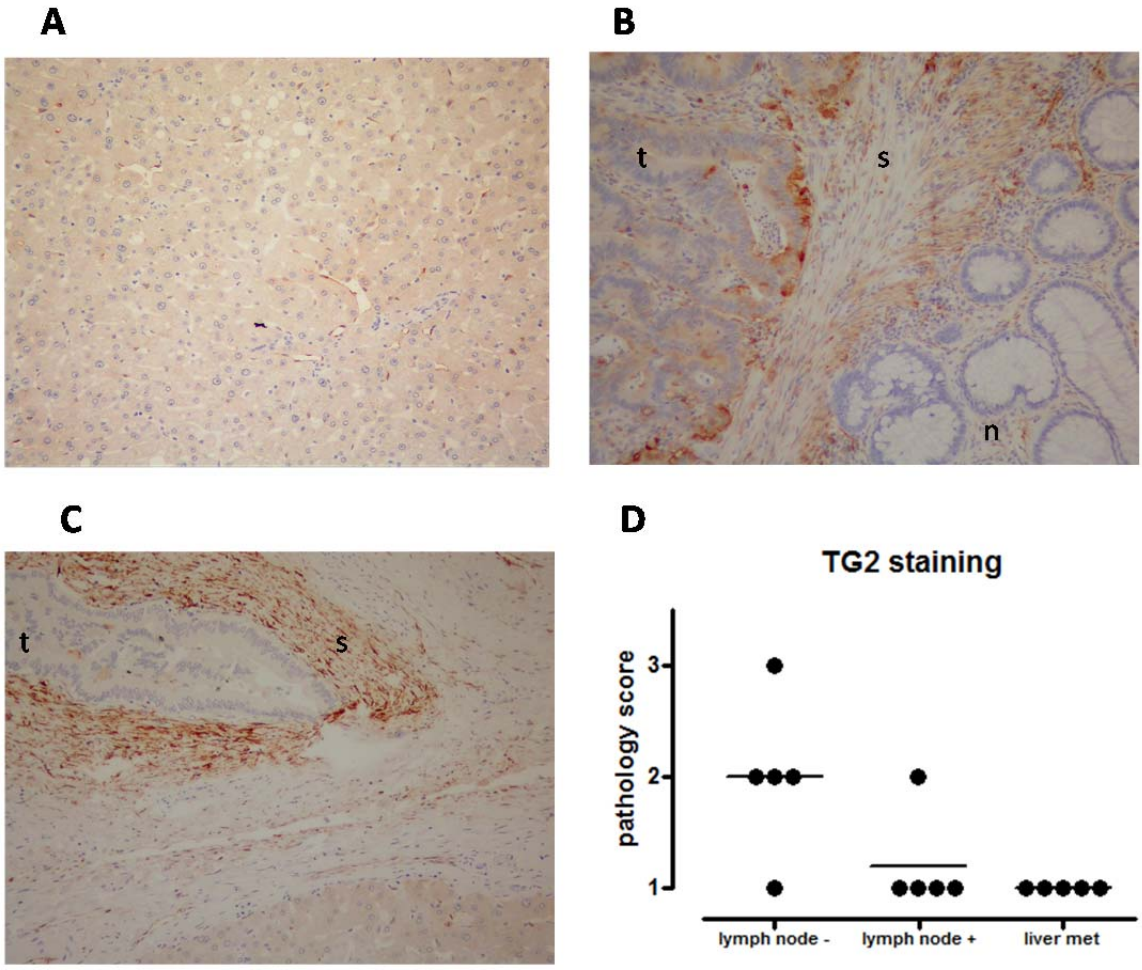

Figure 3.10 – IHC staining for TG2 (red). Images referring to 1 out of 5 patients scored. Panel A, section of healthy colon mucosa. Panel B, section of primary tumour with no LN involvement. Panel C, section of liver metastasis. Panel D, scoring graph. All images taken at magnification 10X. t=tumour, s=stroma, n=normal mucosa

3.5 Discussion

Very little is known about the anti-tumoral role of tumour-expressed intracellular TG2. Understanding the underlying mechanisms of such phenotype is essential for the development of a targeted anti-cancer treatment. To this purpose, in this chapter I aimed to: i) characterise TG2 in different cancer cell lines in order to find the most interesting models to investigate its tumour suppressor role, and ii) carry out more extensive analyses of TG2 in such selected *in vitro* models, as well as in human cancer tissue sections.

Initially, I screened a number of solid and hematologic tumour cell lines for their expression of TG2 protein, and compared them to a known model of high and low TG2-expressing cells, constituted by the CF cell lines IB3-1 (high TG2) and C38 (low TG2)[115]. The Western blot results in Figure 3.1 showed a very interesting pattern: the 77kDa full-length TG2 was very high in a primary colon cancer cell line (SW480), but very low in its patient-matched metastatic counterpart (SW620); conversely, the 55kDa TG2 splice variant showed the opposite pattern in these cell lines. Both cell lines were selected for this study and screened for their levels of TG2 mRNA, along with various other cell lines that served as reference. In doing so, I found out that all TG2 mRNA variants assessed were around 1000-fold more abundant in SW480 compared to SW620, except for the TGM2_v2 (coding for the 55kDa protein) that was just 100-fold more abundant, i.e. one order of magnitude below the other variants (Figure 3.2). Considering that the TGM2_v2 splice variant lacks the original 3' UTR, this result suggested the possibility of a miRNA-specific translation regulation which would affect all variants here analysed except the TGM2_v2.

Next, in order to investigate the intracellular or cell surface TG2 localization of TG2 protein, I analysed SW480 and SW620 by flow cytometry. Results in figures 3.3 and 3.6 show that: a) >99% of the non-metastatic SW480 and the metastatic SW620 cells expressed intracellular TG2, b) SW480 expressed ~3.5 fold more intracellular TG2 than SW620, and c) this phenomenon was independent of cell size. Interestingly, the flow cytometry analysis

also showed that the amount of intracellular TG2/cell (represented by the MFI values) in SW480 was quite variable, and much more so than in SW620. This might indicate that the population of SW480 cells is overall more heterogeneous than the population of SW620 cells in the batches currently being used. A very low proportion of SW480 and SW620 (< 1%) expressed detectable levels of cell surface TG2; however, the proportion of SW480 positive cells was significantly larger (~2-fold) than SW620. Interestingly, the amount of cell surface TG2 (represented by the MFI values) expressed by positive cells was also ~2-fold higher in SW480 than in SW620, although this difference was not statistically significant, perhaps due to the very high variance. Thus, it may be concluded that surface TG2 molecules make a negligible contribution to the overall TG2 protein levels seen in the two colon cancer lines.

The results so far strongly indicated that a prominent role may be played by intracellular TG2 in SW480 and SW620 colon cancer cell lines. Therefore, I assessed levels of one of TG2 enzymatic activities occurring intracellularly, namely the cross-linking activity, and found out that this activity was globally higher in SW480 than in SW620 (Figure 3.7). This result was consistent with the amount of TG2 protein and mRNA expressed by these cell lines, however, no conclusions about the actual enzymatic reaction rate could be drawn from this experiment. Interestingly, this experiment revealed that nearly half of SW480 cells did not express detectable levels of TG2-mediated cross-linking, despite the strong staining for TG2 protein. In both cell lines the staining for TG2 protein was clearly limited to the cytoplasm, whereas the staining for TG2 activity seemed to be present both in the cytoplasm and in the nucleus; however such a discrepancy is likely attributable to “leakage” of the blue fluorescent signals (corresponding to the nuclear counterstain DAPI) into the detection channel for the green-fluorescent TG2 activity. Hence, I suggest that any positive signal for TG2 activity that is not simultaneously positive for TG2 protein must be considered as technical artefact; conversely, any signal for TG2 protein that is not simultaneously positive for TG2 activity can be considered as genuine. It is

noteworthy that the bio-MDC substrate (used here for measuring TG2 activity) is also employed in experiments for inhibition of TG2 cross-linking activity. This is based on the fact that MDC is competitive inhibitor for TG2[177], hence short-term treatments (up to 2h, as used here) are useful for measuring total TG2 cross-linking[66], whereas long-term treatment (12-24h) are used for inhibition experiments[108]. Coherently with a high cross-linking activity, in my experiments SW480 showed also a very high concentration of free intracellular Ca^{++} compared to SW620 (Figure 3.8).

After these initial experiments aimed at characterising the levels and localisation of TG2, I sought to determine whether mechanisms of protein turnover such as SUMOylation or Ubiquitylation could be held responsible for the high difference in TG2 protein levels between SW480 and SW620. Analysis of the linear amino acid sequence revealed that TG2 possesses three KxE sites which are similar to ΨKxE sites typically recognised by SUMO/Ub molecules, but lack the initial hydrophobic residue (Ψ). Furthermore, an important study clearly shows SUMOylation of TG2 in human CF cell lines[151]. Results obtained here indicated that TG2 in SW480 is less often found Ubiquitylated than SUMOylated, whereas TG2 in SW620 is more often found Ubiquitylated than SUMOylated. Furthermore, when comparing the two cell lines, TG2 was found much less Ubiquitylated in SW480 than in SW620 (Figure 3.9). Hence, it is conceivable that decreased Ubiquitylation in SW480 promotes intracellular persistence of TG2 protein, whereas increased Ubiquitylation in SW620 leads to faster turnover. Noticeably, despite TG2 being homogenously distributed in the cytoplasm, its association with SUMO and Ubiquitin was mainly seen at the border between the cytoplasm and the plasma cell membrane, suggesting a more tightly regulated turnover at these locations, and an involvement of TG2 in either motility/invasion or early cell signalling mediation.

Because of the above finding and the knowledge that in the SW model of colorectal cancer TG2 was downregulated in the metastatic SW620 line, we investigated the expression of TG2 in sections obtained from CRC patients. Positive TG2 staining was

detected in primary tumour sections, mainly at the invasive front (figure 3.10B), but not in liver metastases (figure 3.10C). Scoring by two independent investigators quantified this differential expression pattern (figure 3.10D), with TG2 expression found to negatively correlate with tumour stage. However, in these sections the most intense staining was detected in the tumour stroma (figure 3.10B-C), with cells surrounding the cancerous cells appearing to produce significant amounts of TG2, both at the primary and metastatic sites. Notably, no TG2 staining was observed in a representative section of normal colon (figure 3.10A); this result is in agreement with another study that found increased TGM2 mRNA in CRC sections compared to healthy colon mucosa and proposed TG2 as a therapeutic target as well as a prognostic marker for CRC[178]. Overall, these results so far mirror those from the *in vitro* characterisation of SW480/SW620.

The differential TG2 protein and activity in SW480 and SW620 cell lines was first noted by Zirvi et al. in 1991[48], however they did not characterise these cell lines for mRNA levels of TG2, check its cellular localisation, or looked at post-translational modifications (such as SUMOylation and Ubiquitylation) that could affect the intracellular turnover. I have investigated all such aspects in this chapter and have shown that, compared with the metastatic SW620, in the non-metastatic SW480 both the production and 'molecular survival' of TG2 are promoted, and that the Ca^{++}-dependent cross-linking activity is kept at high levels. Importantly, I have shown that >99% of SW480 and SW620 cells express intracellular TG2, whereas only 0.75% of SW480 and 0.35% of SW620 cells express TG2 on the cell surface. This strengthens the idea that statements about the role of TG2 in the progression from primary to metastatic colon cancer, should take into account only the intracellular enzymatic activities of this protein. Finally, I have shown that the pattern of expression of TG2 *in vitro* mimics the one seen *ex vivo* in colorectal cancer patients.

Findings in this chapter (summarised in Table 3.1) raise the question as to why and how, in the SW480-SW620 model of colon cancer progression, TG2 protein and activity is maintained at a very high level in the primary tumour line. What is the biological event that

links the massive decrease in TG2 with acquisition of the SW620 metastatic phenotype? What is the functional advantage that the primary colon cancer line gains from keeping its levels of TG2 high, and/or what is the advantage that the metastatic colon cancer cell line gains from a massive decrease in TG2? Furthermore, which are the mechanisms behind this switch? Is there a role for miRNA in regulating TG2 expression through the different phases of colorectal cancer progression?

Through the experiments performed and reported in the next chapters I will try to provide an answer to these questions.

Cell line	TG2 mRNA	TG2 protein	TG2 activity	Free cytosolic Ca^{++}	FACS TG2		TG2/ SUMO-1	TG2/ Ubiq.
					Intracell. % of molecules/cell	Surface % of +ve cells		
SW480 Primary tumour	+++	+++ (V1) + (V2)	+++	+++	+++	++	++	+
SW620 Metastatic tumour	+	+ (V1) ++ (V2)	+	+	+	+	++	+++

Table 3.1 – Summary of the characterisation of TG2 carried out in SW480 and SW620 cell lines. Intracell.=intracellular, +ve=positive, Ubiq.=Ubiquitin. Values arbitrarily assigned.

4. Strategies for modulating TG2, and its functional effects in the SW480/SW620 CRC model

4.1 Introduction

As mentioned at the end of the previous chapter, the clear dichotomy existing in SW480/SW620 regarding TG2 levels led me to question what the biological significance of such differences was, and which the mechanisms that lead to its onset were. The aim of this section is to investigate the relationship between TG2 and autophagy, immune escape, tumour invasion, for reasons that will be stated here below. To this end, I first optimised tools for manipulating TG2 expression *in vitro*, which were essential for the subsequent functional experiments performed.

TG2 and Autophagy. A growing body of evidence (mainly in *in vitro* cancer models) has promoted the idea of autophagy as a bi-phasic process[53,54]. Specifically, autophagy has been hypothesised to act as a tumour suppressive mechanism within the primary tumour, whilst acting as a promoter of metastasis at more advanced stages[54]. Such a hypothesis is based on the discovery that autophagy plays a physiological role in helping to resolve stressful conditions (e.g. oxidative stress, ER stress, UPR)[44], and in promoting cell survival during starvation, hypoxia[44] and anoikis[50]. During tumour initiation and progression, cells are highly likely to face some or all of these stressful conditions, hence autophagy becomes crucial for: i) clearing stressors or stress-related by-products from normal cells, ii) supporting proliferation of tumour cells even within the most hypoxic areas of the tumour mass, and iii) survival of tumour cells following their detachment form the ECM (which is a pre-requisite for the formation of distant metastasis)[179]. Importantly, the only caveat to the above theory is that it has not yet been demonstrated in a model of full tumour development, i.e. from normal tissue to primary tumour, to metastatic.

Along with playing an important role in tumour initiation and progression, autophagy is also essential in gut homeostasis[180]. Mutations in autophagy-related genes (*ATG* genes) confer susceptibility to Crohn's disease[127], a type of IBD that is naturally associated with increased risk of small intestine, colon and colorectal cancer[125]. On this basis, a strong

association between autophagy and colorectal cancer can be hypothesised, where basal levels of autophagy might be high in normal colon cells, then undergo a decrease during oncogenic transformation (formation of primary adenocarcinoma), and might increase again during metastasis formation. In this context, defective autophagy might favour the progression from normal (or dysplastic) colon mucosa to primary adenocarcinoma, but impair the formation of metastasis at more advanced stages.

Interestingly, results in Chapter 3 of this study have highlighted a similar bi-phasic pattern of TG2 expression in the SW480/SW620 model of colon cancer progression. An inverse relationship between levels of TG2 and autophagy has already been established in pancreatic cancer[69] and Cystic Fibrosis[66]. In particular, the latter study showed that it is possible to distinguish between low levels of autophagy that occur naturally, and low levels of autophagy resulting from a malfunctioning of this biological process. Such a distinction was made by assessing the levels of key autophagy-related proteins (including Beclin-1, ATG7, ATG14, Vps34) and the p62 protein, whose role is to tag Ubiquitylated protein aggregates for autophagic degradation. Impairment of autophagy and the subsequent lack of formation of autophagosomes resulted in decreased levels of the above mentioned genes, but increased levels of p62. Such a relationship was due to the inability of autophagy to clear p62-tagged protein aggregates[77]. Based on this evidence, I hypothesise that an inverse relationship exists between levels of TG2 and autophagy in the SW480/SW620 model of colon cancer progression. Specifically, I hypothesise that TG2 prevents autophagy from occurring in the SW480 colon primary adenocarcinoma cell line, whilst downregulation of TG2 permits autophagy-mediated metastatic progression in the SW620 colon cell line.

TG2 and tumour invasion. TG2 is involved in migration and invasion of cancer cells. Until now, intracellular tumour-expressed TG2 has been positively associated only with increased migratory and invasive properties[103,173], mainly by interacting with the FAK kinase (an essential mediator of cell motility) at the leading edges of the cells[58]. Conversely, surface and extracellular (stromal) TG2 has been associated with suppression of tumour

expansion[176,181]. Furthermore, one study carried out in a TG2 $^{-/-}$ colon cancer cell line showed that exogenous addition of TG2 caused decreased cell migration *in vitro*[182]. However, in none of the experiments where TG2 was shown to suppress tumour cell migration/invasion were intracellular tumour-expressed TG2 levels manipulated. The results I obtained in colon cancer cell lines (Chapter 3) indicated that, despite TG2 being homogenously distributed in the cytoplasm, it was found in a SUMOylated and Ubiquitylated form mainly at the edges of the cell, thus supporting a role for TG2 in migration/invasion also in the SW480/SW620 colon cancer model. Based on this evidence, in this chapter I will test whether the levels of TG2 expressed by SW480 and SW620 colon cancer cells affect their ability to invade through an ECM-like compound, and whether this is mediated by an increased expression of MMPs.

TG2 and immune escape. Tumour initiation, progression and metastasis are linked to immune evasion. A study from 1981 carried out in PBMCs showed that exogenously administered TG2 is able to cross-link and cause intracellular aggregation of β2-microglobulin[75]. β2-microglobulin plays an essential role in the assembly and cell surface expression of HLA-I molecules[76]. A variable degree of downregulation (but not loss) of HLA-I molecules has been demonstrated to occur in colon cancer cell lines and in histological sections from human patients[183,184]. This phenomenon is associated with reduced immune recognition which, in turn, allows the tumour to expand and makes possible the formation of distant metastases. To date, no relationship between intracellular levels of TG2 (protein and activity) and β2-microglobulin has been established. Here, I will test whether high TG2 levels in the SW480 primary colon cancer cell line cause cross-linking and downregulation of β2-microglobulin, leading to reduced expression of HLA-I at the cell surface.

Among the strategies likely adopted by tumour cells to guarantee their growth is to increase the abundance of oncosuppressor-targeting miRNA while decreasing the abundance of oncogene-targeting ones. Within the former category of miRNA lie miR-19a and miR-19b, whose levels are found to be altered (upregulated or downregulated) in many

cancers[165]. Interestingly, using 4 online databases (Targetscan, miRanda, miR Walk, Diana) for the prediction of miRNA targets, I have found that miR-19a and miR-19b are predicted to bind to a conserved UUUGCACA sequence at position 1588-1595 of the 3'-UTR of TG2. Furthermore, data published by our internal collaborators Dr Karen Pickard and Dr Alex Mirnezami, demonstrate that miR-19a is significantly more abundant in metastatic CRC compared to primary[185,186]. Hence in this chapter I will test whether the levels of miR-19a are inversely correlated with levels of TG2 in SW480 and SW620, and what (if any) are the biological consequences of such regulation.

To summarise, in this chapter I aim first to carry out a series of optimisations to identify the best method for modulating the levels of TG2; these include: i) transfection of a TG2-encoding DNA plasmid in SW620, in order to increase their levels of TG2, and ii) transfection of TG2-specific siRNA in SW480, in order to decrease their levels of TG2.

Contextually, I aim to transfect sense miR-19a into the high TG2-expressing SW480, and antisense miR-19a into the low TG2-expressing SW620, to find out whether a miRNA-dependent modulation of TG2 expression may occur.

In order to be able to define TG2 ways of action in our model, I will also assess whether any modulation of TG2 levels also affects its intracellular crosslinking activity.

For functional investigations over the biological role of TG2, I aim to assess: i) basal levels of autophagy in SW480 and SW620 colon cancer cell lines, ii) ability to activate autophagy following starvation, iii) relationship between autophagy and TG2 levels, iv) invasive properties of SW480 and SW620 basally and following modulation of intracellular TG2 levels, v) expression of total HLA-I molecules in SW480 and SW620 in basal conditions and following modulation of intracellular TG2 levels, vi) expression of pro/anti-inflammatory cytokines and MMPs in basal conditions and upon TG2 silencing.

The results from the proposed experiments are important in order to establish a functional role for TG2 in colon cancer. Indeed, its differential expression between primary and metastatic colon adenocarcinoma suggests a role for TG2 in the progression of this

tumour type. However, given the potentially adverse effects of targeting TG2 pharmacologically (explained in section 1.4.3.), only by uncovering the exact mechanisms of TG2-mediated tumour suppression can a targeted therapy for colon cancer be designed.

4.2 Materials and methods

Optimisation of TG2 plasmid DNA transfection was carried out in SW620 cells. Cells were seeded in 24-well plates at 6.4 x 10^5 cells/mL in a total volume of 500 μL complete DMEM. Cells were transfected at 70% confluence, which was reached ~24 h after seeding. Transfection was carried out for 48h (section 2.13) using the range of conditions shown in Table 4.1. At the end of this period, cells lysates were prepared (section 2.7), and SDS-PAGE and Western blotting performed (sections 2.8 and 2.9, respectively).

Lipofectamine (μL)	**PLUS reagent (μL)**	**Plasmid DNA (μg)**
4.0	1.0	1.0
3.0	2.0	2.0
3.0	2.0	3.0
3.0	3.0	3.0
2.0	1.0	0.0
0.0	0.0	0.0

Table 4.1 –DNA transfection optimisation conditions in SW620

Optimisation of siRNA-mediated TG2 RNAi was carried out in SW480 cells. Cells were seeded in 24-well plates at 2.6 x 10^5 cells/mL, in a total volume of 500 μL/well of complete DMEM, and were transfected at 40% confluence which was reached ~24 h after seeding. Delivery of RNA duplexes was carried out for 48h (section 2.13). Optimisation conditions were set up as shown in the tables below for SW480 (Table 4.2). At the end of this period, cell lysates were prepared (section 2.7), and SDS-PAGE and Western blotting performed (sections 2.8 and 2.9, respectively).

Hiperfect (μL)	Each siRNA (nM)	High GC negative control (nM)
1.5	5	-
3.0	5	-
4.5	5	-
1.5	20	-
3.0	20	-
4.5	20	-
1.5	50	-
3.0	50	-
4.5	50	-
2.0	-	30
2.0	-	-
0.0	0	-

Table 4.2 – RNAi optimisation conditions in SW480

Optimisation of miRNA transfection was carried out in SW480 and SW620 colon cancer cell lines. Cells were transfected at the same time as they were seeded (fast-forward transfection protocol), as broadly explained in section 2.14. The range of conditions used for optimisation is shown in Table 4.3. An identical protocol was used for transfection of miRNA using Hiperfect reagent (Qiagen UK, #301704) or Interferin reagent (Polyplus UK, #409-10). Briefly, 4 μL of 6.25 μM miRNA (final concentration 50 nM) was diluted in a total volume of 100 μL of Opti-MEM I, in one well of a 96-well round-bottomed plate. Next, 3 or 4 μL of the transfection reagent (Table 4.3) was added and the plate vortexed for 3 sec, then incubated for 10 min at R.T.

When each of the transfection mixes was ready, SW480 and SW620 cells were seeded in 24-well plates in a total volume of 500 μL/well of complete DMEM, SW480 at 2.6 x 10^5 cells/mL and SW620 at 6.4 x 10^5 cells/mL. The mixes were dispensed immediately on top of the seeded cells.

Transfections of all RNA oligos were carried out for 48h. At the end of this period, RNA was extracted (section 2.10) and quantitative PCR of cDNA was performed (section 2.11) to

assess the levels of expression of TG2 and PTK9 (the latter used as an internal positive control) target genes.

Cell line	Transfection reagent	Type of oligo	miRNA 50 nM	qPCR targets
SW480	Hiperfect 4.0 μL	Sense	miR-1	PTK9
SW480	Hiperfect 4.0 μL	Sense	miR-19a	TG2
SW480	Hiperfect 4.0 μL	Sense	miR-19b	TG2
SW480	Hiperfect 4.0 μL	Sense	negative control	TG2 and PTK9
SW480	Interferin 3.0 μL	Sense	miR-1	PTK9
SW480	Interferin 3.0 μL	Sense	miR-19a	TG2
SW480	Interferin 3.0 μL	Sense	miR-19b	TG2
SW480	Interferin 3.0 μL	Sense	negative control	TG2 and PTK9
SW620	Hiperfect 4.0 μL	Antisense	miR-19a	TG2
SW620	Hiperfect 4.0 μL	Antisense	miR-19b	TG2
SW620	Hiperfect 4.0 μL	Antisense	negative control	TG2
SW620	Interferin 3.0 μL	Antisense	miR-19a	TG2
SW620	Interferin 3.0 μL	Antisense	miR-19b	TG2
SW620	Interferin 3.0 μL	Antisense	negative control	TG2

Table 4.3 – miRNA transfection optimisation conditions in SW480 and SW620

Invasion assay was carried out as described in section 2.3. Cells were seeded on top of the polymerised Matrigel layer at a density of 2.5 x 10^5 cells/mL in a total volume of 200 μL serum-free DMEM. After 24h, cells were harvested and counted using a CASY TTC Counter (Roche Innovatis AG).

For the analysis of autophagy markers, SW480 and SW620 cells were serum- and additive-starved for 6, 12 and 18h. These time points were chosen according to the suggestions of our collaborator Prof Luigi Maiuri who successfully showed increase of the autophagy marker Beclin-1 in C38 cells with as little as 6h starvation[66].

At each time point, cell lysates or total RNA were collected (section 2.7 and section 2.10, respectively). Control sample is indicated in graphs as “0h” or “unstarved”.

RNA extraction and cDNA synthesis were performed as in section 2.10. PCR for TG2 (697 bp) and Actin (550 bp), and qPCR for ATG7 (380 bp), ATG14 (192 bp), VPS34 (199 bp) were performed as in section 2.11, using the primer pairs listed in Appendix C (page C). Relative expression of genes analysed by qPCR was obtained by using the ΔΔCt calculation method, with β-actin used as normaliser gene.

Flow cytometry analysis of surface stained cells was performed as described in section 2.15. Anti-HLA I primary antibody (Abcam) and Goat anti-mouse PE-conjugated secondary antibody (Abcam) were used at the concentrations stated in Appendix B (page B).

For the TG2 activity assay, cells were seeded on coverslips pre-coated with Poly-L-Lysine, which were placed at the bottom of wells in a 24-well plate. Cells were seeded in a total volume of 500 μL/well of complete DMEM, SW480 at 2.6 x 10^5 cells/mL, SW620 at 6.4 x 10^5 cells/mL. The following day (~16 hrs later), SW480 were transfected with TG2 siRNA, whereas SW620 were transfected with TG2 plasmid. Transfection was carried out for 48h, at the end of which period the TG2 activity assay protocol was performed (section 2.6).

4.3 Results

4.3.1 Optimisation of plasmid DNA and oligo RNA transfection

Figure 4.1 shows Western blot analysis and densitometry data for plasmid DNA transfection optimisation carried out in SW620 cells. Results indicate that transfection of 3 μg of pLPCX-TG2 plasmid using 3 μL of Lipofectamine LTX + 3 μL of PLUS reagent achieved the greatest overexpression (12-fold) of TG2 protein compared to control cells treated only with the transfection reagent mix.

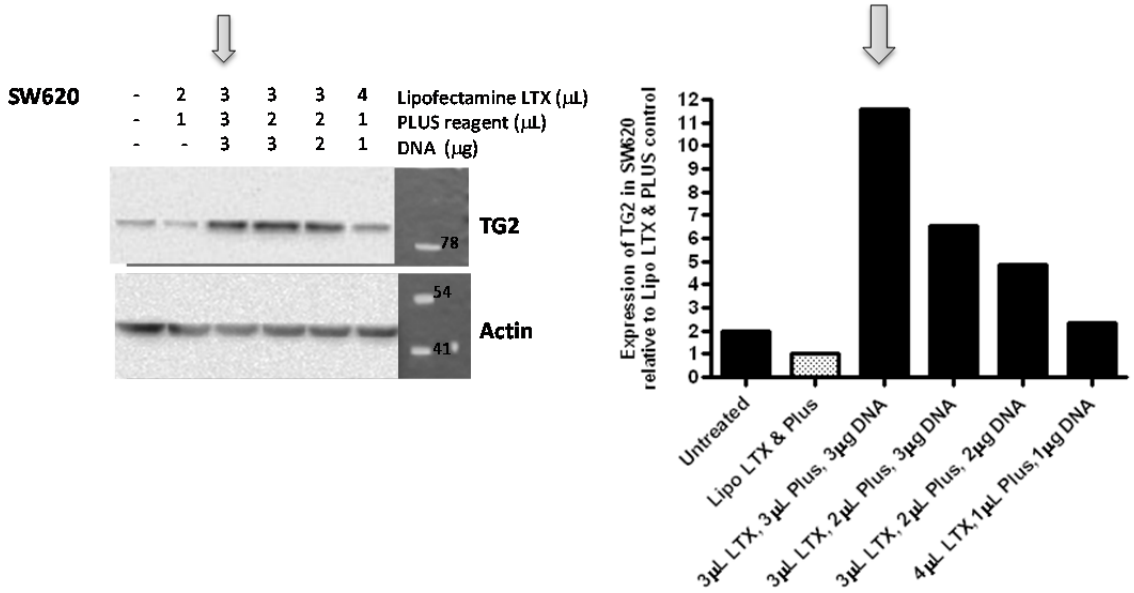

Figure 4.1 – Western blot and densitometry analysis of SW620 cells transfected with pLPCX DNA plasmid encoding full length TG2. Arrows indicate the optimal condition. Results here shown are representative of 1 out of 2 experiments.

Results in Figure 4.2 show Western blot analysis and densitometry data for TG2-specific siRNA transfection optimisation carried out in SW480. Results indicate that transfection of 50 nM of each of the three TG2-specific siRNA oligo using 4.5 μL of Hiperfect reagent achieved the greatest knock-down of TG2 protein (55%), compared to control cells transfected with a Hi-GC siRNA duplex control.

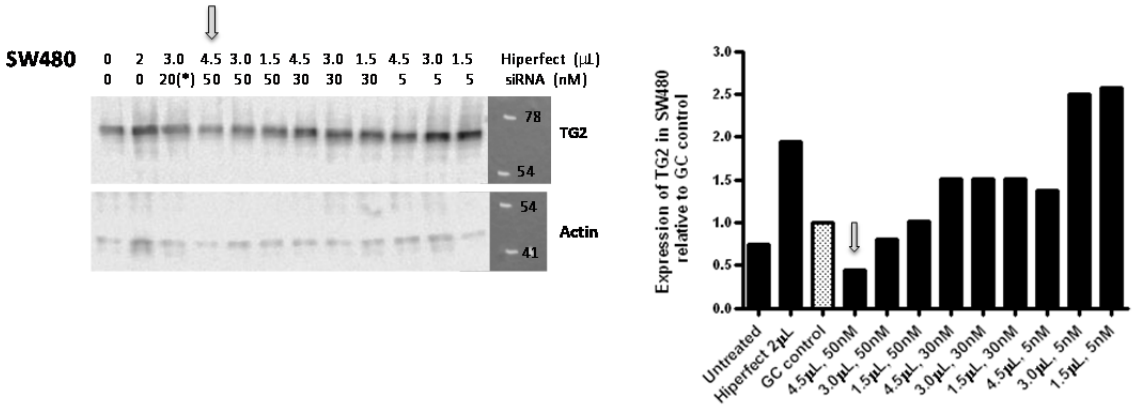

Figure 4.2 – Western blot and densitometry analysis of SW480 cells treated with siRNA for TG2, except conditions marked with (*) which represent hi-GC siRNA duplex control. Arrows indicate the optimal condition. Results here shown are representative of 1 out of 2 experiments.

4.3.2 Manipulation of TG2 protein levels by miR-19a and antimiR-19a

In order to verify whether miR-19a and miR-19b target TG2 mRNA as predicted *in silico* SW480 cells were transfected with sense oligos for miR-19a and miR-19b, as well as miR-1 which was used as an internal positive control. SW620 were transfected with antisense oligos for miR-19a and miR-19b. The mRNA of PTK9 is known to be downregulated by miR-1[187], hence it was used here as a positive control for the efficacy of transfection and as a reference for optimising the technique.

Figure 4.3 shows the relative expression of TG2 and PTK9 genes following transfection of 50nM synthetic oligo miRNA with different transfection reagents (as laid out in Table 4.3). Chart **a** (Figure 4.3, top left) shows that transfection of sense miR-19a or miR-19b in SW480 with either Hiperfect or Interferin caused respectively an ~80% or ~60% decrease in TG2 mRNA expression compared to control. Chart **b** (Figure 4.3, top right) shows that transfection of antisense miR-19a with Hiperfect in SW620 caused a ~300% increase of TG2 mRNA expression; however, transfection of the same antisense oligo with Interferin did not generate a noteworthy increase compared to control. Similarly, transfection of antisense miR-19b with either reagent did not generate a noteworthy increase of TG2 mRNA. Chart **c** (Figure 4.3, bottom) shows that transfection of sense miR-1 in SW480 with either Hiperfect or Interferin caused >90% decrease of its validated target PTK9, thus confirming the effectiveness of our transfection method.

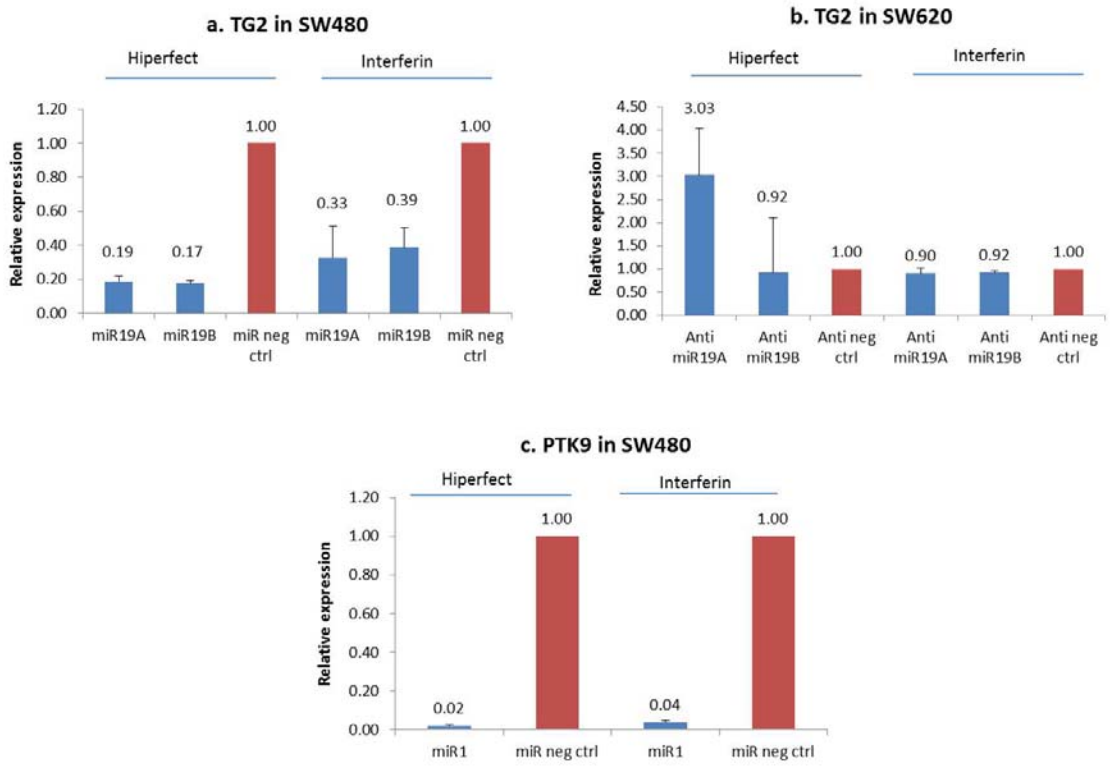

Figure 4.3 – Quantitative PCR of TG2 (charts a and b) and PTK9 positive control (chart c). SW480 were transfected with miR-19a, miR-19b and miR-1 oligo precursors (charts a and c), SW480 were transfected with antisense oligos for miR-19a, miR-19b and miR-1 (chart b). Bar charts indicate relative expression of samples (blue bars) compared to controls (red bars). n=2

Once confirmed that miR-19a was effective in reducing TG2 mRNA levels in SW480 and that antimiR-19a was effective in increasing TG2 mRNA in SW620, we sought to stably transfect these cells with a miR-19a or an antimiR-19a expressing DNA plasmid. For the initial transfection, the best condition as determined in section 4.3.1 (Figure 4.1) was used. Results in Figure 4.4 show a significant decrease of TG2 protein achieved in SW480 upon transfection of miR-19a plasmid, compared to control plasmid (SSC).

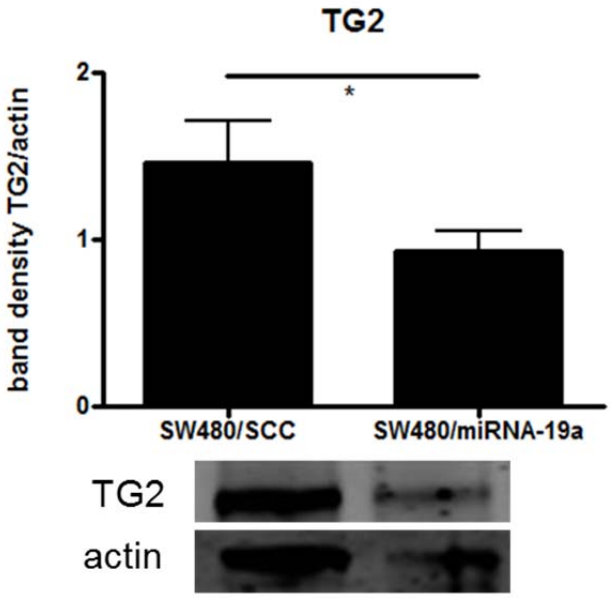

Figure 4.4 - Densitometric analysis of Western blots measuring the expression of TG2 upon transfection of miR19A. Data represent average + SEM of n=3 ; plus one representative Western blot

SW620 cells were transfected with a MirZip GFP-tagged antimiR-19a expressing plasmid (+Zip in Figure 4.5) or with a MirZip control plasmid (-Zip in Figure 4.5) for 24h or 72h. Results in Figure 4.5 show that 72h post transfection, a concomitant increase in TG2 and GFP in the +Zip condition was achieved, which was ~7-fold higher compared to the 72h -Zip condition.

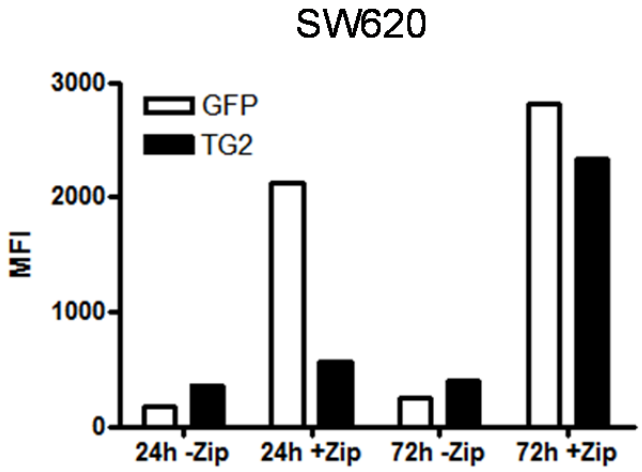

Figure 4.5 - Expression of TG2 and GFP in SW620 cells transfected with antimiR-19a plasmid ("Zip" in the graph) measured by flow cytometry

4.3.3 TG2 activity

In order to understand whether manipulation of TG2 protein levels was reflected by an alteration of its cross-linking enzymatic activity, we silenced TG2 in SW480 and transfected TG2 in SW620.

SW480 cells were silenced with 50 nM of each siRNA and 4.5 μL of Hiperfect reagent for 48 h, at the end of which period TG2 activity was assayed. Results in Figure 4.6 show that silencing of TG2 caused a ~20% decrease in TG2 activity vs. untreated cells.

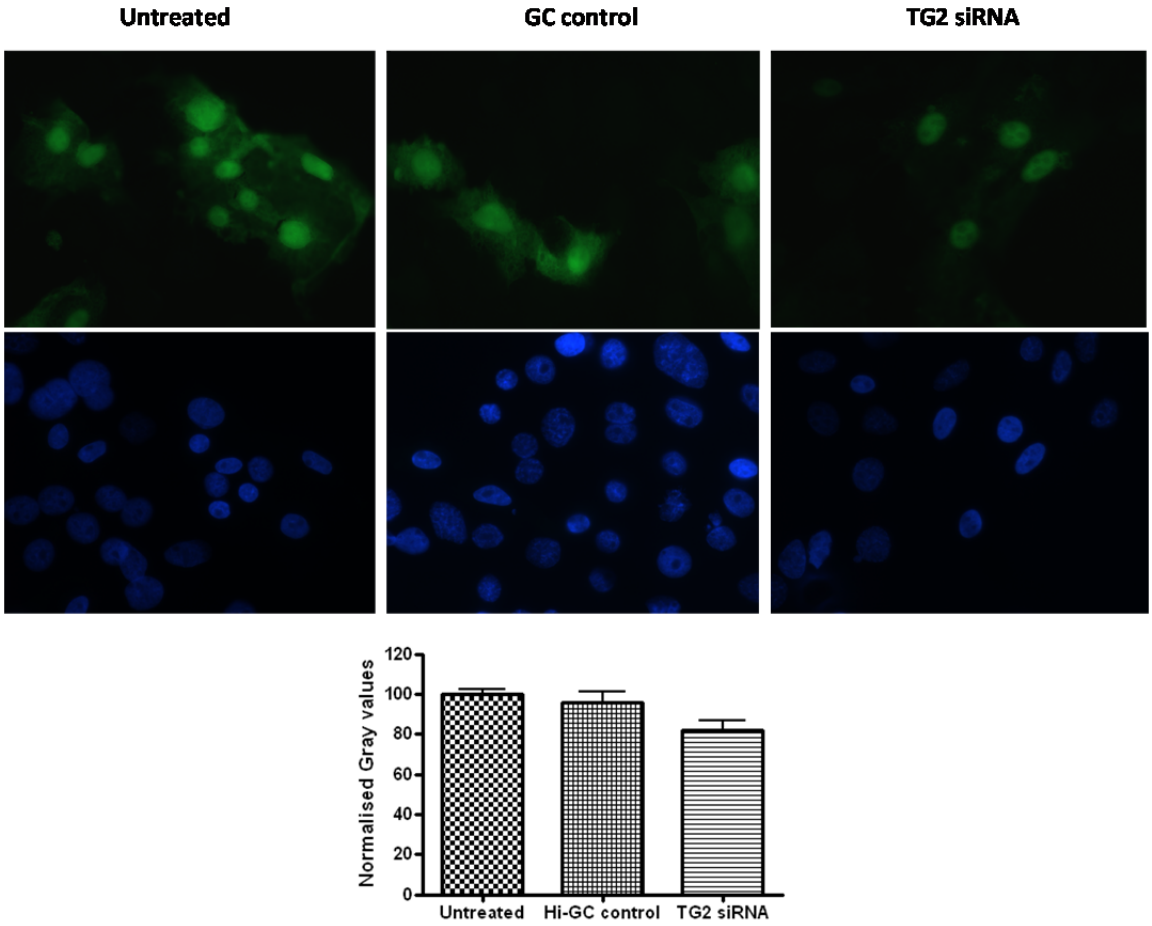

Figure 4.6 - TG2 activity assay upon treatment with TG2 siRNA in SW480. Data are representative of 1 of 2 experiments performed. Images taken at 100X magnification (TG2 activity in displayed in green, nuclei displayed in blue). All images were acquired with the same parameters. For each slide, 4 or 5 regions are selected and Gray value (intensity of fluorescence) measured. Bar charts show mean Gray values + SEM of n=3

SW620 cells were transfected with 3 μg of pLPCX-TG2 plasmid using 3 μL of Lipofectamine LTX + 3 μL of PLUS reagent. Results in Figure 4.7 show that transfection of a TG2-encoding plasmid caused a ~20% increase in TG2 activity compared to untreated cells.

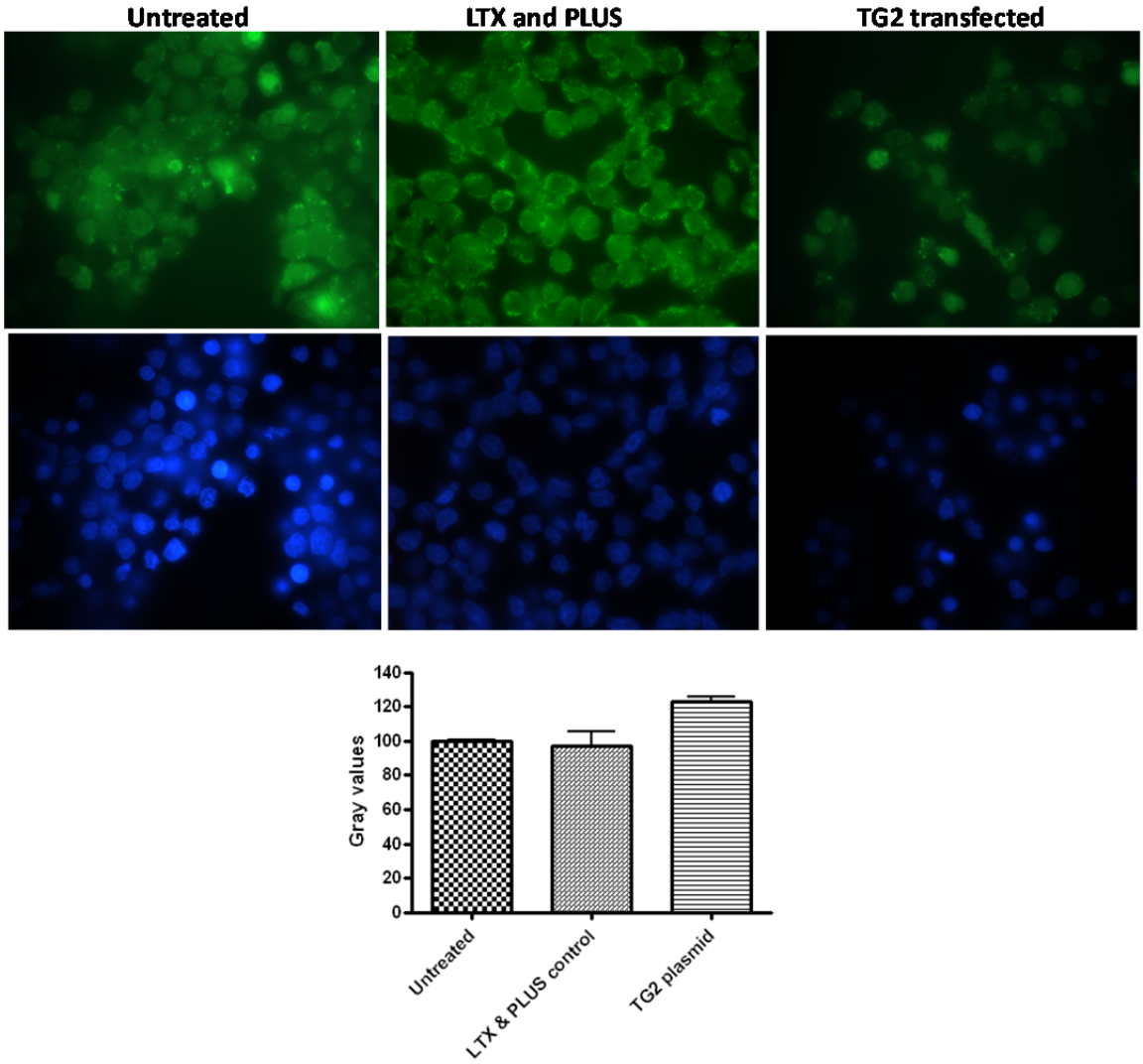

Figure 4.7 - TG2 activity assay upon transfection of a TG2-encoding plasmid in SW620. Data are representative of 1 out of 2 experiments performed. Images taken at 100X magnification (TG2 activity in displayed in green, nuclei displayed in blue). All images were acquired with the same parameters, however for printing purposes the luminosity of "Untreated" and "LTX-PLUS" conditions have been increased. For each slide, 4 or 5 regions of the raw images were selected and Gray value (intensity of fluorescence) was measured. Bar chart shows mean Gray values + SEM of n=2.

4.4 Biological significance of differential levels of TG2 in primary and metastatic colon cancer

4.4.1 Expression of autophagy markers

Results in Figure 4.8 show that starvation of SW480 (**a**) and SW620 (**b**) cells for 6-18h caused a progressive increase in expression of the autophagy markers ATG7, ATG14 and Vps34. Comparisons within each cell line were made to their respective unstarved control (0h). In SW480, the levels of each of the three genes analysed after 18h of starvation were higher compared to their respective levels measured after 6h and 12h, and compared to the unstarved control (0h). In SW620, the levels of the three genes analysed after 18h of starvation were higher compared to the control; additionally, the levels of ATG14 analysed after 18h were higher compared to 6h. Furthermore, the levels of Vps34 analysed at an earlier time point (12h of starvation) were also different compared to the control.

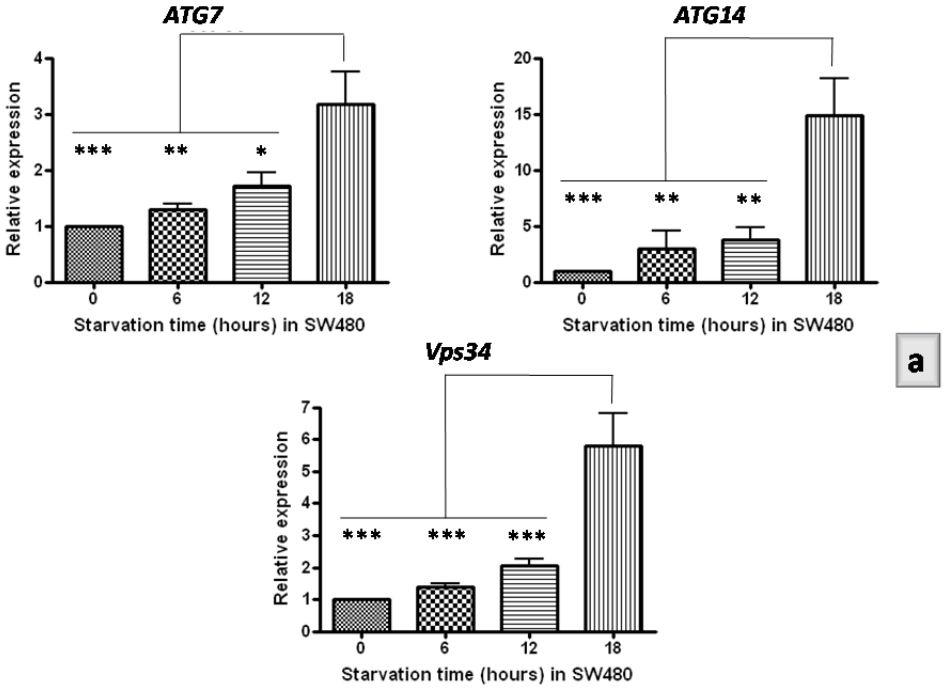

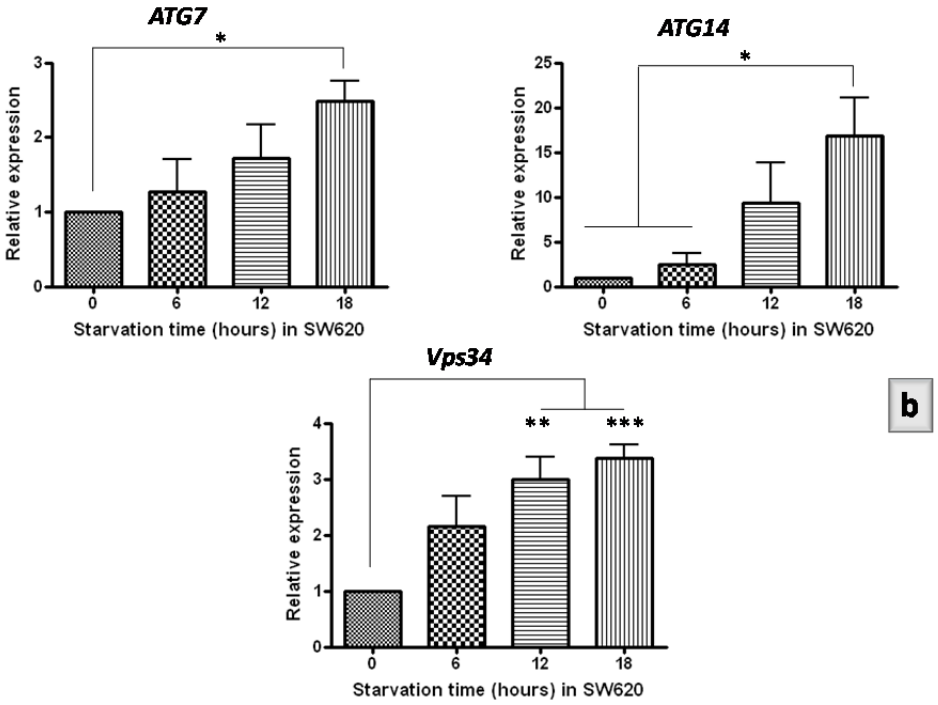

Figure 4.8 - Gene expression of ATG7, ATG14, Vps34 (relative to β-actin) measured by qPCR after 6-18h starvation in SW480 (a) and SW620 (b) cells. Data represent mean + SEM of 3 or 4 independent experiments; statistics analysis carried out by one-way ANOVA

Figure 4.9 shows the same data as in Figure 4.8, but differently plotted in order to highlight the differences between cell lines. In this graph, all data were normalised to SW480 unstarved control. Results in Figure 4.9 show that there were no differences in the levels of ATG7 and ATG14 between cell lines, either basally or following starvation. Conversely, levels of Vps34 were consistently ~3-5-fold higher in SW620 than in SW480, with significant differences observed at 6h (p=0.032) and 18h starvation (p=0.044).

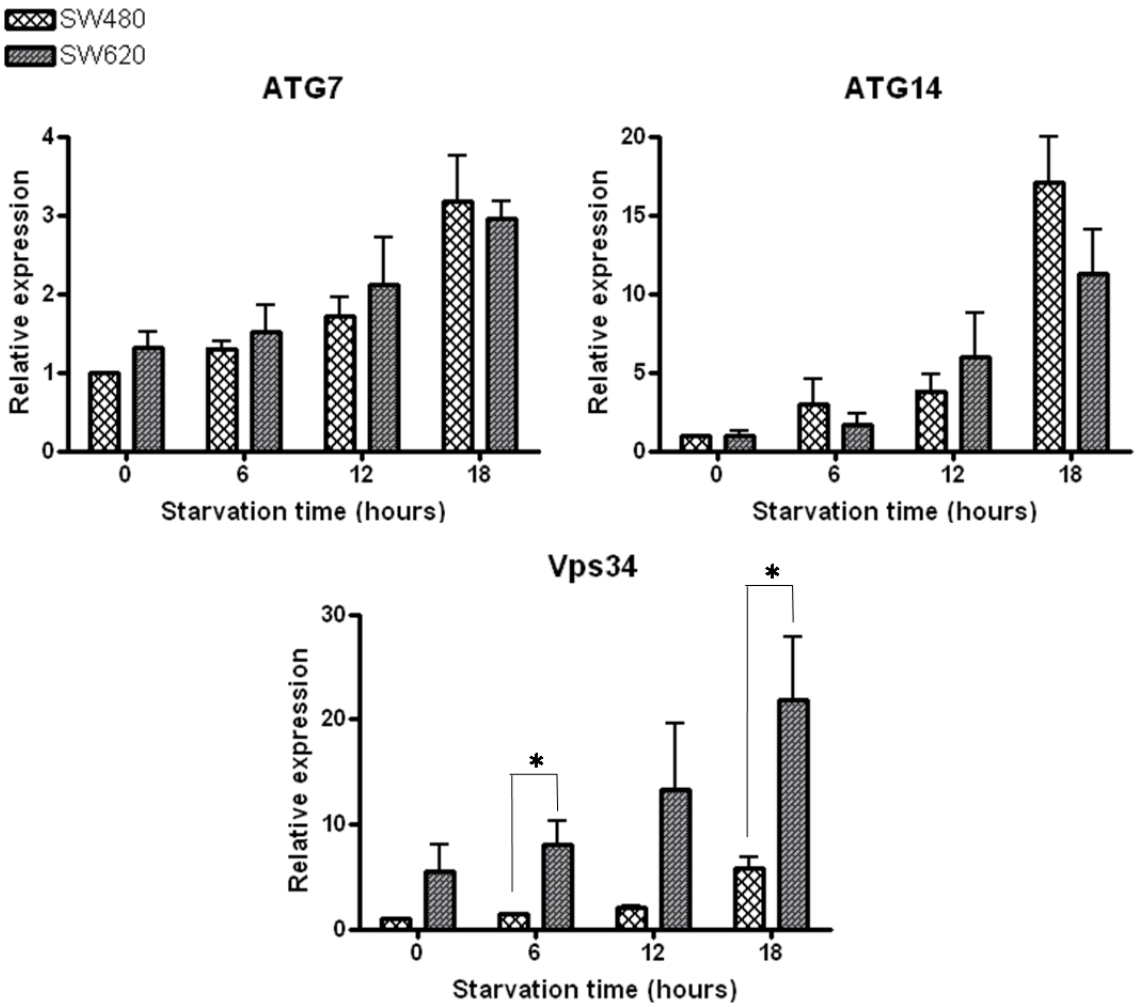

Figure 4.9- Gene expression of ATG7, ATG14, Vps34 (relative to β-actin) measured by qPCR after 6-18h starvation of SW480 (a) and SW620 (b) cells. In each plot, data are normalised to the unstarved SW480 sample. Data represent mean + SEM of at least 3 independent experiments.

4.4.2 Expression of TG2 following starvation

Figure 4.10 shows the analysis of TG2 cDNA in samples that had undergone the same treatment as above (control, and starved for 6-18h). Results show a progressive reduction of TG2 cDNA levels in SW620, but not in SW480, following 6-18h starvation, compared to controls (0h).

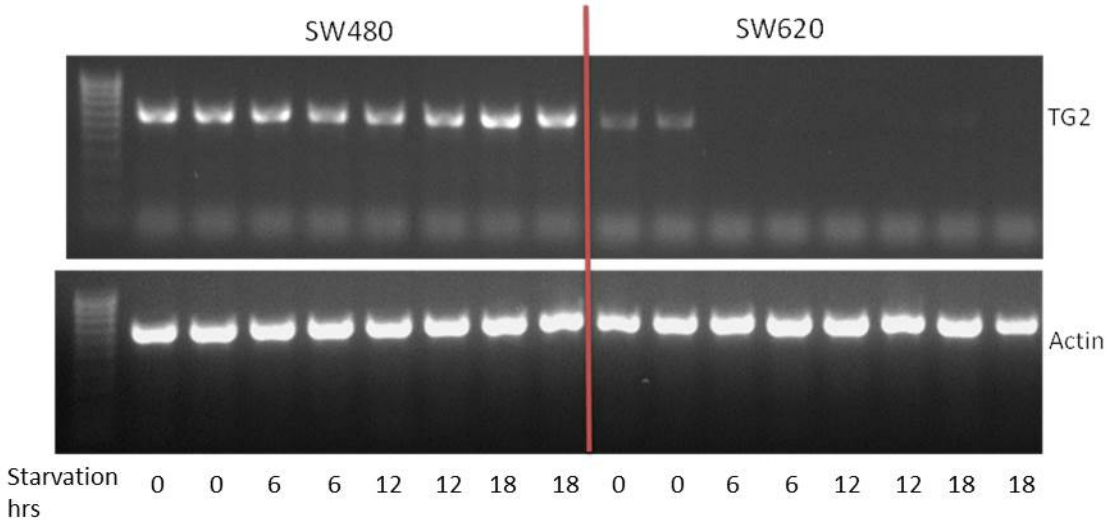

Figure 4.10– Gel electrophoresis of TG2 (upper gel) and Actin (lower gel) cDNA amplified by PCR. The table below the image indicates the loading order of the samples. Results here displayed combine 2 out of 3 experiments performed

4.4.3 Expression of Beclin-1 and p62 proteins following starvation

Figure 4.11 shows Western blot analysis of p62 and Beclin-1 proteins in SW480 and SW620 following 6-18h starvation. Panel **a** shows that, in SW480, p62 protein was barely detectable in the non-starved control or at any duration of starvation. In panel **a** it is also possible to see that Beclin-1 protein was abundant in non-starved SW480 cells (compared to the Actin internal control) and showed a slight but progressive decrease following starvation. Panel **b** shows that, in SW620, the levels of p62 protein were not visibly different between starved and non-starved samples. In panel **b** it can be seen that Beclin-1 protein was abundant (compared to the Actin internal control) in non-starved SW620 cells and showed a slight but progressive decrease following starvation. Furthermore, Figure 4.11 shows that Beclin-1 protein is more abundant in SW620 than in SW480.

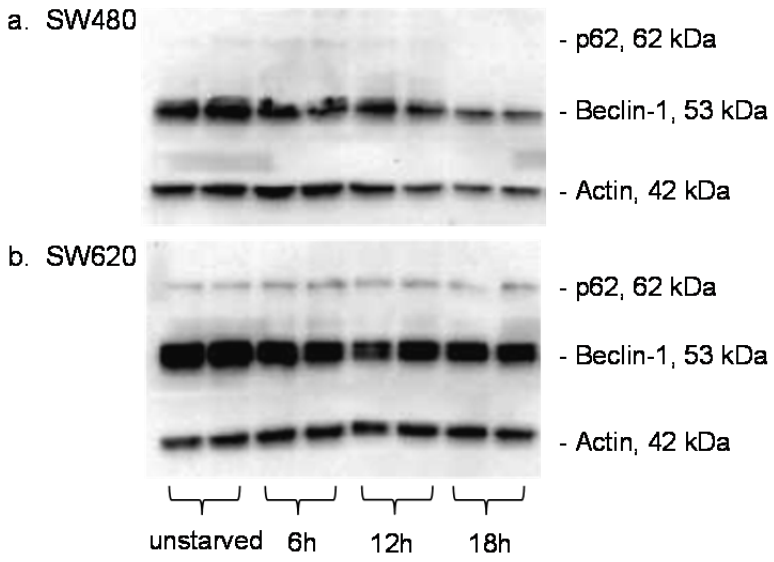

Figure 4.11– Western blot analysis of p62 and Beclin-1 in SW480 and SW620 cells starved for 6, 12, 18h or unstarved. Actin was used here as a loading control, as well as an internal reference for comparing the abundance of the proteins of interest. Results here displayed combine 2 out of 3 experiments performed

4.4.4 Invasion assay and MMP analysis

Results in Figure 4.12 panel **a** show that SW620 were more invasive compared to SW480, and compared to Cystamine-treated SW620 (p<0.001 in both cases). In panel **b** it is shown that transfection of a TG2 plasmid to SW620 decreased invasiveness when compared to the same cells transfected with a TG2 mutant plasmid lacking crosslinking activity, or to the control conditions (p<0.001 in all cases). In panel **c** it is shown that silencing of TG2 in SW480 increased invasiveness when compared to the control conditions. In panel **d** it is shown that SW480 stably transfected with miR-19a were more invasive than control (SSC); furthermore, when the miR-19a SW480 clone was transfected with a TG2 plasmid, invasion decreased despite staying higher than in control cells.

To further clarify whether the effect of TG2 on invasive behaviour was mediated by changes in the matrix metalloproteases profile, the gene expression of 11 MMPs was assessed by qPCR. Figure 4.13 left panel shows significant differences in the levels of MMP-7 (higher in SW620) and MMP-14 (higher in SW480). The right-hand panel shows no

significant differences in the expression of any of the tested MMPs in TG2-silenced SW480 compared to control SW480.

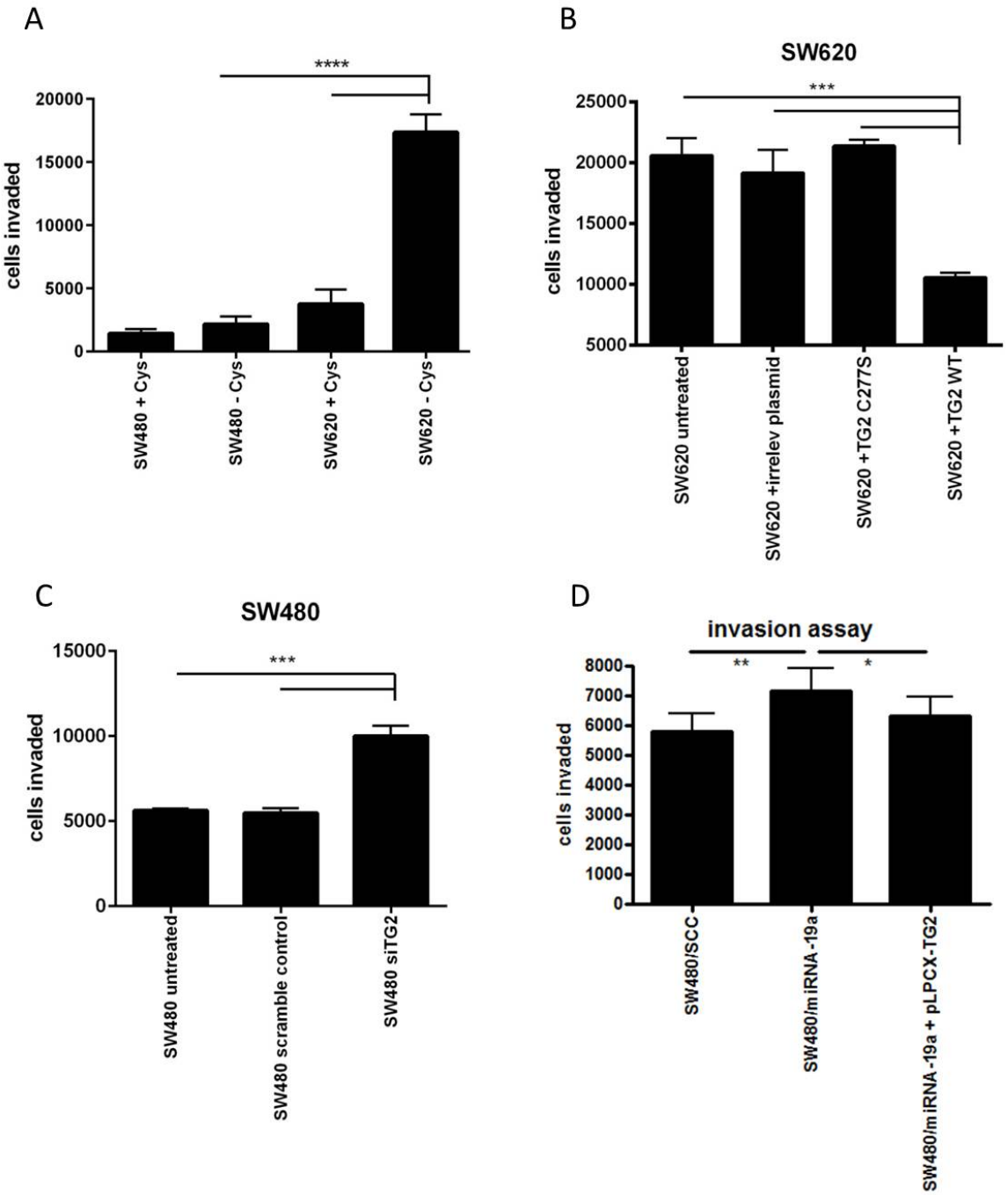

Figure 4.12 – 24h invasion assay of: SW480 and SW620 treated with Cystamine (a); SW620 transfected with TG2 wt and TG2 C277S mutant plasmid (b); SW480 with silenced TG2 (c); SW480/miR19a clones transfected with TG2 (d). Data represent mean + SEM of 3 independent experiments.

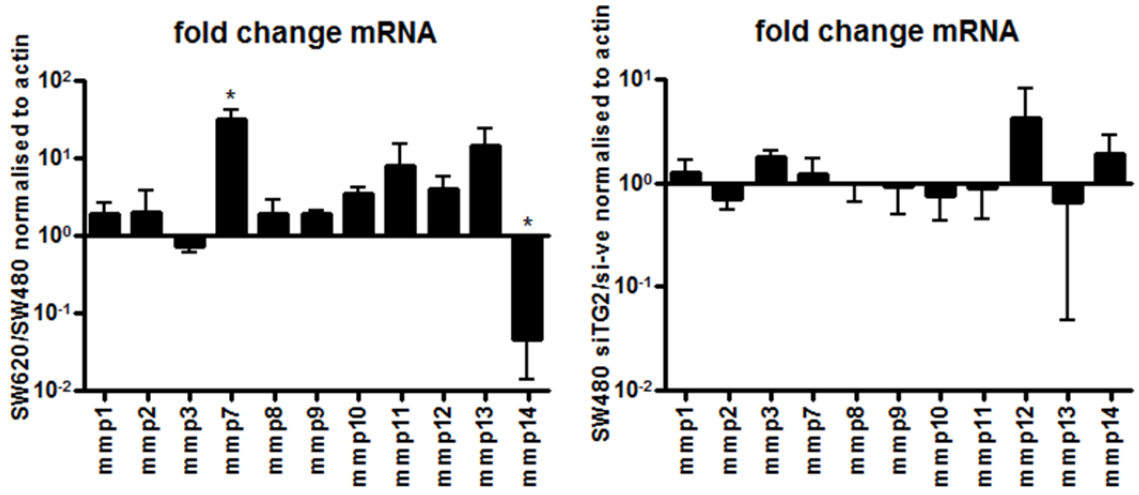

Figure 4.13 - Gene expression values of MMPs expressed as ratio SW620/SW480, pre-normalised for their respective actin content (left panel). Gene expression values of the same MMPs expressed as ratio SW480 siTG2/SW480 –ve control, pre-normalised for their respective actin content (right panel). Values represent mean ± SEM of n=3

4.4.5 Effects of TG2 silencing on the production of pro-inflammatory cytokines

Expression of COX-2, IL-8, IL-10, IL-15, TGF-β, and TNF-α was assessed by qPCR. Figure 4.14 left panel shows significantly higher gene expression of IL-8, IL-10, IL-15 and TGF-β in SW480 compared to SW620. The right-hand panel shows no significant differences in the expression of any of the tested cytokines in TG2-silenced SW480 compared to control SW480.

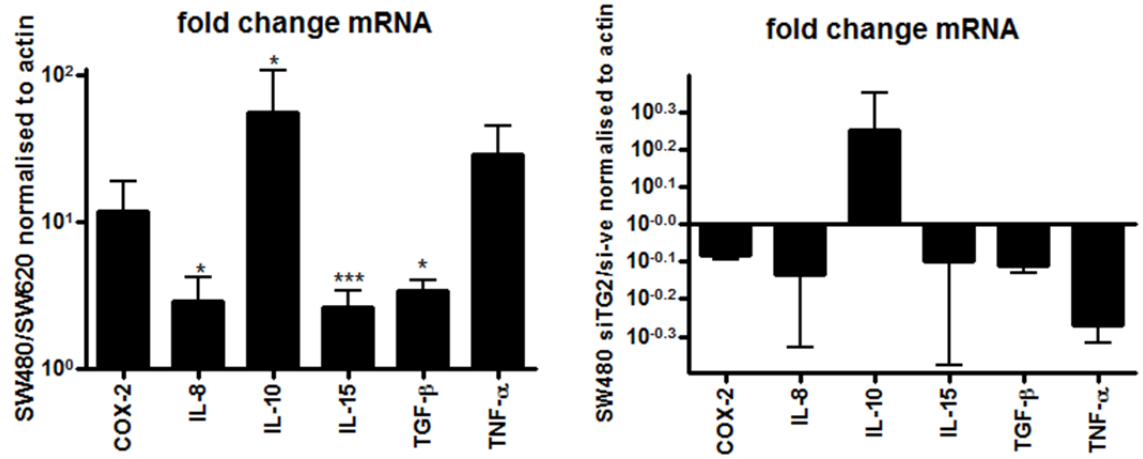

Figure 4.14 – Gene expression values of cytokines expressed as ratio SW480/SW620, pre-normalised for their respective actin content (left panel). Gene expression values of the same cytokines expressed as ratio SW480 siTG2/SW480 neg control, pre-normalised for their respective actin content (right panel). Values represent mean ± SEM of n=3.

4.4.6 Expression of HLA-I following modulation of TG2.

Results in Figure 4.15 show that 10% of the main population of SW480 cells basally expressed HLA-I molecules on their surface (blue dots in panel **a**, percentage in panel **b**), whereas no SW620 cells expressed HLA-I (blue dots in panel **a**, percentage in panel **b**). Silencing of TG2 in SW480 decreased the number of HLA-I positive cells to 7.5% (panel **c**), whereas transfection of TG2 into SW620 slightly increased the number of HLA-I positive cells to 0.2% (panel **f**). Mean results from the 2 experiments performed (summarised in the bar chart below the FACS plots) show that ~12% of SW480 cells expressed HLA-I molecules on their surface, which decreased to ~8% following silencing of TG2. In addition, ~7% of SW620 cells expressed HLA-I molecules on their surface, which significantly increased to ~32% (p=0.032) following transfection of a TG2 plasmid. To clarify whether the increase in HLA-I molecules observed in the latter condition was due to a direct effect of TG2 on HLA-I trafficking from the endoplasmic reticulum (E.R.) towards the cell membrane, an EndoH assay was performed (as described in section 2.18). Results in Figure 4.16 show that in all EndoH-treated samples we could detect both a Resistant and a Sensitive form of HLA-I, serving as an internal control for the success of the experiment. However, the relative quantities of such forms did not vary upon either transfection or silencing of TG2.

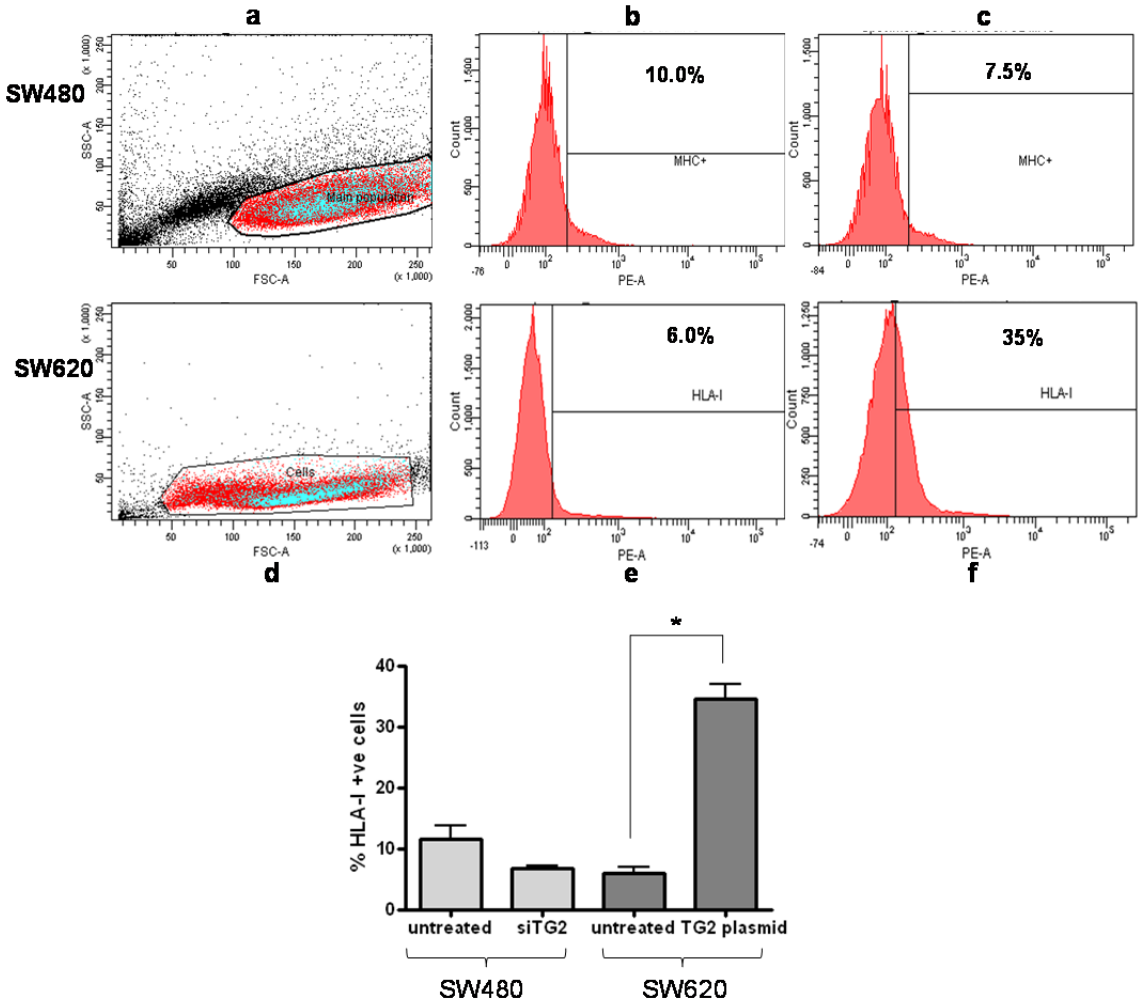

Figure 4.15 – Flow cytometry analysis of total HLA I molecules in SW480 and SW620 cells. Panel a and d show size (FSC) and granularity (SSC) of untreated SW480 and SW620 (respectively), and their basal expression of HLA-I (blue dots within the main population). Panel b and e are histogram plots of basal HLA-I expression in SW480 and SW620, respectively. Panels c and f are histogram plots of TG2-silenced SW480 (c) and TG2-transfected SW620 (f). In histogram plots, the percentages indicate the proportion of cells expressing HLA-I molecules. Best FACS plots from 1 out of 2 experiments performed. Bar chart shows mean + SEM. n=2

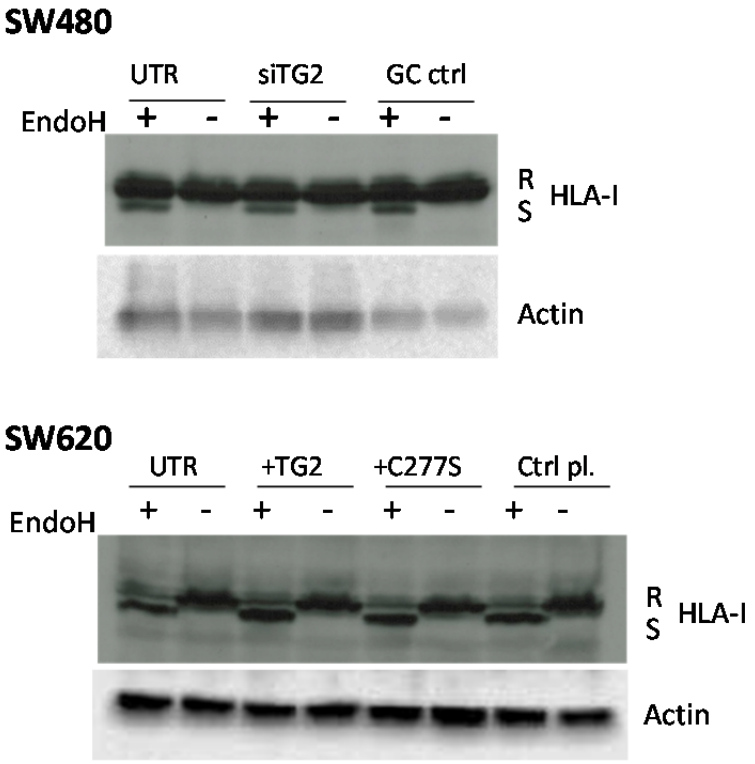

Figure 4.16 – Western blots results of EndoH treatment in SW480 (above) and SW620 (below) cells. HLA-I was detected by HC10 clone antibody. (R) and (S) respectively indicate the resistant (uncleaved) and sensitive (cleaved) form of HLA-I detected. Results are representative of 3 experiments performed

4.5 Discussion

In this chapter I first developed and optimised different strategies for manipulating TG2 levels in SW480 and SW620 cells, by targeting its expression directly (via TG2 DNA plasmid or TG2 siRNA), or indirectly (via miR-19). Secondly, after these optimisations had been carried out and their effectiveness been confirmed, I used these tools in the SW480-SW620 model to understand at a functional level: a) whether the observed difference in TG2 mRNA and protein variants was linkable and attributable to their known difference in miR-19a/b levels, b) whether direct or indirect manipulation of TG2 protein and activity levels would impact on the invasive ability of these cells, c) whether manipulation of TG2 levels would impact on the expression of key autophagy markers, d) whether manipulation of TG2 levels would impact on the surface expression of HLA-I molecules, e) whether by decreasing TG2 I could observe a change in some key pro/anti-inflammatory cytokines.

Manipulation of TG2 levels. In order to decrease abundance of TG2 in SW480, I tested both transfection of a TG2-specific siRNA and transfection of miR19; the latter both in its RNA oligo form, or inserted within a DNA plasmid. In order to increase abundance of TG2 in SW620, I tested both transfection of a TG2-encoding plasmid and transfection of antimiR19a; the latter both in its RNA oligo form, or inserted within a DNA plasmid.

Overexpression of TG2 in SW620 cell line was best achieved by transfection of 3 μg of a TG2-encoding plasmid with 3 μL of Lipofectamine LTX reagent and 3 μL of PLUS enhancer. This condition generated a 12-fold increase in protein expression, compared to the mock-transfected control (Figure 4.1). Being these cells known as hard-to-transfect, and having tried many other transfection methods (not reported here) unsuccessfully, this result was considered satisfactory.

Silencing of TG2 mRNA in SW480 was best achieved by transfection of 50 nM TG2 siRNA with 4.5 μL Hiperfect reagent. This condition generated a 60% decrease in TG2 protein, compared to a control transfected with a Hi-GC scramble RNA (Figure 4.2). Being these cells known as hard-to-transfect, this result was considered satisfactory.

Optimisation of transfection of sense miRNA was technically successful, since the positive control miR-1 caused >90% decrease in one of its validated targets (PTK9), when 50nM were transfected with either Hiperfect or Interferin reagents (Figure 4.3).

Results from transfection of sense miR-19a/b in SW480 showed an effect for both of these miRNAs in reducing TG2 mRNA levels, with the highest reduction achieved by the use of Hiperfect reagent. The opposite effect, i.e. increase of TG2 mRNA was achieved in SW620 only through transfection of antisense miR-19a with Hiperfect. Interestingly, antisense miR-19b did not achieve any significant increase regardless of the transfection reagent used. The results summarised in Figure 4.3 allowed us to conclude that in SW480 both miR-19a and miR-19b can target TG2 mRNA for downregulation; however only miR-19a when silenced can mediate an upregulation of TG2 mRNA.

In view of later performing functional assays that relied on a stable knock-in or knock-down of miR-19a, it was felt that a DNA plasmid-based transfection of these oligos would be the best technique to use. In fact, in Figure 4.4 it is shown that transfection of a miR-19a-containing plasmid successfully downregulated TG2 in SW480; moreover, Figure 4.5 shows that transfection of an antimiR-19A-containing plasmid successfully upregulated TG2 in SW620.

Altogether, these experiments did not simply provide tools for manipulating TG2 levels, but demonstrated for the first time a direct effect of miR-19a on TG2. [N.B. the specificity of miR-19a binding to the TG2 mRNA 3'UTR was confirmed through a Luciferase Reporter Assay performed by our collaborator Dr Karen Pickard, whose results are reported in the publication included in the Supporting Material section of this dissertation].

After having set the conditions for upregulating and downregulating TG2, I sought to determine the impact of TG2 silencing and overexpression on TG2 cross-linking activity. Results in Figures 4.6 and 4.7 indicate that silencing of TG2 in SW480 generated a decrease in TG2 activity (20%), whilst overexpression of TG2 in SW620 generated an increase in TG2 activity (20%). Whereas such a modest increase in TG2 activity in SW620 could be due to TG2 overexpression not being tolerated by SW620, the modest decrease in TG2 activity seen in SW480 upon its downregulation could perhaps be due to a mechanism of compensatory hyperactivity. Whether such a modest increase or decrease in TG2 activity is biologically relevant, it will be assessed through a series of functional studies, hereafter discussed.

Functional studies. Once the tools for manipulating TG2 protein and activity were optimised, I proceeded with the functional characterisation of TG2 in the SW480-SW620 colon cancer model. Firstly I sought to determine whether TG2 had a role in the inhibition of autophagy also in CRC, as already demonstrated in Cystic Fibrosis[134] and pancreatic cancer[69]. It is currently believed that autophagy undergoes a bi-phasic activation in cancer; specifically, high levels of autophagy are believed to prevent oncogenic transformation of

normal cells, but can promote metastasis and acquisition of an MDR phenotype at more advanced stages[119]. Hence, we speculated that the downregulation of TG2 seen in SW620 may represent a way in which metastatic colon cancer cells re-activate autophagy to sustain their phenotype. However, the results in Figure 4.8 and 4.9 show that basal levels of three key autophagy genes (ATG7, ATG14 and Vps34) were not significantly different between SW480 and SW620. Following a period of 6-18h starvation, each of these genes underwent a significant increase above basal levels (thus implying that serum starvation was effective in stimulating autophagy); however, the extent of the increase in ATG7 and ATG14 observed in SW620 was not greater than that observed in SW480. Only Vps34 was greater in SW620 than in SW480, however the significance of this result in this context is unclear.

Further results in Figure 4.10 show that serum starvation did not have any effects on the levels of TG2 in SW480, whereas it did deplete completely TG2 in SW620 starting from 6h starvation through 18h. This last result inverted my thesis, now suggesting that starvation-induced autophagy was having a knock-down effect on TG2. To clarify the matter I therefore proceeded to analysing p62 (whose accumulation is regarded as a marker of impaired "selective autophagy")[147] and Beclin-1 (regarded as the primer of the autophagy process)[188] upon serum starvation. Interestingly, results in Figure 4.11 show that both proteins were expressed at a much higher level in SW620 than SW480, although no differences could be seen upon starvation or upon TG2 silencing or transfection (data not shown here). Taken together, **these results rule out a connection between the different expression of TG2 seen in SW480 and SW620 and autophagy.** On a side note, a possible explanation for the constantly higher levels of p62 in SW620 than in SW480, may lie in the fact that p62 has been demonstrated to mediate Ras-induced activation of NF-kB and, thus, promote proliferation of tumour cells, at least in lung adenocarcinoma[188].

The below Table 4.4 summarizes findings for the set of experiments relating to autophagy and TG2

		TG2	ATG7	ATG14	Vps34	Beclin-1	p62
SW480	unstarved	+++	+	+	+	+++	+
	6h	+++	+	+	+	++	+
	12h	+++	+	+	+	++	+
	18h	+++	++	++	++	++	+
SW620	unstarved	+	+	+	++	++++	++
	6h	-	+	+	++	+++	++
	12h	-	+	+	+++	+++	++
	18h	-	++	++	+++	+++	++

Table 4.4 -Summary of the assessment of autophagy markers in SW480 and SW620 cell lines. Scores arbitrarily assigned.

Next, I sought to determine the invasive potential of SW480 and SW620 cell lines, and if/how this changed upon alterations of TG2 levels. Results in Figure 4.12 panel **a** show SW620 cells had an intrinsically greater ability to invade through an ECM-substitute (Matrigel), which was expected given that SW620 are the metastatic counterpart of SW480. Furthermore, use of a chemical inhibitor of TG2 activity (Cystamine) decreased invasion of both SW620 (to a significant degree) and SW480 (to an almost significant degree), in relation to controls. This result alone indicates that inhibition of TG2 crosslinking activity through use of Cystamine may be useful to decrease further invasion of metastatic cells, whereas at the primary tumour stage this drug would not be effective enough to prevent cells from invading. Results in panel **b** show that transfection of w.t. TG2 in SW620 greatly reduced invasion, compared to controls and compared to the same cells transfected with a mutant TG2 lacking crosslinking activity. These results do confirm that cell invasion is a crosslinking-dependent event (as demonstrated through the use of the activity mutant plasmid), however raise the possibility that Cystamine may act on targets other than TG2. Results in panel **c** show that silencing TG2 greatly increased invasion in SW480 cells

compared to the controls. Importantly, increased invasion was also observed when SW480 were stably transfected with a miR-19a-encoding plasmid; this effect was partially reverted when w.t. TG2 was co-transfected.

The impact that TG2 has on the invasive abilities of SW480 and SW620 does not directly involve key metalloproteases, as it is possible to see in Figure 4.13. This shows that basal expression levels of all MMPs (except MMP-14) were higher in SW620 compared to SW480. These features do not seem to be correlated with the levels of TG2 in these cell lines, since silencing TG2 in SW480 did not significantly raise MMP expression levels to a degree comparable to SW620 .

Overall, these data suggest that in this model miR-19a-induced reduction of TG2 increases invasion, and that TG2 naturally acts a repressor of invasion through its cross-linking activity.

As described in the introduction, cancer formation and growth is favoured by an inflammatory milieu that promotes tissue remodelling and neoangiogenesis both in the primary tumour site and in the metastatic one. Furthermore, in 2008 our research group discovered that high levels of TG2 promote inflammation in chronic inflammatory diseases such as Cystic Fibrosis and Coeliac Disease[115]. For this reason, I proceeded to first assessing the gene expression levels of key pro/anti-inflammatory cytokines in SW480 compared to SW620; and secondly, how such levels changed upon TG2 silencing in SW480. As showed in Figure 4.14 there are basal differences in the levels of expression of IL-8, IL-10, IL-15 and TGF-β between SW480 and SW620; however these do not seem to be correlated with TG2, since silencing in SW480 did not generate a significant change of expression. As a consequence, these differences were not explored further and **it was ruled out that TG2 could act as a promoter of inflammation in the SW480/SW620 cancer model.**

Finally, in an effort to understand whether TG2 may be decreased in SW620 for reasons linked to immune escape, I analysed the basal expression of HLA-I in the SW480/SW620 model, and how this changed upon alteration of TG2 expression. Figure 4.15 shows that

transfection of a w.t. TG2 plasmid in SW620 caused an increased presence of HLA-I on the cell surface; the same figure also shows a decreased HLA-I expression upon silencing of TG2 in SW480 (although not to a statistically significant extent in this case).

I then proceeded to assess whether the increased HLA-I observed in SW620 was due to an increased release of mature (i.e. peptide loaded) HLA-I molecules from the E.R. . Results in Figure 4.16 rule out this possibility, as no differences were detected in the relative amounts of EndoH sensitive (empty) and resistant (loaded) forms of HLA-I upon silencing of TG2 in SW480 or transfection of TG2 w.t. and mutant in SW620.

Taken together, findings in this chapter tell that in SW480 and SW620: i) starvation-induced autophagy decreases expression of TG2 (although only in SW620); ii) TG2 levels do not affect autophagy; iii) reduction of TG2 achieved by direct gene silencing promotes cell invasion, although this is not linked to alteration of the levels of matrix metalloproteases; iv) miR-19a also promotes cell invasion through reduction of TG2; v) TG2 naturally represses cell invasion through its crosslinking activity; vi) TG2 expression is positively correlated with surface expression of HLA-I, but this is not due to a better stabilization of the HLA-I:peptide complexes at the E.R. level; and vii) TG2 is not linked to tumour inflammation.

These findings, with a particular focus on the relationship TG2/cell invasion and TG2/HLA-I lead us to hypothesize another relationship, e.g. TG2/EMT. The reason for speculating this lies in the fact that both cell invasion and HLA-I downregulation are consequential effects of TGFβ-induced EMT[189]. This will be addressed in the next chapter through comparing the behaviour of CRC cell lines (where TGFβ pathway is usually impaired) with that of HCC cell lines (where TGFβ pathway is usually intact).

5. Relationship between TG2 expression and EMT status in CRC and HCC cell lines

5.1 Introduction

Epithelial-to-Mesenchymal Transition (EMT) is the process whereby epithelial cells downregulated their cell adhesion markers in order to acquire a mesenchymal phenotype. This is a physiological process in the context of embryo development. However, in the context of carcinomas, this permits cancer cells to detach from the primary tumour mass and migrate towards distant sites in order to form a metastasis[31].

In molecular terms, this implies loss of cell polarity, downregulation of epithelial cell-specific adhesion molecules (E-cadherin) and intermediate filaments (Keratins), and upregulation of stromal cell-specific adhesion molecules (N-cadherin) and intermediate filaments (Vimentin).

The Transforming Growth Factor beta (TGFβ) acts as an essential EMT mediator during both embryogenesis and cancer, by inducing the transcription of key EMT master regulator genes (among which Snail1, Zeb1, Zeb2/Sip1) either directly through the SMAD pathway, or indirectly through the MAPK pathway[190]. Another fundamental role of TGFβ is suppression of proliferation, both in normal epithelial cells and in cells of the immune system. As such, within a tumour, activation or repression of TGFβ secretion, as well as activation of either the cytostatic or the oncogenic TGFβ-SMAD pathway are cell-type dependent and stage-dependent[191]. Of interest for this study, TGFβ is known to increase cell adhesion and migration through upregulation of TG2 as demonstrated in several *in vitro* models[192,193,194].

The EMT program can also be initiated through the direct engagement of the EGFR and Frizzled receptors by EGF and WNT ligands, resulting in the activation of the MAPK pathway which leads to proliferation and cellular remodeling. Activated RAS-MAPK pathway in turn mediates the switch between cytostatic TGFβ and oncogenic TGFβ, and promotes the autocrine secretion of TGFβ, ultimately creating a synergistic proliferative effect for cancer cells[195,196].

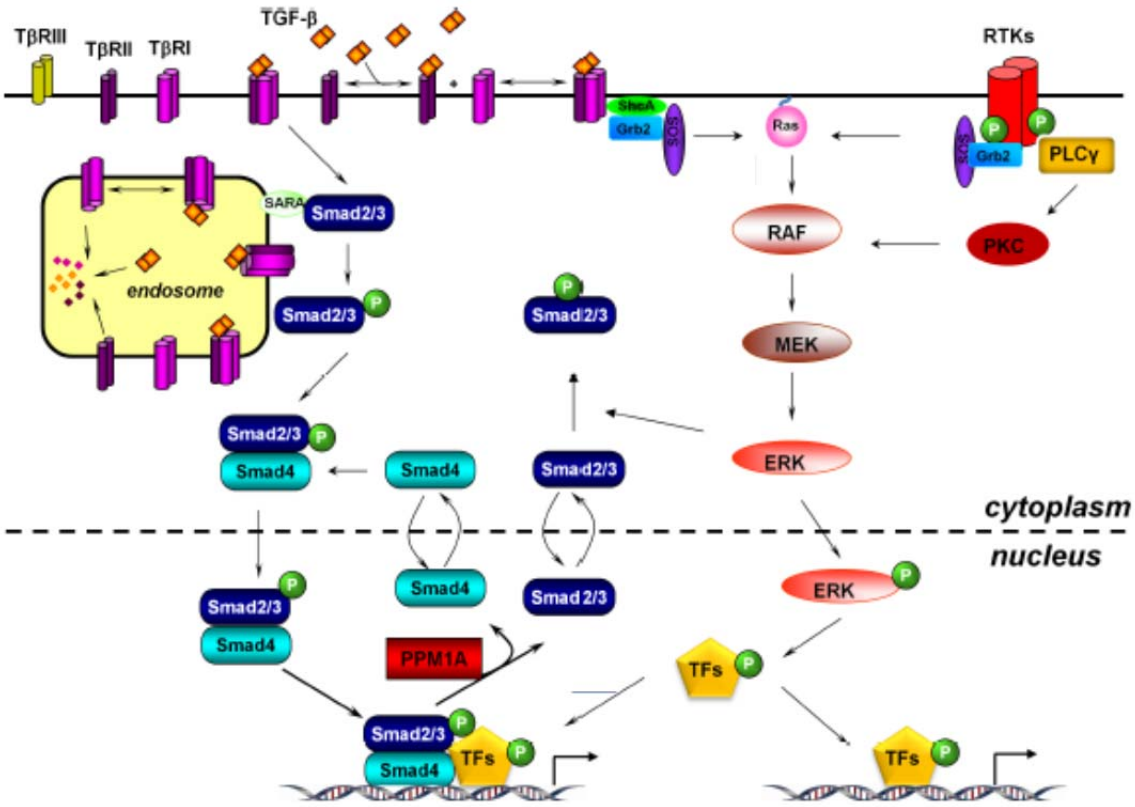

Figure 5.1 – Crosstalks between TGFb pathway and Ras/MAPK pathway, adapted from Chapnik A et al.[197]

Based on this knowledge it is not surprising that most cancers, among which Colorectal Carcinoma (CRC) and Hepatocellular Carcinoma (HCC), accumulate genetic and epigenetic mutations that allow for constitutive activation of the MAPK pathway and/or for the promotion of TGFβ oncogenic functions.

CRC is a heterogeneous group of tumours that can be broadly divided into those characterized by chromosomal instability (CIN), and those characterized by microsatellite instability (MSI). It has been estimated that 16-25% of all CRC carry loss-of function SMAD4 mutations, and that 40-65% of them carry gain-of-function K-RAS mutations; furthermore 75-90% of MSI+ CRC show mutations in the TGFBRII gene[36]. Of the CRC cell lines that will be used in this section of the study, three are MSI- (namely SW480, SW620, Colo205) characterised by intact TGFBRII gene, but absent SMAD4 gene; whereas one is MSI+ (namely HCT116) characterised by intact SMAD4 gene, and homozigously mutated TGFBRII

gene[198]. Loss of SMAD4 seems to be particularly advantageous in CRC, since this event promotes migration, invasion and drug resistance[199,200].

The EGFR pathway is frequently found constitutively active in CRC, due to gain-of-function mutations affecting key molecules of this pathway, among which K-RAS, B-RAF[201] and the EGFR itself[202]. The scenario is made more complicated by the fact that this pathway may be mutated at different levels, hence therapies aimed at restoring the function of one protein of the pathway may not be sufficient to arrest replication of cancer cells; furthermore, following the first cycles of chemotherapy cells acquire drug resistance whose mechanisms are still unclear[203].

HCC is the most common type of liver cancer, and similarly to most cancers, it develops within a context of persistent inflammation. It is currently believed that hyperactivation of the EGFR pathway in HCC (due to EGFR overexpression) is what drives production of inflammatory mediators, which in turn are essential for fast tumour proliferation, neo-angiogenesis and metastasis[204].

Virtually all cells at all physiological developmental stages remain sensitive to TGFβ and its cytostatic effects. In cancer, however, cells quickly try to blunt TGFβ cytostatic pathway in order to warrant their hyperproliferation, and/or limit TGFβ action to those tumour-promoting effects (e.g. ECM remodeling, expansion of cancer-associated fibroblasts, recruitment of immunosuppressive T-regs). Therefore, cancers may partially retain or completely lose functionality of TGFβ pathway by accumulating mutations either upstream (affecting TGFBRI or TGFBRII), or downstream (affecting SMADs)[205].

HCC is one such model where TGFβ pathway is still functional, yet skewed towards just pro-tumoral changes, such as EMT activation. Conversely, in CRC an increasing loss of functionality of TGFβ pathway is seen during the adenoma-carcinoma-metastasis progression[206]. Therefore in HCC and CRC cell lines, the response to *in vitro* administration of TGFβ is expected to be different and perhaps involving different intracellular mediators.

Currently, there is very limited literature exploring the link between TG2 with the TGFβ/EMT pathway or the EGFR/proliferation pathway (earlier reviewed in section 1.2).

In this chapter I aim at assessing firstly whether TG2 presence correlates with expression of key EMT markers; secondly, whether activation or inhibition of the TGFβ and EGFR pathways can alter the expression of TG2 and of EMT markers. Findings will help elucidate whether TG2 plays a mediator role in TGFβ–induced EMT.

5.2 Materials and methods

For this section of the study, a total of 4 CRC cell lines (2 epithelial, 2 mesenchymal) and 4 HCC cell lines (2 epithelial, 2 mesenchymal) were used. The main mutations affecting these cell lines are shown in table 5.1 below.

For TG2 overexpression and silencing experiments, the best conditions as determined in Section 4.3.1 were used experiment. For experiments of manipulations of the TGFβ and EGFR pathway, all epithelial cell lines were exposed to 4ng/mL soluble hTGFβ1 (RnD, #100-B) for 72h, or to 5ng/mL soluble EGF (Cell Signaling, #8916) for 24h; all mesenchymal cell lines were exposed either to 4 μM TGFβRI kinase inhibitor V (ALK V, Calbiochem, #627536-09-8) or to 10μM MEK1/2 inhibitor (UO126, Calbiochem, #109511-58-2) for 24h. Cells treated with soluble EGF and UO126 were serum-starved overnight before drug being added. At the end of the treatments, cell lysates were prepared as detailed in Section 2.7, and Western blotting performed as of Sections 2.8-2.9.

Cell line	Main known mutations
SW480	SMAD4 neg ; K-RAS mut ; APC mut ; p53 mut
SW620	SMAD4 neg ; K-RAS mut ; APC mut ; p53 mut
HCT116	TGFBRII mut; K-RAS mut; b-Catenin mut
Colo205	SMAD4 neg; APC mut, p53 mut
HUH7	p53 mut
PLC/PRF	p53 mut
SNU475	p53 mut
SKHEP-1	B-raf mut

Table 5.1 – Main known mutations found in HCC and CRC cell lines used in this section

5.3 Results

5.3.1 Effects of TG2 modulation on key EMT markers in CRC

Expression of EMT markers Zeb1, Snail1, Vimentin, E-Cadherin, and of the cytoskeleton-associated protein β-Catenin was assessed by Western blot upon silencing TG2 in SW480, The analysis of β-Catenin in this context was deemed important as the β-catenin gene in SW480 and SW620 is wild type and its pathway constitutively active, despite the presence of a mutated APC gene[207].

Results in Figure 5.2 show that SW480 shows a moderate mesenchymal phenotype, with low basal expression of Zeb1 and Vimentin. Silencing TG2 in these cells caused a reduction of Zeb1 and Vimentin expression, whereas E-Cadherin was not affected.

The abundance of Snail1, one of the master regulators of EMT, did not show any changes upon silencing of TG2. The levels of β-Catenin, a protein involved in cytoskeleton rearrangement occurring during EMT, did decrease upon TG2 silencing.

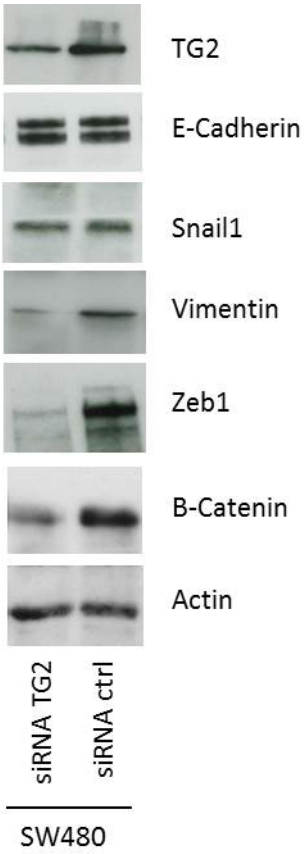

Figure 5.2 – Western blot analysis upon TG2 silencing in SW480. 20μg total cell lysate loaded. Best results out of n=3 experiments performed.

5.3.2 Effects of modulation of TGFβ and EGFR pathway in CRC and HCC

Epithelial cancer cell lines were exposed to TGFβ or EGF, whereas mesenchymal cancer cell lines were exposed to TGFβRI inhibitor and MEK1/2 inhibitor. Results shown in Figure 5.3 below show that treatment with EGF in HCC cells with an epithelial phenotype, causes a marked decrease of EGFR, suggestive of an enhanced recycling of this receptor at the cell surface. All other markers suffered minor or no variations compared to control. Interestingly though, in both cell lines it is possible to observe a decrease of pSMAD2/3.

Treatment with TGFβ in these cells, causes a marked increase in TG2, Vimentin, pSMAD2/3 and pERK1/2. It also causes increase of pAKT in HUH7 and a slight decrease of total ERK1/2 in PLC. The efficacy of TGFβ treatment itself is demonstrated by the increase in the phosphorylated forms of transcription factors SMAD2 and SMAD3.

Treatment with UO126 in HCC cells with a mesenchymal phenotype caused a slight increase in total ERK1/2 in SKHEP1 cells, and a slight decrease in pERK1/2 in SNU475. Furthermore a slight increase in pAKT accompanied by a decrease of total AKT could be observed in SNU475 only.

Treatment with TGFβRI-inhibitor caused a marked decrease in pERK1/2 in both cell lines. Furthermore it caused a slight increase in levels of total ERK1/2 in SKHEP1, as well as a slight increase in pAKT in SNU475.

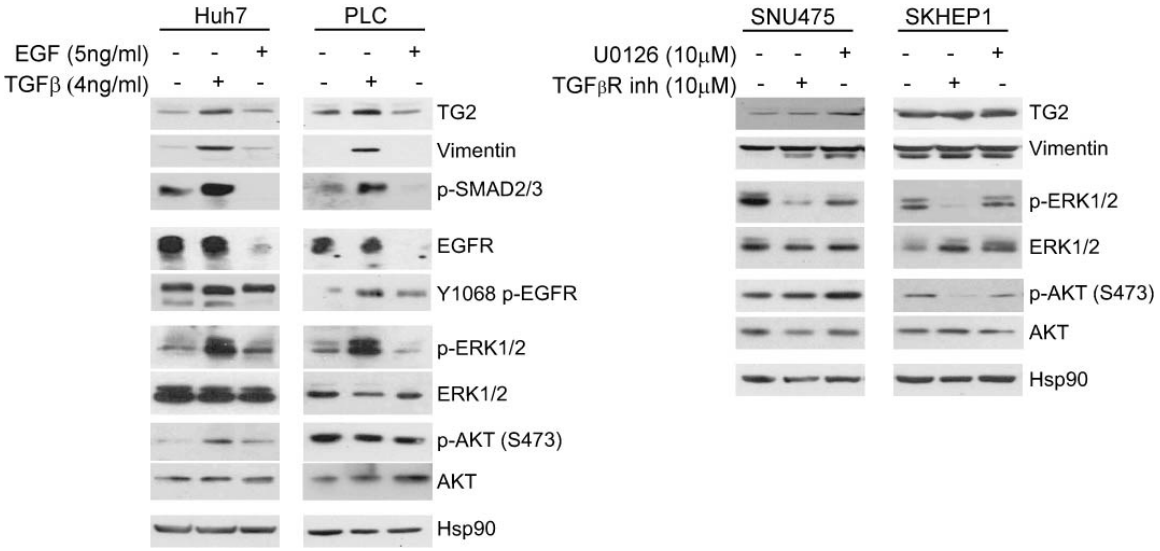

Figure 5.3 – Western Blot analysis of markers in HCC cell lines. 30 μg total cell lysate loaded. Best results out of n=2 experiments performed.

Results shown in Figure 5.4 below show that treatment with EGF in CRC cells with an epithelial phenotype, caused a marked decrease of EGFR suggestive of an enhanced recycling of this receptor at the cell surface. Furthermore, levels of pEGFR and pAKT were markedly increased in Colo205 but not in HCT116. Levels of pERK1/2 were also sharply increased in both cell lines.

Following treatment with TGFβ, a marked increase affecting only HCT116 cell line could be observed for the following markers: TG2, EGFR, pEGFR, total ERK1/2, pAKT.

Treatment with UO126 in CRC cells with a mesenchymal phenotype caused a sharp decrease in pERK1/2 in both cell lines. It also caused an opposite effect on Vimentin (decrease in SW620, increase in SW480).

Treatment with TGFβRI-inhibitor caused a slight decrease in pERK1/2 as well as total AKT in SW620 only. On the contrary, it caused a slight increase in Vimentin and total ERK1/2 in SW480 only.

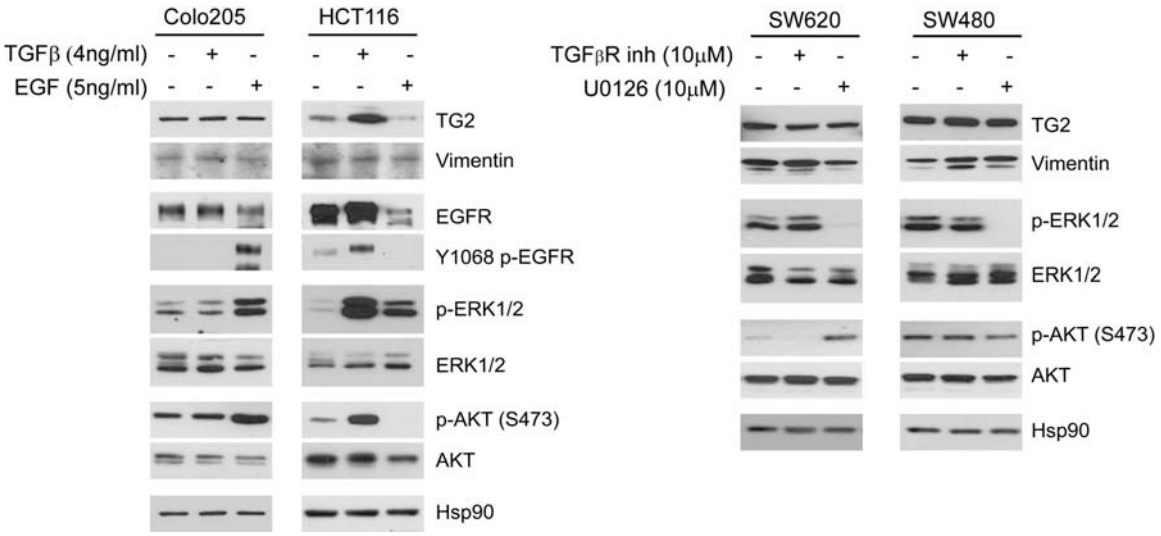

Figure 5.4 - Western Blot analysis of markers in HCC cell lines. 30 μg total cell lysate loaded. Best results out of n=2 experiments performed.

5.4 Discussion

The association between TG2 and EMT has already been proven in experimental models of ovarian cancer[208], breast cancer[209], epidermal cancer[125], pancreatic cancer[210], but not in HCC or CRC.

Experiments performed in this chapter were aimed at determine whether a correlation between TG2 and EMT exists in HCC and CRC, and if so, whether such correlation relies on either the TGFβ or the EGFR pathway. Both HCC and CRC *in vitro* models carry a degree of alterations to the TGFβ and EGFR pathways; however, unlike in CRC, TGFβ pathway is intact in HCC and still able to induce EMT.

Based on the existing literature and genetic backgrounds of these two cancer types, we had speculated that TG2 would act as an EMT promoter in HCC, and as an EMT suppressor in CRC.

The first observation that could be made in CRC was that SW480 show higher basal levels of mesenchymal markers, compared to SW620 which show higher basal levels of epithelial markers. This phenotype was in keeping with their microscope appearance (Figure 3.5) as well as with other reports of the literature describing the same phenomenon[211,212], and it is due to the fact that SW480 were generated from an already advanced stage of primary CRC, whereas SW620 were generated from an established metastasis where it is highly likely that cells had undergone the so-called Mesenchymal-to-Epithelial transition. Furthermore it has been reported in these cells that loss of SMAD4 is correlated with loss of the invasion suppressor E-Cadherin[213].

TG2 may have an important role in maintaining a mesenchymal phenotype in SW480, in fact when TG2 in these cells was silenced, the markers Zeb1 and Vimentin decreased neatly; such a decrease, however, was not mirrored by a reactive increase in the epithelial marker E-Cadherin, which suggests that blunting TG2 expression is not in itself enough to generate a complete phenotypical switch.

Importantly, we found out that **TG2 abundance is directly proportional to β-Catenin abundance**; this represents a novel link between TG2 and β-Catenin in CRC cells. The analyses performed do not allow us to comment over the intracellular localization of β-Catenin upon manipulation of TG2 levels; however by consolidating results shown in the previous chapters we speculate that SUMO-TG2 may form a tight complex with β-Catenin at the cell-cell junctions (Figure 3.9), thus controlling tumour cell invasion (Figure 4.12). As a consequence to this theory, downregulation of TG2 in CRC leading to disruption of tight junctions would become a prerogative for cells in order to detach from the primary tumour mass and metastasize.

With regards to the comparison between HCC and CRC, we observed that **exposure of epithelial HCC cells to TGFβ caused TG2 to increase and initiate EMT**, as demonstrated by increase of the mesenchymal marker Vimentin. Such result indeed confirmed our hypothesis and represents a novel finding in HCC, never to our knowledge reported before; it also suggests a pro-tumoral role for TG2 in HCC, in keeping with the GeneHub-GEPIS database which reports increased levels of the TGM2 transcript in tumour compared to normal liver, and with a proteomic study that presented TG2 as a novel and reliable oncomarker for those AFP-deficient HCC[214].

Another observed effect of TGFβ, which was evident in all epithelial HCC apart from Colo205, was to promote phosphorylation (i.e. activation) of ERK1/2, thus demonstrating here a direct link between the TGFβ and the EGF pathway. Paradoxically, it was interesting to note that **TGFβ activated downstream mediators of the EGFR/RAS pathway more powerfully than EGF itself**, thus suggesting a synergistic activation of the EGFR/RAS pathway by both proper EGFR ligands and TGFβ in SMAD4 competent epithelial cell lines. Demonstration that the EGFR pathway was indeed active, was given by the disappearance of EGFR protein, which is a distinctive feature of the negative feedback loop activated upon EGF binding[215].

On the contrary, blockade of the TGFβ pathway at the receptorial level either in HCC or CRC mesenchymal cells did not have any effects on TG2 expression, thus suggesting the existence of redundant ways of keeping TG2 expression high. It is nonetheless worth highlighting that at least in HCC blockade of the TGFβ pathway did reduce considerably the amount of pERK and pAKT, thus confirming again the direct effect of TGFβ on the EGFR/RAS pathway. This interaction has already been reported a small number of times in the literature, with one proposed mechanism involving generation of an EGF-like fragment through proteolysis activated via the TGFβ/SMAD4 route[216], and another mechanism

suggesting direct phosphorylation of the ShcA adapter which leads to the activation of the Grb2/SOS/RAS/RAF cascade[197].

Finally, despite the existence of studies reporting the direct effect of EGF and oncogenic RAS on the levels of TG2 (reviewed in Section 1.2), none of the CRC and HCC cell lines tested showed any changes in TG2 levels following either activation or blockade of the EGFR/RAS pathway. This result was somehow surprising, considering that we selected cell lines both with and without mutations affecting the EGFR/RAS pathway.

6. Conclusions

Cancer is a complex pathology that affects 14 million new patients every year, claiming 8 million lives every year. As such it represents an urgent global health matter, as well as being a heavy burden on worldwide health services providers. The use of broad-spectrum anti-cancer treatments (whether in combination or not with surgery), is not always effective as most cancers show a recurrence after a disease-free period. Recurrences are usually more aggressive than the original tumour, and require more radical chemotherapies, which leave the patient severely immunodepressed. In the last decade the worldwide scientific community has reached a consensus over the need for a more "personalised medicine" which would first scan the genome of the cancer patient for unique alterations, then develop a treatment aimed at arresting the cancer at the earliest possible stage and with minimum impact over bystander organs. This approach is not far from becoming reality in the most medically advanced parts of the world, due to the lowering costs of whole genome sequencing. In light of this, the discovery of more specific predictive and prognostic oncologic markers, and the discovery of new "druggable" key regulators of carcinogenesis and metastasis are important focuses of current cancer research.

In such a context, my study had the purpose of providing a better understanding of the role of intracellular tumour-expressed TG2 as an anti-tumoral factor. The *in vitro* model I selected for this study was made up mainly by two CRC cell lines, SW480 and SW620, the former being a high-TG2 expressing line derived from a primary colon tumour, and the latter being a low-TG2 expressing line derived from a lymph-node metastasis of the same patient. The usefulness and uniqueness of these cell lines to study progression of colorectal carcinogenesis had already been confirmed in 2001[217]. Furthermore, a study carried out in 1991 did already show that TG2 activity in these cells was inversely correlated with their metastatic potential[95], but the functions of TG2 as a tumour suppressor have not since been assessed in further depth.

In order to fully comprehend the model, I first carried out extensive characterisation of TG2 showing that its levels of mRNA, protein, and cross-linking enzymatic activity were

consistently higher in SW480 than in SW620 (Fig. 3.1, 3.2, 3.7); accordingly, TG2 staining in CRC tissue sections was higher in primary compared to metastatic tumour (Fig. 3.10).

Importantly, I discovered that one of TG2 mRNA variants and its corresponding protein isoform were relatively higher in SW620 compared to SW480 (Fig. 3.2). Considering that the main variant TGM2_v1 and the secondary TGM2_v2 differ in their 3'UTR, I hypothesized a miRNA-mediated regulation of TG2 expression, substantiated also by the knowledge that miRNA can affect mRNA stability as well as translation[187]. *In silico* and experimental analyses conducted in parallel by our project collaborators, identified miR-19a as a regulator of TG2 expression, due to it being expressed at much higher levels in metastatic CRC compared to primary CRC both *in vitro* and in tissue sections. This theory was confirmed by 3'UTR Luciferase assay (performed by collaborator Dr K. Pickard). Furthermore, functional assays I performed proved that in the CRC model miR-19a reduced TG2 expression, and this downregulation was responsible for invasion and metastasis (Fig. 4.3, 4.4, 4.5, 4.12).

As revealed by flow cytometry analysis in SW480 and SW620, almost all TG2 molecules were expressed intracellularly, rather than on the cell surface (Fig. 3.6), thus reinforcing the idea that the intracellular form of TG2 was responsible for controlling cell invasion. Furthermore, I showed for the first time that, together with a translational regulation of TG2 mediated by miR-19a, a higher SUMOylation/Ubiquitylation may be responsible for extending TG2 protein half-life in SW480 compared to SW620 (Fig. 3.9). Importantly, the majority of the events of SUMOylation and Ubiquitylation took place at the edges of the cells, thus suggesting a possible interaction (via enzymatic cross-linking) of TG2 on proteins of the adherent junctions complex. This interaction was clearly demonstrated in SW480 where silencing of TG2 caused a marked decrease in β-Catenin (Fig. 5.2), thus suggesting that the event of TG2 downregulation observed during the transition carcinoma-metastasis in CRC is essential to allow disruption of cell-cell interaction and promote metastasis.

Future work might help shed a light on the exact mechanisms of interaction between TG2 and β-Catenin, as well as the fate and location of β-Catenin upon removal of TG2.

In an attempt to explore other functional roles for TG2 in CRC which could be compatible with the dual expression seen in the SW480/620 model (i.e. high in the primary tumour, low in the metastatic), other hypotheses were considered and tested.

One such hypothesis, was the correlation between levels of TG2 and HLA-I, which was based on the knowledge that TG2 can cross-link β2-microglobulin[75], an essential molecule for the maturation and cell surface display of HLA-I[76]. As such an inverse correlation was hypothesised between TG2 and HLA-I expression; however, what was found was even more interesting. In fact, results showed that silencing of TG2 decreased the proportion of SW480 cells expressing HLA-I, whereas transfection of a TG2 plasmid in SW620 increased such proportion. This suggests that downregulation of TG2 during the carcinoma-metastasis transition in CRC may be functional also to reduce Cytotoxic T Cells-mediated killing which would otherwise occur through engagement of HLA-I. Future work might shed a light on the exact mechanisms and location of the interaction between TG2 and HLA-I, as well as its consequences on $CD8^+$-mediated killing of cancer cells.

Another one of those functional hypotheses, which had already been proven true in the context of chronic inflammatory diseases[117], was the correlation TG2/autophagy. Given the dual role of autophagy in cancer (anti-tumoral at early stages, pro-tumoral at later ones), its correlation with TG2 levels was tested, but in this case no relationship was found.

Finally, given the already established correlation between TG2 and TGFβ-induced EMT in several cancer types[125,208–210], I tested whether the same correlation could be found in HCC cells (where TGFβ pathway is functional) and in CRC cells (where TGFβ pathway is dysfunctional). Results showed clearly that TGFβ induced EMT and TG2 increase only in HCC. Additionally, I discovered that TGFβ was able to strongly induce the EGFR/RAS pathway in HCC cells and in CRC TGFBRII-defective epithelial cells, but not in CRC SMAD4-defective cells. This observation in itself may benefit of further studies since, in my

knowledge, to date there is only one study reporting non-canonical TGFβ signalling occurring through interactions between TGBRI and TGFBRIII in a *Tgfbr2* mutant mouse model[218].

SMAD4 loss or inactivation represents an early event in MSS subtypes (due to chromosome instability at the 18q region), and a late/advanced stage event in all other subtypes. It is quite a common finding in CRC and associated with a very poor prognosis[219]. Furthermore, SMAD4 is also one of mir-19a targets[220]. MiR-19a is located on Chromosome 13q which is often found amplified in advanced CRC, hence miR-19a likely mediates SMAD4 inactivation in all advanced CRC, independent of their microsatellite stability.

The results obtained so far offer a rationale for trying to prevent TG2 loss at the primary stage of colorectal tumours. Among the various strategies that could be adopted to this purpose, the most viable appears to be direct sequestration of miR-19a, an approach already being trialled for other disease-associated miRNA[221]. Targeting miR-19a would also have the added advantage of reducing the silencing effect on SMAD4, thus contributing to restore its function in those tumour subtypes where the gene copy is not deleted.

To summarize, this work which was focused around the role of TG2 in colorectal cancer has confirmed some of the initial hypotheses, discarded others, and offered new interesting ones to be explored. The areas that could be explored further include:

- Verifying whether the TG2-mediated repression of cell invasion *in vitro*, is due to a direct interaction with β-catenin protein. If such an interaction exists, verifying in which cellular compartment it occurs

- Exploring in further detail the mechanisms and mediators that lead to HLA-I downregulation following TG2 silencing. Furthermore, understanding whether TG2 levels directly affect the ability of immune system cells to kill cancer cells through engagement of HLA-I.

- Evaluating the phenotype of a miR19a$^{-/-}$ mouse model. Furthermore, evaluating the effects of sequestering miR19a in a mouse model of colon cancer.

7. References

1. Katsumoto, K., Shiraki, N., Miki, R. & Kume, S. Embryonic and adult stem cell systems in mammals: ontology and regulation. *Dev. Growth Differ.* **52,** 115–29 (2010).
2. Fink, S. L. & Cookson, B. T. Apoptosis, pyroptosis, and necrosis: mechanistic description of dead and dying eukaryotic cells. *Infect. Immun.* **73,** 1907–1916 (2005).
3. Prochownik, E. V. Functional and physical communication between oncoproteins and tumor suppressors. *Cell. Mol. Life Sci.* **62,** 2438–59 (2005).
4. Pitot, H. C. & Dragan, Y. P. Facts and theories concerning the mechanisms of carcinogenesis. *FASEB J.* **5,** 2280–2286 (1991).
5. Boyland, E. Tumour initiators, promoters, and complete carcinogens. *Br. J. Ind. Med.* **42,** 716–718 (1985).
6. Woo, D. K. & Eide, M. J. Tanning beds, skin cancer, and vitamin D: An examination of the scientific evidence and public health implications. *Dermatol. Ther.* **23,** 61–71
7. Stämpfli, M. R. & Anderson, G. P. How cigarette smoke skews immune responses to promote infection, lung disease and cancer. *Nat. Rev. Immunol.* **9,** 377–84 (2009).
8. Li, L. F. *et al.* Cigarette smoking and gastrointestinal diseases: the causal relationship and underlying molecular mechanisms (review). *Int. J. Mol. Med.* **34,** 372–80 (2014).
9. Friedrich, R. E., Sperber, C., Jäkel, T., Röser, K. & Löning, T. Basaloid lesions of oral squamous epithelial cells and their association with HPV infection and P16 expression. *Anticancer Res.* **30,** 1605–12 (2010).
10. Walboomers, J. M. *et al.* Human papillomavirus is a necessary cause of invasive cervical cancer worldwide. *J. Pathol.* **189,** 12–9 (1999).
11. Ashley, D. J. The two 'hit' and multiple 'hit' theories of carcinogenesis. *Br. J. Cancer* **23,** 313–328 (1969).
12. Levin, I. the Mechanisms of Metastasis Formation in Experimental Cancer. *J. Exp. Med.* **18,** 397–405 (1913).

13. Fearon, E. R. & Vogelstein, B. A genetic model for colorectal tumorigenesis. *Cell* **61,** 759–67 (1990).

14. Miles, A. K., Matharoo-Ball, B., Li, G., Ahmad, M. & Rees, R. C. The identification of human tumour antigens: Current status and future developments. *Cancer Immunol. Immunother.* **55,** 996–1003 (2006).

15. Aptsiauri, N. *et al.* MHC class I antigens and immune surveillance in transformed cells. *Int. Rev. Cytol.* **256,** 139–89 (2007).

16. Ljunggren, H. G. & Kärre, K. In search of the 'missing self': MHC molecules and NK cell recognition. *Immunol. Today* **11,** 237–44 (1990).

17. Melero, I. *et al.* Evolving synergistic combinations of targeted immunotherapies to combat cancer. *Nat. Rev. Cancer* **15,** 457–472 (2015).

18. Riordan, J. R. & Ling, V. Genetic and biochemical characterization of multidrug resistance. *Pharmacol. Ther.* **28,** 51–75 (1985).

19. Fojo, A. *et al.* Molecular biology of drug resistance. *Breast Cancer Res. Treat.* **9,** 5–16 (1987).

20. Alphonso, A. & Alahari, S. K. Stromal cells and integrins: conforming to the needs of the tumor microenvironment. *Neoplasia* **11,** 1264–71 (2009).

21. Balkwill, F. & Mantovani, A. Inflammation and cancer: back to Virchow? *Lancet* **357,** 539–45 (2001).

22. Mantovani, A., Allavena, P., Sica, A. & Balkwill, F. Cancer-related inflammation. *Nature* **454,** 436–44 (2008).

23. Federico, A., Morgillo, F., Tuccillo, C., Ciardiello, F. & Loguercio, C. Chronic inflammation and oxidative stress in human carcinogenesis. *Int. J. Cancer* **121,** 2381–6 (2007).

24. Kessenbrock, K., Plaks, V. & Werb, Z. Matrix metalloproteinases: regulators of the tumor microenvironment. *Cell* **141,** 52–67 (2010).

25. De Luca, A. *et al.* The role of the EGFR signaling in tumor microenvironment. *J. Cell. Physiol.* **214,** 559–67 (2008).

26. Stover, D. G., Bierie, B. & Moses, H. L. A delicate balance: TGF-beta and the tumor microenvironment. *J. Cell. Biochem.* **101,** 851–61 (2007).

27. Chiodoni, C., Colombo, M. P. & Sangaletti, S. Matricellular proteins: from homeostasis to inflammation, cancer, and metastasis. *Cancer Metastasis Rev.* **29,** 295–307 (2010).

28. Borrello, M. G. *et al.* Induction of a proinflammatory program in normal human thyrocytes by the RET/PTC1 oncogene. *Proc. Natl. Acad. Sci. U. S. A.* **102,** 14825–30 (2005).

29. Edge, S. B. & Compton, C. C. The American Joint Committee on Cancer: the 7th edition of the AJCC cancer staging manual and the future of TNM. *Ann. Surg. Oncol.* **17,** 1471–4 (2010).

30. Yokota, J. Tumor progression and metastasis. *Carcinogenesis* **21,** 497–503 (2000).

31. Klymkowsky, M. W. & Savagner, P. Epithelial-mesenchymal transition: a cancer researcher's conceptual friend and foe. *Am. J. Pathol.* **174,** 1588–93 (2009).

32. Nguyen, D. X., Bos, P. D. & Massagué, J. Metastasis: from dissemination to organ-specific colonization. *Nat. Rev. Cancer* **9,** 274–84 (2009).

33. van't Veer, L. J. & Bernards, R. Enabling personalized cancer medicine through analysis of gene-expression patterns. *Nature* **452,** 564–70 (2008).

34. Vineis, P. & Perera, F. Molecular epidemiology and biomarkers in etiologic cancer research: the new in light of the old. *Cancer Epidemiol. Biomarkers Prev.* **16,** 1954–65 (2007).

35. Nisticò, P., Bissell, M. J. & Radisky, D. C. Epithelial-mesenchymal transition: general principles and pathological relevance with special emphasis on the role of matrix metalloproteinases. *Cold Spring Harb. Perspect. Biol.* **4,** a011908– (2012).

36. Takayama, T., Miyanishi, K., Hayashi, T., Sato, Y. & Niitsu, Y. Colorectal cancer: genetics of development and metastasis. *J. Gastroenterol.* **41,** 185–92 (2006).

37. Rubin, D. C., Shaker, A. & Levin, M. S. Chronic intestinal inflammation: inflammatory bowel disease and colitis-associated colon cancer. *Front. Immunol.* **3,** 107 (2012).

38. Weitz, J. *et al.* Colorectal cancer. *Lancet* **365,** 153–65 (2005).

39. Wilson, P. M., Ladner, R. D. & Lenz, H.-J. Predictive and prognostic markers in colorectal cancer. *Gastrointest. Cancer Res.* **1,** 237–46 (2007).

40. Narayan, S. & Roy, D. Role of APC and DNA mismatch repair genes in the development of colorectal cancers. *Mol. Cancer* **2,** 41 (2003).

41. Shibata, T. & Aburatani, H. Exploration of liver cancer genomes. *Nat. Rev. Gastroenterol. Hepatol.* **11,** 340–9 (2014).

42. Kudo, M. Targeted therapy for liver cancer: updated review in 2012. *Curr. Cancer Drug Targets* **12,** 1062–72 (2012).

43. Klionsky, D. J. & Emr, S. D. Autophagy as a regulated pathway of cellular degradation. *Science* **290,** 1717–21 (2000).

44. Matus, S. *et al.* The stress rheostat: an interplay between the unfolded protein response (UPR) and autophagy in neurodegeneration. *Curr. Mol. Med.* **8,** 157–72 (2008).

45. Kaushik, S. & Cuervo, a. M. Chaperone-mediated autophagy. *Methods Mol. Biol.* **445,** 227–244 (2008).

46. He, C. & Klionsky, D. J. Regulation mechanisms and signaling pathways of autophagy. *Annu. Rev. Genet.* **43,** 67–93 (2009).

47. Yang, Z. & Klionsky, D. J. Eaten alive: a history of macroautophagy. *Nat. Cell Biol.* **12,** 814–22 (2010).

48. Yu, L. *et al.* Termination of autophagy and reformation of lysosomes regulated by mTOR. *Nature* **465,** 942–6 (2010).

49. Qu, X. *et al.* Promotion of tumorigenesis by heterozygous disruption of the beclin 1 autophagy gene. *J. Clin. Invest.* **112,** 1809–20 (2003).

50. Jain, K., Paranandi, K. S., Sridharan, S. & Basu, A. Autophagy in breast cancer and its implications for therapy. *Am. J. Cancer Res.* **3,** 251–65 (2013).

51. Mathew, R. *et al.* Autophagy suppresses tumorigenesis through elimination of p62. *Cell* **137,** 1062–75 (2009).

52. Young, A. R. J. *et al.* Autophagy mediates the mitotic senescence transition. *Genes Dev.* **23,** 798–803 (2009).

53. Ogier-Denis, E. & Codogno, P. Autophagy: a barrier or an adaptive response to cancer. *Biochim. Biophys. Acta - Rev. Cancer* **1603,** 113–128 (2003).

54. Chen, N. & Debnath, J. Autophagy and tumorigenesis. *FEBS Lett.* **584,** 1427–35 (2010).

55. Singh, S. B., Davis, A. S., Taylor, G. a & Deretic, V. Human IRGM induces autophagy to eliminate intracellular mycobacteria. *Science* **313,** 1438–41 (2006).

56. Birmingham, C. L., Smith, A. C., Bakowski, M. a, Yoshimori, T. & Brumell, J. H. Autophagy controls Salmonella infection in response to damage to the Salmonella-containing vacuole. *J. Biol. Chem.* **281,** 11374–83 (2006).

57. Crotzer, V. L. & Blum, J. S. Autophagy and its role in MHC-mediated antigen presentation. *J. Immunol.* **182,** 3335–41 (2009).

58. Lleo, A. *et al.* Autophagy: highlighting a novel player in the autoimmunity scenario. *J. Autoimmun.* **29,** 61–8 (2007).

59. Bernstein, C. N., Blanchard, J. F., Kliewer, E. & Wajda, A. Cancer risk in patients with inflammatory bowel disease: a population-based study. *Cancer* **91,** 854–62 (2001).

60. Schirbel, A. & Fiocchi, C. Inflammatory bowel disease: Established and evolving considerations on its etiopathogenesis and therapy. *J. Dig. Dis.* **11,** 266–76 (2010).

61. Barrett, J. C. *et al.* Genome-wide association defines more than 30 distinct susceptibility loci for Crohn's disease. *Nat. Genet.* **40,** 955–62 (2008).

62. Kaser, A. *et al.* XBP1 links ER stress to intestinal inflammation and confers genetic risk for human inflammatory bowel disease. *Cell* **134,** 743–56 (2008).

63. Cheung, J. C. & Deber, C. M. Misfolding of the cystic fibrosis transmembrane conductance regulator and disease. *Biochemistry* **47,** 1465–73 (2008).

64. Quinton, P. M. Role of epithelial $HCO3^-$ transport in mucin secretion: lessons from cystic fibrosis. *Am. J. Physiol. Cell Physiol.* **299,** C1222–33 (2010).

65. Nakamura, H., Yoshimura, K., McElvaney, N. G. & Crystal, R. G. Neutrophil elastase in respiratory epithelial lining fluid of individuals with cystic fibrosis induces interleukin-8 gene expression in a human bronchial epithelial cell line. *J. Clin. Invest.* **89,** 1478–84 (1992).

66. Luciani, A. *et al.* Defective CFTR induces aggresome formation and lung inflammation in cystic fibrosis through ROS-mediated autophagy inhibition. *Nat. Cell Biol.* **12,** 863–75 (2010).

67. Ciechanover, A. The ubiquitin – proteasome pathway : on protein death and cell life. **17,** 7151–7160 (1998).

68. Wang, J. & Maldonado, M. a. The ubiquitin-proteasome system and its role in inflammatory and autoimmune diseases. *Cell. Mol. Immunol.* **3,** 255–61 (2006).

69. Sun, Y. Targeting E3 ubiquitin ligases for cancer therapy. *Cancer Biol. Ther.* **2,** 623–629 (2003).

70. Hershko, A., Leshinsky, E., Ganoth, D. & Heller, H. ATP-dependent degradation of ubiquitin-protein conjugates. *Proc. Natl. Acad. Sci. U. S. A.* **81,** 1619–23 (1984).

71. Ikeda, F. & Dikic, I. Atypical ubiquitin chains: new molecular signals. 'Protein Modifications: Beyond the Usual Suspects' review series. *EMBO Rep.* **9,** 536–42 (2008).

72. Hicke, L. & Dunn, R. Regulation of membrane protein transport by ubiquitin and ubiquitin-binding proteins. *Annu. Rev. Cell Dev. Biol.* **19,** 141–72 (2003).

73. Su, H.-L. & Li, S. S.-L. Molecular features of human ubiquitin-like SUMO genes and their encoded proteins. *Gene* **296,** 65–73 (2002).

74. Saitoh, H. & Hinchey, J. Functional heterogeneity of small ubiquitin-related protein modifiers SUMO-1 versus SUMO-2/3. *J. Biol. Chem.* **275,** 6252–8 (2000).

75. Hay, R. T. SUMO: a history of modification. *Mol. Cell* **18,** 1–12 (2005).

76. Galluzzi, L. *et al.* To die or not to die: that is the autophagic question. *Curr. Mol. Med.* **8,** 78–91 (2008).

77. Bjørkøy, G. *et al.* p62/SQSTM1 forms protein aggregates degraded by autophagy and has a protective effect on huntingtin-induced cell death. *J. Cell Biol.* **171,** 603–14 (2005).

78. Ande, S. R., Chen, J. & Maddika, S. The ubiquitin pathway: an emerging drug target in cancer therapy. *Eur. J. Pharmacol.* **625,** 199–205 (2009).

79. Bedford, L., Lowe, J., Dick, L. R., Mayer, R. J. & Brownell, J. E. Ubiquitin-like protein conjugation and the ubiquitin-proteasome system as drug targets. *Nat. Rev. Drug Discov.* **10,** 29–46 (2011).

80. Bonnevier, J. L., Zhang, R. & Mueller, D. L. E3 ubiquitin ligases and their control of T cell autoreactivity. *Arthritis Res. Ther.* **7,** 233–42 (2005).

81. Adams, J. & Kauffman, M. Development of the proteasome inhibitor Velcade (Bortezomib). *Cancer Invest.* **22,** 304–11 (2004).

82. Griffin, M., Casadio, R. & Bergamini, C. M. Transglutaminases : Nature ' s biological glues. **396,** 377–396 (2002).

83. Park, S.-S., Kim, D.-S., Park, K.-S., Song, H.-J. & Kim, S.-Y. Proteomic analysis of high-molecular-weight protein polymers in a doxorubicin-resistant breast-cancer cell line. *Proteomics. Clin. Appl.* **1,** 555–60 (2007).

84. Facchiano, A. & Facchiano, F. Transglutaminases and their substrates in biology and human diseases: 50 years of growing. *Amino Acids* **36,** 599–614 (2009).

85. Zemskov, E. a, Mikhailenko, I., Strickland, D. K. & Belkin, A. M. Cell-surface transglutaminase undergoes internalization and lysosomal degradation: an essential role for LRP1. *J. Cell Sci.* **120,** 3188–99 (2007).

86. Lorand, L. & Graham, R. M. Transglutaminases: crosslinking enzymes with pleiotropic functions. *Nat. Rev. Mol. Cell Biol.* **4,** 140–56 (2003).

87. Lee, K. N. *et al.* Site-directed mutagenesis of human tissue transglutaminase: Cys-277 is essential for transglutaminase activity but not for GTPase activity. *Biochim. Biophys. Acta* **1202,** 1–6 (1993).

88. Achyuthan, K. E. & Greenberg, C. S. Identification of a guanosine triphosphate-binding site on guinea pig liver transglutaminase. Role of GTP and calcium ions in modulating activity. *J. Biol. Chem.* **262,** 1901–6 (1987).

89. Nakaoka, H. *et al.* Gh: a GTP-binding protein with transglutaminase activity and receptor signaling function. *Science* **264,** 1593–6 (1994).

90. Mastroberardino, P. G. *et al.* 'Tissue' transglutaminase contributes to the formation of disulphide bridges in proteins of mitochondrial respiratory complexes. *Biochim. Biophys. Acta* **1757,** 1357–65

91. Akimov, S. S., Krylov, D., Fleischman, L. F. & Belkin, a M. Tissue transglutaminase is an integrin-binding adhesion coreceptor for fibronectin. *J. Cell Biol.* **148,** 825–38 (2000).

92. Mishra, S. & Murphy, L. J. Tissue transglutaminase has intrinsic kinase activity: identification of transglutaminase 2 as an insulin-like growth factor-binding protein-3 kinase. *J. Biol. Chem.* **279,** 23863–8 (2004).

93. Mehta, K., Kumar, A. & Kim, H. I. Transglutaminase 2: a multi-tasking protein in the complex circuitry of inflammation and cancer. *Biochem. Pharmacol.* **80,** 1921–9 (2010).

94. Park, D., Choi, S. S. & Ha, K.-S. Transglutaminase 2: a multi-functional protein in multiple subcellular compartments. *Amino Acids* **39,** 619–31 (2010).

95. Zirvi, K. A., Keogh, J. P., Slomiany, A. & Slomiany, B. L. Transglutaminase activity in human colorectal carcinomas of differing metastatic potential. *Cancer Lett.* **60,** 85–92 (1991).

96. Fraij, B. M., Birckbichler, P. J., Patterson, M. K., Lee, K. N. & Gonzales, R. a. A retinoic acid-inducible mRNA from human erythroleukemia cells encodes a novel tissue transglutaminase homologue. *J. Biol. Chem.* **267,** 22616–23 (1992).

97. Tee, A. E. L. *et al.* Opposing effects of two tissue transglutaminase protein isoforms in neuroblastoma cell differentiation. *J. Biol. Chem.* **285,** 3561–7 (2010).

98. Datta, S., Antonyak, M. a & Cerione, R. a. GTP-binding-defective forms of tissue transglutaminase trigger cell death. *Biochemistry* **46,** 14819–29 (2007).

99. Phatak, V. M. *et al.* Expression of transglutaminase-2 isoforms in normal human tissues and cancer cell lines: dysregulation of alternative splicing in cancer. *Amino Acids* **44,** 33–44 (2013).

100. Kotsakis, P. & Griffin, M. Tissue transglutaminase in tumour progression: friend or foe? *Amino Acids* **33,** 373–84 (2007).

101. Herman, J. F., Mangala, L. S. & Mehta, K. Implications of increased tissue transglutaminase (TG2) expression in drug-resistant breast cancer (MCF-7) cells. *Oncogene* **25,** 3049–58 (2006).

102. Sieg, D. J. *et al.* FAK integrates growth-factor and integrin signals to promote cell migration. *Nat. Cell Biol.* **2,** 249–56 (2000).

103. Verma, A. *et al.* Increased expression of tissue transglutaminase in pancreatic ductal adenocarcinoma and its implications in drug resistance and metastasis. *Cancer Res.* **66,** 10525–33 (2006).

104. Huang, W.-C. & Hung, M.-C. Induction of Akt activity by chemotherapy confers acquired resistance. *J. Formos. Med. Assoc.* **108,** 180–94 (2009).

105. Falasca, M. PI3K/Akt signalling pathway specific inhibitors: a novel strategy to sensitize cancer cells to anti-cancer drugs. *Curr. Pharm. Des.* **16,** 1410–6 (2010).

106. Antonyak, M. a *et al.* Tissue transglutaminase is an essential participant in the epidermal growth factor-stimulated signaling pathway leading to cancer cell migration and invasion. *J. Biol. Chem.* **284,** 17914–25 (2009).

107. Li, B. *et al.* EGF potentiated oncogenesis requires a tissue transglutaminase-dependent signaling pathway leading to Src activation. *Proc. Natl. Acad. Sci. U. S. A.* **107,** 1408–13 (2010).

108. Yuan, L. *et al.* Tissue transglutaminase 2 inhibition promotes cell death and chemosensitivity in glioblastomas. *Mol. Cancer Ther.* **4,** 1293–302 (2005).

109. Stambolic, V. *et al.* Negative regulation of PKB/Akt-dependent cell survival by the tumor suppressor PTEN. *Cell* **95,** 29–39 (1998).

110. Stiles, B. *et al.* Essential role of AKT-1/protein kinase B alpha in PTEN-controlled tumorigenesis. *Mol. Cell. Biol.* **22,** 3842–51 (2002).

111. Salvesen, H. B., Stefansson, I., Kalvenes, M. B., Das, S. & Akslen, L. a. Loss of PTEN expression is associated with metastatic disease in patients with endometrial carcinoma. *Cancer* **94,** 2185–91 (2002).

112. Hwang, P. H. *et al.* Suppression of tumorigenicity and metastasis in B16F10 cells by PTEN. *Cancer Lett.* **172,** 83–91 (2001).

113. Verma, A. *et al.* Tissue transglutaminase regulates focal adhesion kinase/AKT activation by modulating PTEN expression in pancreatic cancer cells. *Clin. Cancer Res.* **14,** 1997–2005 (2008).

114. Farrow, B. & Evers, B. M. Activation of PPARgamma increases PTEN expression in pancreatic cancer cells. *Biochem. Biophys. Res. Commun.* **301,** 50–3 (2003).

115. Maiuri, L. *et al.* Tissue Transglutaminase Activation Modulates Inflammation in Cystic Fibrosis via PPAR Down-Regulation. *J. Immunol.* **180,** 7697–7705 (2008).

116. Mann, A. P. *et al.* Overexpression of tissue transglutaminase leads to constitutive activation of nuclear factor-kappaB in cancer cells: delineation of a novel pathway. *Cancer Res.* **66,** 8788–95 (2006).

117. Luciani, A. *et al.* Cystic fibrosis: a disorder with defective autophagy. *Autophagy* **7,** 104–6 (2011).

118. Akar, U. *et al.* Tissue transglutaminase inhibits autophagy in pancreatic cancer cells. *Mol. Cancer Res.* **5,** 241–9 (2007).

119. Thiery, J. P. Epithelial-mesenchymal transitions in tumour progression. *Nat. Rev. Cancer* **2,** 442–54 (2002).

120. Shao, M. *et al.* Epithelial-to-mesenchymal transition and ovarian tumor progression induced by tissue transglutaminase. *Cancer Res.* **69,** 9192–201 (2009).

121. Chua, H. L. *et al.* NF-kappaB represses E-cadherin expression and enhances epithelial to mesenchymal transition of mammary epithelial cells: potential involvement of ZEB-1 and ZEB-2. *Oncogene* **26,** 711–24 (2007).

122. Kim, D.-S., Park, S.-S., Nam, B.-H., Kim, I.-H. & Kim, S.-Y. Reversal of drug resistance in breast cancer cells by transglutaminase 2 inhibition and nuclear factor-kappaB inactivation. *Cancer Res.* **66,** 10936–43 (2006).

123. Park, M. K. *et al.* Transglutaminase-2 induces N-cadherin expression in TGF-β1-induced epithelial mesenchymal transition via c-Jun-N-terminal kinase activation by protein phosphatase 2A down-regulation. *Eur. J. Cancer* **49,** 1692–705 (2013).

124. Kumar, A. *et al.* Tissue transglutaminase promotes drug resistance and invasion by inducing mesenchymal transition in mammary epithelial cells. *PLoS One* **5,** e13390 (2010).

125. Fisher, M. L. *et al.* Type II transglutaminase stimulates epidermal cancer stem cell epithelial-mesenchymal transition. *Oncotarget* (2015).

126. Satpathy, M., Shao, M., Emerson, R., Donner, D. B. & Matei, D. Tissue transglutaminase regulates matrix metalloproteinase-2 in ovarian cancer by modulating cAMP-response element-binding protein activity. *J. Biol. Chem.* **284,** 15390–9 (2009).

127. Fesijs, L., Falus, A., Erdei, A. & Laki, K. Human b2-microglobulin is a Substrate of Tissue Transglutaminase : Polymerization in Solution and on the Cell Surface Preparation of Human Peripheral Blood Shedding of Surface-labeled Human PBMC and Adsorption of the Shed Supernate on Sephadex. **89,** (1981).

128. Krangel, M. S., Orr, H. T. & Strominger, J. L. Assembly and maturation of HLA-A and HLA-B antigens in vivo. *Cell* **18,** 979–91 (1979).

129. Verma, A. *et al.* Therapeutic significance of elevated tissue transglutaminase expression in pancreatic cancer. *Clin. Cancer Res.* **14,** 2476–83 (2008).

130. Aeschlimann, D. & Thomazy, V. Protein crosslinking in assembly and remodelling of extracellular matrices: the role of transglutaminases. *Connect. Tissue Res.* **41,** 1–27 (2000).

131. Verderio, E. *et al.* Regulation of cell surface tissue transglutaminase: effects on matrix storage of latent transforming growth factor-beta binding protein-1. *J. Histochem. Cytochem.* **47,** 1417–32 (1999).

132. Jones, R. a *et al.* Matrix changes induced by transglutaminase 2 lead to inhibition of angiogenesis and tumor growth. *Cell Death Differ.* **13,** 1442–53 (2006).

133. Haroon, Z. A. *et al.* Tissue transglutaminase is expressed as a host response to tumor invasion and inhibits tumor growth. *Lab. Invest.* **79,** 1679–86 (1999).

134. Hand, D., Elliott, B. M. & Griffin, M. Expression of the cytosolic and particulate forms of transglutaminase during chemically induced rat liver carcinogenesis. *Biochim. Biophys. Acta - Mol. Cell Res.* **970,** 137–145 (1988).

135. Johnson, T. S. *et al.* Transfection of tissue transglutaminase into a highly malignant hamster fibrosarcoma leads to a reduced incidence of primary tumour growth. *Oncogene* **9,** 2935–42 (1994).

136. Ahn, J.-S. *et al.* Tissue transglutaminase-induced down-regulation of matrix metalloproteinase-9. *Biochem. Biophys. Res. Commun.* **376,** 743–7 (2008).

137. Liu, T. *et al.* Activation of tissue transglutaminase transcription by histone deacetylase inhibition as a therapeutic approach for Myc oncogenesis. *Proc. Natl. Acad. Sci. U. S. A.* **104,** 18682–7 (2007).

138. Smethurst, P. A. & Griffin, M. Measurement of tissue transglutaminase activity in a permeabilized cell system : its regulation by Ca 2 + and nucleotides. **808,** 803–808 (1996).

139. Brookes, P. S., Yoon, Y., Robotham, J. L., Anders, M. W. & Sheu, S.-S. Calcium, ATP, and ROS: a mitochondrial love-hate triangle. *Am. J. Physiol. Cell Physiol.* **287,** C817–33 (2004).

140. Fesus, L. *et al.* Apoptotic hepatocytes become insoluble in detergents and chaotropic agents as a result of transglutaminase action. *FEBS Lett.* **245,** 150–4 (1989).

141. Rodolfo, C. *et al.* Tissue transglutaminase is a multifunctional BH3-only protein. *J. Biol. Chem.* **279,** 54783–92 (2004).

142. Oliverio, S. *et al.* Tissue transglutaminase-dependent posttranslational modification of the retinoblastoma gene product in promonocytic cells undergoing apoptosis. *Mol. Cell. Biol.* **17,** 6040–8 (1997).

143. Tatsukawa, H. *et al.* Dual induction of caspase 3- and transglutaminase-dependent apoptosis by acyclic retinoid in hepatocellular carcinoma cells. *Mol. Cancer* **10,** 4 (2011).

144. Chhabra, A., Verma, A. & Mehta, K. Tissue transglutaminase promotes or suppresses tumors depending on cell context. *Anticancer Res.* **29,** 1909–19 (2009).

145. Dieterich, W. *et al.* Identification of tissue transglutaminase as the autoantigen of celiac disease. *Nat. Med.* **3,** 797–801 (1997).

146. Dørum, S. *et al.* The preferred substrates for transglutaminase 2 in a complex wheat gluten digest are Peptide fragments harboring celiac disease T-cell epitopes. *PLoS One* **5,** e14056 (2010).

147. Qiao, S.-W., Sollid, L. M. & Blumberg, R. S. Antigen presentation in celiac disease. *Curr. Opin. Immunol.* **21,** 111–7 (2009).

148. Diosdado, B. & Wijmenga, C. Molecular mechanisms of the adaptive, innate and regulatory immune responses in the intestinal mucosa of celiac disease patients. *Expert Rev. Mol. Diagn.* **5,** 681–700 (2005).

149. Garrote, J. A., Gómez-González, E., Bernardo, D., Arranz, E. & Chirdo, F. Celiac disease pathogenesis: the proinflammatory cytokine network. *J. Pediatr. Gastroenterol. Nutr.* **47 Suppl 1,** S27–32 (2008).

150. Schuppan, D., Junker, Y. & Barisani, D. Celiac disease: from pathogenesis to novel therapies. *Gastroenterology* **137,** 1912–33 (2009).

151. Luciani, A. *et al.* SUMOylation of tissue transglutaminase as link between oxidative stress and inflammation. *J. Immunol.* **183,** 2775–84 (2009).

152. Lesort, M., Tucholski, J., Miller, M. L. & Johnson, G. V. Tissue transglutaminase: a possible role in neurodegenerative diseases. *Prog. Neurobiol.* **61,** 439–63 (2000).

153. Wilhelmus, M. M. M., van Dam, A.-M. & Drukarch, B. Tissue transglutaminase: a novel pharmacological target in preventing toxic protein aggregation in neurodegenerative diseases. *Eur. J. Pharmacol.* **585,** 464–72 (2008).

154. Choi, K. *et al.* Chemistry and biology of dihydroisoxazole derivatives: selective inhibitors of human transglutaminase 2. *Chem. Biol.* **12,** 469–75 (2005).

155. Elbashir, S. M., Lendeckel, W. & Tuschl, T. RNA interference is mediated by 21- and 22-nucleotide RNAs. *Genes Dev.* **15,** 188–200 (2001).

156. Wightman, B., Ha, I. & Ruvkun, G. Posttranscriptional regulation of the heterochronic gene lin-14 by lin-4 mediates temporal pattern formation in C. elegans. *Cell* **75,** 855–62 (1993).

157. Lee, R. C., Feinbaum, R. L. & Ambros, V. The C. elegans heterochronic gene lin-4 encodes small RNAs with antisense complementarity to lin-14. *Cell* **75,** 843–54 (1993).

158. Bartel, D. P., Lee, R. & Feinbaum, R. MicroRNAs : Genomics , Biogenesis , Mechanism , and Function Genomics : The miRNA Genes. **116,** 281–297 (2004).

159. Yi, R., Qin, Y., Macara, I. G. & Cullen, B. R. Exportin-5 mediates the nuclear export of pre-microRNAs and short hairpin RNAs. *Genes Dev.* **17,** 3011–6 (2003).

160. Winter, J., Jung, S., Keller, S., Gregory, R. I. & Diederichs, S. Many roads to maturity: microRNA biogenesis pathways and their regulation. *Nat. Cell Biol.* **11,** 228–34 (2009).

161. Zamore, P. D., Tuschl, T., Sharp, P. A. & Bartel, D. P. RNAi: double-stranded RNA directs the ATP-dependent cleavage of mRNA at 21 to 23 nucleotide intervals. *Cell* **101,** 25–33 (2000).

162. Guo, H., Ingolia, N. T., Weissman, J. S. & Bartel, D. P. Mammalian microRNAs predominantly act to decrease target mRNA levels. *Nature* **466,** 835–40 (2010).

163. Valencia-Sanchez, M. A., Liu, J., Hannon, G. J. & Parker, R. Control of translation and mRNA degradation by miRNAs and siRNAs. *Genes Dev.* **20,** 515–24 (2006).

164. Mallory, A. C. & Vaucheret, H. Functions of microRNAs and related small RNAs in plants. *Nat. Genet.* **38 Suppl,** S31–6 (2006).

165. Olive, V., Jiang, I. & He, L. mir-17-92, a cluster of miRNAs in the midst of the cancer network. *Int. J. Biochem. Cell Biol.* **42,** 1348–54 (2010).

166. Xiang, J. & Wu, J. Feud or Friend? The Role of the miR-17-92 Cluster in Tumorigenesis. *Curr. Genomics* **11,** 129–35 (2010).

167. Knuutila, S. *et al.* DNA copy number losses in human neoplasms. *Am. J. Pathol.* **155,** 683–94 (1999).

168. Diosdado, B. *et al.* MiR-17-92 cluster is associated with 13q gain and c-myc expression during colorectal adenoma to adenocarcinoma progression. *Br. J. Cancer* **101,** 707–14 (2009).

169. Lin, Y. *et al.* Original Paper Loss of Heterozygosity at Chromosome 13q in Hepatocellular Carcinoma : Identification of Three Independent Regions. **35,** 1730–1734 (1999).

170. Zhang, L. *et al.* microRNAs exhibit high frequency genomic alterations in human cancer. *Proc. Natl. Acad. Sci. U. S. A.* **103,** 9136–41 (2006).

171. Petrocca, F., Vecchione, A. & Croce, C. M. Emerging role of miR-106b-25/miR-17-92 clusters in the control of transforming growth factor beta signaling. *Cancer Res.* **68,** 8191–4 (2008).

172. Hwang, J. Y. *et al.* Clinical and biological significance of tissue transglutaminase in ovarian carcinoma. *Cancer Res.* **68,** 5849–58 (2008).

173. Mangala, L. S., Fok, J. Y., Zorrilla-Calancha, I. R., Verma, a & Mehta, K. Tissue transglutaminase expression promotes cell attachment, invasion and survival in breast cancer cells. *Oncogene* **26,** 2459–70 (2007).

174. Mehta, K. Biological and therapeutic significance of tissue transglutaminase in pancreatic cancer. *Amino Acids* **36,** 709–16 (2009).

175. Fredriksson, S. *et al.* Protein detection using proximity-dependent DNA ligation assays. *Nat. Biotechnol.* **20,** 473–7 (2002).

176. Di Giacomo, G., Lentini, a, Beninati, S., Piacentini, M. & Rodolfo, C. In vivo evaluation of type 2 transglutaminase contribution to the metastasis formation in melanoma. *Amino Acids* **36,** 717–24 (2009).

177. Murthy, P., Wilson, J., Zhang, Y. & Lorandf, L. Residue Gln-30 of Human Erythrocyte Anion Transporter Is a Prime Site. 22907–22911 (1994).

178. Miyoshi, N. *et al.* TGM2 is a novel marker for prognosis and therapeutic target in colorectal cancer. *Ann. Surg. Oncol.* **17,** 967–72 (2010).

179. Fung, C., Lock, R., Gao, S., Salas, E. & Debnath, J. Induction of autophagy during extracellular matrix detachment promotes cell survival. *Mol. Biol. Cell* **19,** 797–806 (2008).

180. Xavier, R. J., Huett, A. & Rioux, J. D. Autophagy as an important process in gut homeostasis and Crohn's disease pathogenesis. *Gut* **57,** 717–20 (2008).

181. Mangala, L. S., Arun, B., Sahin, A. a & Mehta, K. Tissue transglutaminase-induced alterations in extracellular matrix inhibit tumor invasion. *Mol. Cancer* **4,** 33 (2005).

182. Zirvi, K. A., Keogh, J. P., Slomiany, A. & Slomiany, B. L. Effects of exogenous transglutaminase on spreading of human colorectal carcinoma cells. *Cancer Biochem. Biophys.* **13,** 283–94 (1993).

183. Menon, A. G. *et al.* Down-regulation of HLA-A expression correlates with a better prognosis in colorectal cancer patients. *Lab. Invest.* **82,** 1725–33 (2002).

184. Kaczmarek, M. *et al.* Analysis of expression of MHC class I molecules and TAP genes in malignant human cell lines. *Folia Histochem. Cytobiol.* **45,** 205–14 (2007).

185. Zhang, L. *et al.* miR-153 supports colorectal cancer progression via pleiotropic effects that enhance invasion and chemotherapeutic resistance. *Cancer Res.* **73,** 6435–47 (2013).

186. Bullock, M. D. *et al.* Stratifying risk of recurrence in stage II colorectal cancer using deregulated stromal and epithelial microRNAs. *Oncotarget* **6,** 7262–79 (2015).

187. Lim, L. P. *et al.* Microarray analysis shows that some microRNAs downregulate large numbers of target mRNAs. *Nature* **433,** 769–73 (2005).

188. Pattingre, S., Espert, L., Biard-Piechaczyk, M. & Codogno, P. Regulation of macroautophagy by mTOR and Beclin 1 complexes. *Biochimie* **90,** 313–23 (2008).

189. Chen, X.-H. *et al.* TGF-β and EGF induced HLA-I downregulation is associated with epithelial-mesenchymal transition (EMT) through upregulation of snail in prostate cancer cells. *Mol. Immunol.* **65,** 34–42 (2015).

190. Yu, L., Hébert, M. C. & Zhang, Y. E. TGF-beta receptor-activated p38 MAP kinase mediates Smad-independent TGF-beta responses. *EMBO J.* **21,** 3749–59 (2002).

191. Akhurst, R. J. & Derynck, R. TGF-beta signaling in cancer--a double-edged sword. *Trends Cell Biol.* **11,** S44–51 (2001).

192. Priglinger, S. G. *et al.* TGF- 2-Induced Cell Surface Tissue Transglutaminase Increases Adhesion and Migration of RPE Cells on Fibronectin through the Gelatin-Binding Domain. *Invest. Ophthalmol. Vis. Sci.* **45,** 955–963 (2004).

193. Jung, S.-A. *et al.* Upregulation of TGF-beta-induced tissue transglutaminase expression by PI3K-Akt pathway activation in human subconjunctival fibroblasts. *Invest. Ophthalmol. Vis. Sci.* **48,** 1952–8 (2007).

194. Welge-Lüssen, U., May, C. A. & Lütjen-Drecoll, E. Induction of tissue transglutaminase in the trabecular meshwork by TGF-beta1 and TGF-beta2. *Invest. Ophthalmol. Vis. Sci.* **41,** 2229–38 (2000).

195. Fischer, A. N. M. *et al.* Integration of Ras subeffector signaling in TGF-beta mediated late stage hepatocarcinogenesis. *Carcinogenesis* **26,** 931–42 (2005).

196. Del Castillo, G. *et al.* Autocrine production of TGF-beta confers resistance to apoptosis after an epithelial-mesenchymal transition process in hepatocytes: Role of EGF receptor ligands. *Exp. Cell Res.* **312,** 2860–71 (2006).

197. Chapnick, D. A., Warner, L., Bernet, J., Rao, T. & Liu, X. Partners in crime: the TGFβ and MAPK pathways in cancer progression. *Cell Biosci.* **1,** 42 (2011).

198. Woodford-Richens, K. L. *et al.* SMAD4 mutations in colorectal cancer probably occur before chromosomal instability, but after divergence of the microsatellite instability pathway. *Proc. Natl. Acad. Sci. U. S. A.* **98,** 9719–23 (2001).

199. Zhang, B. *et al.* Antimetastatic role of Smad4 signaling in colorectal cancer. *Gastroenterology* **138,** 969–80.e1–3 (2010).

200. Zhang, B. *et al.* Loss of Smad4 in colorectal cancer induces resistance to 5-fluorouracil through activating Akt pathway. *Br. J. Cancer* **110,** 946–57 (2014).

201. Corcoran, R. B. *et al.* EGFR-mediated re-activation of MAPK signaling contributes to insensitivity of BRAF mutant colorectal cancers to RAF inhibition with vemurafenib. *Cancer Discov.* **2,** 227–35 (2012).

202. Danner, B. C. *et al.* Comparison of chromosomal aberrations in primary colorectal carcinomas to their pulmonary metastases. *Cancer Genet.* **204,** 122–8 (2011).

203. Lee, M. S. & Kopetz, S. Current and Future Approaches to Target the Epidermal Growth Factor Receptor and Its Downstream Signaling in Metastatic Colorectal Cancer. *Clin. Colorectal Cancer* (2015). doi:10.1016/j.clcc.2015.05.006

204. Huang, P. *et al.* The role of EGF-EGFR signalling pathway in hepatocellular carcinoma inflammatory microenvironment. *J. Cell. Mol. Med.* **18,** 218–30 (2014).

205. Massagué, J. TGFbeta in Cancer. *Cell* **134,** 215–30 (2008).

206. Neuzillet, C. *et al.* Targeting the TGFβ pathway for cancer therapy. *Pharmacol. Ther.* **147,** 22–31 (2015).

207. El-Bahrawy, M. *et al.* Characterization of the E-cadherin/catenin complex in colorectal carcinoma cell lines. *Int. J. Exp. Pathol.* **85,** 65–74 (2004).

208. Cao, L. *et al.* Tissue transglutaminase links TGF-β, epithelial to mesenchymal transition and a stem cell phenotype in ovarian cancer. *Oncogene* **31,** 2521–34 (2012).

209. Kumar, A. *et al.* Evidence that GTP-binding domain but not catalytic domain of transglutaminase 2 is essential for epithelial-to-mesenchymal transition in mammary epithelial cells. *Breast Cancer Res.* **14,** R4 (2012).

210. Ashour, A. A. *et al.* Elongation factor-2 kinase regulates TG2/β1 integrin/Src/uPAR pathway and epithelial-mesenchymal transition mediating pancreatic cancer cells invasion. *J. Cell. Mol. Med.* **18,** 2235–2251 (2014).

211. Tomita, N. *et al.* Isolation and Characterization of a Highly Malignant Variant of the SW480 Human Colon Cancer Cell Line. *Cancer Res.* **52,** 6840–6847 (1992).

212. Pálmer, H. G. *et al.* Vitamin D(3) promotes the differentiation of colon carcinoma cells by the induction of E-cadherin and the inhibition of beta-catenin signaling. *J. Cell Biol.* **154,** 369–87 (2001).

213. Reinacher-Schick, A. *et al.* Loss of Smad4 correlates with loss of the invasion suppressor E-cadherin in advanced colorectal carcinomas. *J. Pathol.* **202,** 412–20 (2004).

214. Sun, Y. *et al.* Quantitative proteomic signature of liver cancer cells: tissue transglutaminase 2 could be a novel protein candidate of human hepatocellular carcinoma. *J. Proteome Res.* **7,** 3847–59 (2008).

215. Avraham, R. & Yarden, Y. Feedback regulation of EGFR signalling: decision making by early and delayed loops. *Nat. Rev. Mol. Cell Biol.* **12,** 104–17 (2011).

216. Stern, J. R., Christley, S., Zaborina, O., Alverdy, J. C. & An, G. Integration of TGF-β- and EGFR-based signaling pathways using an agent-based model of epithelial restitution. *Wound Repair Regen.* **20,** 862–71

217. Hewitt, R. E. *et al.* Validation of a model of colon cancer progression. *J. Pathol.* **192,** 446–54 (2000).

218. Iwata, J. *et al.* Modulation of noncanonical TGF-β signaling prevents cleft palate in Tgfbr2 mutant mice. *J. Clin. Invest.* **122,** 873–85 (2012).

219. Kozak, M. M. *et al.* Smad4 inactivation predicts for worse prognosis and response to fluorouracil-based treatment in colorectal cancer. *J. Clin. Pathol.* **68,** 341–5 (2015).

220. Zoni, E., van der Pluijm, G., Gray, P. C. & Kruithof-de Julio, M. Epithelial Plasticity in Cancer: Unmasking a MicroRNA Network for TGF-β-, Notch-, and Wnt-Mediated EMT. *J. Oncol.* **2015,** 198967 (2015).

221. Van Rooij, E., Purcell, A. L. & Levin, A. A. Developing microRNA therapeutics. *Circ. Res.* **110,** 496–507 (2012).

APPENDIX A

TNM Classification	
T1	the tumour is confined to the submucosa
T2	the tumour has grown into (but not through) the muscularis propria
T3	the tumour has grown into (but not through) the serosa
T4	the tumour has penetrated through the serosa and the peritoneal surface. If extending directly into other nearby structures (such as other parts of the bowel or other organs/body structures) it is classified as T4a. If there is perforation of the bowel, it is classified as T4b.
N0	no lymph nodes contain tumour cells
N1	there are tumour cells in up to 3 regional lymph nodes
N2	there are tumour cells in 4 or more regional lymph nodes
M0	no metastasis to distant organs
M1	metastasis to distant organs

Dukes Classification	
Stage A	T1N0M0 or T2N0M0
Stage B	T3N0M0 or T4N0M0
Stage C	any T, N1, M0 or any T, N2, M0
Stage D	any T, any N, M1

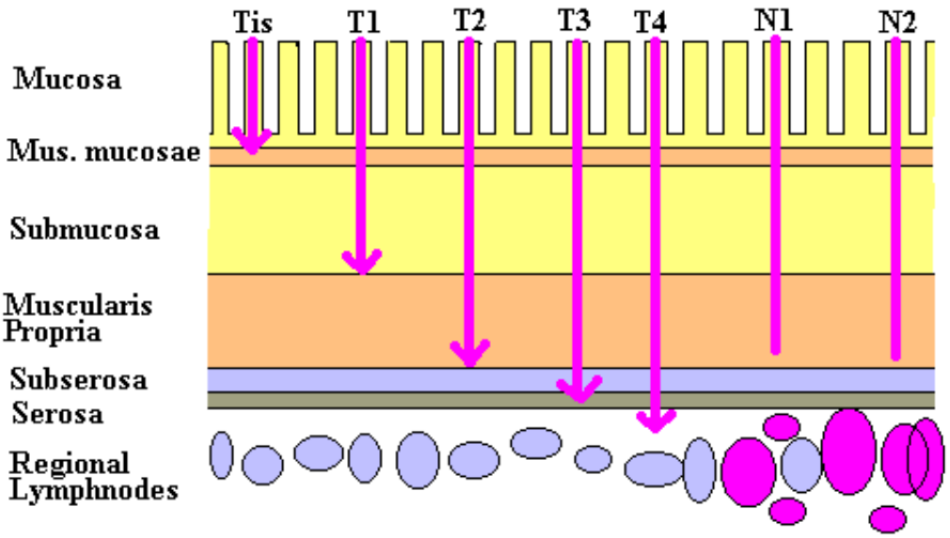

APPENDIX B

A table of all antibodies used throughout this study is provided below, stating the working concentration for each application.

Unconjugated antibodies

Name	Brand, product number	Application
Mouse anti-human TG2 clone CUB7402	Abcam, ab2386	IHC, IF (1:100), FACS (0.3 μg/10^6 cells), WB (1:500)
Rabbit anti-human TG2 clone H237	Santa Cruz, sc20621	WB (1:200), IF and PLA (1:50)
Actin	Santa Cruz, sc1615	WB (1:4000)
Mouse anti-human Ubiquitin clone P4D1	Santa Cruz, sc-8017	IF and PLA (1:50)
Mouse anti-human SUMO-1 clone D11	Santa Cruz, sc5308	IF and PLA (1:50)
Mouse anti-human HLA I clone W6/32	Abcam, ab23755	FACS (1 μg/10^6 cells)
Mouse anti-human SQSTM1/p62	Abcam, ab56416	WB (1:1000)
Mouse anti-human Beclin-1 clone 1B7	Abcam, ab79937	WB (1:1000)

Conjugated antibodies, and other dyes

Name	Brand, product number	Application
Goat-anti-mouse IgG-FITC	Sigma, F0257	IF (1:300), FACS (1:100)
Goat-anti-Rabbit IgG-FITC	Sigma, F9887	IF (1:100)
Goat-anti-mouse IgG-Alexa594	Molecular Probes, A11005	IF (1:300)
Goat anti-mouse IgG-HRP	Santa Cruz, sc2005	WB (1:2000)
Donkey anti-goat IgG-HRP	Santa Cruz, sc2020	WB (1:2000)
Mouse anti-rabbit IgG-HRP	Santa Cruz, sc2357	WB (1:2000)
Anti-Streptavidin-FITC	BD Pharmingen, 554060	IF (1:150)
Goat anti-mouse IgG-PE	Abcam, ab7002	FACS (1:200)
Diamidino-2-phenylindole dihydrochloride (DAPI)	Sigma, 32670	IF (1 μg/mL)

APPENDIX C

LIST OF PRIMERS

TG2 forward - 5’ cagtgtcgtgaccggcccagcccctagc 3’

TG2 reverse - 5’ ccaggcacctcagcactgtgcaggccacg 3’

ACTIN forward 5’ ctggcatcgtgatggactccggtga 3’

ACTIN reverse 5’ caatgaagatcaagatcattgctcc 3’

ATG7 forward 5’ cactgtgagtcgtccaggac 3’

ATG7 reverse 5’ cgctcatgtcccagatctca 3’

ATG14L forward 5’ atgagcgtctggcaaatctt 3’

ATG14L reverse 5’ cccatcgtcctgagaggtaa 3’

VPS34 forward 5’ aagcagtgcctgtaggagga 3’

VPS34 reverse 5’ tgtcgatgagctttggtgag 3’

Supporting material

Published OnlineFirst May 1, 2015; DOI: 10.1158/1541-7786.MCR-14-0466

Chromatin, Gene, and RNA Regulation

Molecular Cancer Research

miR-19–Mediated Inhibition of Transglutaminase-2 Leads to Enhanced Invasion and Metastasis in Colorectal Cancer

D. Cellura[1], K. Pickard[1], S. Quaratino[1], H. Parker[2], J.C. Strefford[2], G.J. Thomas[1], R. Mitter[3], A.H. Mirnezami[1,4], and N.J. Peake[1]

Abstract

Transglutaminase-2 (TG2) is a critical cross-linking enzyme in the extracellular matrix (ECM) and tumor microenvironment (TME). Although its expression has been linked to colorectal cancer, its functional role in the processes that drive disease appears to be context dependent. There is now considerable evidence of a role for microRNAs (miRNA) in the development and progression of cancer, including metastasis. A cell model of metastatic colon adenocarcinoma was used to investigate the contribution of miRNAs to the differential expression of TG2, and functional effects on inflammatory and invasive behavior. The impact of TG2 in colorectal cancer was analyzed in human colorectal tumor specimens and by manipulations in SW480 and SW620 cells. Effects on invasive behavior were measured using Transwell invasion assays, and cytokine production was assessed by ELISA. TG2 was identified as a target for miR-19 by *in silico* analysis, which was confirmed experimentally. Functional effects were evaluated by overexpression of pre-miR-19a in SW480 cells. Expression of TG2 correlated inversely with invasive behavior, with knockdown in SW480 cells leading to enhanced invasion, and overexpression in SW620 cells the opposite. TG2 expression was observed in colorectal cancer primary tumors but lost in liver metastases. Finally, miR-19 overexpression and subsequent decreased TG2 expression was linked to chromosome-13 amplification events, leading to altered invasive behavior in colorectal cancer cells.

Implications: Chromosome-13 amplification in advanced colorectal cancer contributes to invasion and metastasis by upregulating miR-19, which targets TG2. *Mol Cancer Res; 13(7); 1095–105. ©2015 AACR.*

Introduction

Colorectal cancer is the fourth most common malignancy worldwide and the third most common malignant cause of mortality in the western world (1, 2). Although advances in screening and treatment have improved life expectancy in recent decades, prognosis remains significantly poorer in later stages when disease has spread to lymph nodes and distant metastatic sites (3). Understanding and preventing this invasive progression would therefore significantly benefit patient outcome worldwide.

Transglutaminase-2 (TG2) activity has been linked to multiple biologic processes associated with tumor development and progression, such as cell adhesion, motility, invasion, apoptosis, chemoresistance, and epithelial–mesenchymal transition (4, 5). The most ubiquitous member of the transglutaminase family of protein cross-linking enzymes, TG2 has been observed in various cancer tissues and cell lines, with activity linked to disease progression and metastasis in tumors with a diverse range of origins (6–10). TG2 has been identified as a potential marker of colorectal cancer progression by immunohistochemical analysis, following previous work demonstrating differential expression of TG2 in colorectal cancer cell lines with different metastatic potential (11–13). However, published studies aiming to identify a definitive role for TG2 in cancer cell biology have demonstrated sometimes contradictory functional roles, such as promoting or inhibiting apoptosis. TG2 therefore appears to act in a context-dependant manner that may relate to cellular location and the availability of its many identified protein substrates (14), or to the balance between different isotypes of the enzyme that have been shown to have opposing consequences on cell behavior (15).

microRNAs (miRNA) are a family of short, noncoding, single-stranded RNAs, which inhibit the function of multiple target genes by binding to their 3′-untranslated region (UTR), leading to direct degradation of target mRNA or inhibiting translation (16). A wide body of work now links miRNA expression to colorectal cancer by altering the expression of oncogenic and tumor-suppressive genes (17, 18). Furthermore, miRNA deregulation is strongly linked to disease progression, with changes in miRNAs linked to metastasis (19, 20). These "metastaMirs" are attractive therapeutic targets for treating metastatic colorectal

[1]Molecular Mechanisms Research Unit, Cancer Research UK Centre, University of Southampton Cancer Sciences Division, Somers Cancer Research Building, Southampton University Hospital NHS Trust, Southampton, United Kingdom. [2]Cancer Genomics, Cancer Sciences, University of Southampton, Southampton, United Kingdom. [3]Bioinformatics Unit, London Research Institute, Cancer Research UK, Lincoln's Inn Fields, London, United Kingdom. [4]Department of Colorectal Surgery, Southampton University Hospital NHS Trust, Southampton, United Kingdom.

Note: Supplementary data for this article are available at Molecular Cancer Research Online (http://mcr.aacrjournals.org/).

A.H. Mirnezami and N.J. Peake contributed equally to this article.

Corresponding Authors: A.H. Mirnezami, Molecular Mechanisms Research Unit, Cancer Research UK Centre, Somers Cancer Research Building, University of Southampton Cancer Sciences Division, Southampton University Hospital NHS Trust, Tremona Road, Southampton SO166YD, United Kingdom. Phone: 44-7790518527; Fax: 44-2380795152; E-mail: ahm@soton.ac.uk; and N.J. Peake, njpeake@soton.ac.uk

doi: 10.1158/1541-7786.MCR-14-0466

Published OnlineFirst May 1, 2015; DOI: 10.1158/1541-7786.MCR-14-0466

cancer, as each miRNA influences the expression of multiple proteins downstream that may contribute to the development of the complex, multifactorial metastatic phenotype (21).

Because TG2 has multiple cell substrates and plays a critical role in cancer cell behavior, its expression is carefully controlled. As well as translational regulation, TG2 abundance is also controlled through the SUMO pathway (22), and enzymatic function is dependent on the presence of calcium and inhibited by GTP (23). To date, few studies have examined miRNA regulation of TG2, despite both TG2 and miRNAs being closely linked to cancer progression. In this study, we investigated the differential expression of TG2 in colon cancer cell lines and tissue sections taken from primary and metastatic tumors, examined how TG2 expression affected invasive characteristics and inflammatory mediators synthesized by these cells, and finally determined how miRNA regulation alters these functional properties.

Materials and Methods

Cell lines and reagents

The primary adenocarcinoma cell line SW480 was obtained from the European Collection of Cell Culture, along with the patient-matched lymph-node metastasis–derived line SW620. Cells were cultured and passaged according to supplied information. siRNA targeted against TG2 was obtained from Invitrogen, and transfected into cells using HiPerFect reagent (Qiagen) according to the manufacturer's recommendations. TG2 expression plasmid (pLPCX-TG2) and the active site mutant (pLPCX-C277S) plasmid were used as previously described (22), along with an empty vector control (pcDNA3.1), and transfected into cells using Lipofectamine LTX (Invitrogen) according to the manufacturer's instructions. Pre-miR-19a plasmid (Genecoepia) and a corresponding scrambled plasmid control (SCC) were transfected into SW480 cells using Fugene 6 (Roche) according to the manufacturer's recommendations (SW480/miR19A and SW480/SCC). Stable transfection was achieved by selecting resistant clones using puromycin (1 μg/mL), cell sorting by FACS for the IRES-driven GFP reporter, and after expansion used at early passage (<10). Twenty-four hours prior to experiments, cells were also transfected with a miR-19A mimic or corresponding scramble control (Qiagen) using HiPerFect reagent (Qiagen) according to the manufacturer's instructions. After 24-hour incubation, cells were trypsinized and used for experimental testing.

Matrigel invasion assay

Invasion assays were performed using 8 μm Transwell plates (Corning). Matrigel (BD Biosciences) was diluted at 1:3 in serum-free medium and allowed to dry in the upper chamber of the wells. A total of 100,000 cells were then added to the upper chamber in serum-free medium, and complete medium was added to the lower chamber as a chemoattractant. After 24 hours, cells invading the Matrigel were released by trypsinization, and counted using a CASY TTC counter (Roche Innovatis).

Western blot analysis

Western blotting was performed to assess cellular expression of TG2, and actin expression was used to confirm equal protein loading. Cells were lysed in PBS + 1% NP-40, and briefly sonicated before centrifugation to remove insoluble material. Alternatively, in some experiments, protein extracts were prepared in 1% SDS following TRizol treatment according to the manufacturer's protocol (Ambion). Total protein content of these preparations was assessed by BCA assay (Thermo Scientific), equal quantities of protein were loaded onto SDS–PAGE gels for electrophoresis, and transferred to nitrocellulose membrane (Amersham). Membranes were blocked with 5% nonfat milk in TBS+0.5% Tween, then probed with appropriate primary antibodies; TG2 (Abcam; clone CUB7402; 1:2,000), and actin to confirm equal protein loading (Santa Cruz Biotechnology, 1:2,000). Bound proteins were detected using horseradish peroxidase (HRP)–labeled secondary antibodies (Santa Cruz Biotechnology, 1:2,000), and ECL chemiluminescent substrate (Thermo scientific).

TG2 activity assay

The assay for TG2 activity was performed as previously described (24). On the basis of incorporation of the TG2 substrate monodanslycadaverin (bio-MDC; Cambridge Bioscience), cells were incubated for 1 hour with the substrate in the presence of 200 mmol/L $CaCl_2$, fixed in 4% paraformaldehyde, and permeabilized with 0.1% Triton X-100 (Sigma). Biotinylated substrate was revealed using streptavidin–FITC (BD Pharmingen; 1:150), and TG2 protein costained using the antibody clone CUB7402 (Abcam; 1:100) and detected by anti-mouse Alexa Fluor-594 antibody (BD Biosciences; 1:300). Cells were counterstained with the nuclear stain DAPI (1:1,000; Invitrogen) before mounting in Slow-fade medium (Invitrogen) and visualized under a fluorescent microscope. Mean corrected total cell fluorescence was calculated from fluorescence intensities obtained in the ImageJ, using the equation: integrated density − (area of cell × background).

Flow cytometry and immunoassay

The expression of TG2 was assessed by flow cytometry in order to compare surface expression and intracellular expression. Cells were trypsinized from culture dishes, washed three times in PBS, and suspended in flow buffer (PBS + 1% FCS, 0.05% sodium azide). Membrane permeabilization was performed where necessary using Fix-perm reagents (eBiosciences, according to the manufacturer's instructions). For both intracellular and cell-surface staining, the primary TG2 antibody CUB7402 was used (1:100; Abcam), and detection performed using anti-mouse FITC-conjugated secondary antibody (1:300; Sigma). IL8 production was measured using a commercial ELISA assay (R&D Systems).

Immunohistochemical and miRNA quantification from colorectal cancer patients

Immunohistochemical staining was performed on formalin-fixed specimens from patients undergoing resections for colorectal cancer at the University Hospital Southampton (Southampton, United Kingdom) as part of an NIHR portfolio study (UK CRN ID6067). Tumor specimens were snap-frozen in liquid nitrogen within 10 minutes of surgery and stored in a designated UK Human Tissue Act–approved tumor bank. Samples were selected from three clinically distinct groups: (i) colonic tissue from early-stage disease (stage I/II), (ii) colonic tissue from late-stage disease (lymph node involvement, stage III/IV), (iii) liver tissue from colorectal cancer metastatic disease (stage IV). Antigen retrieval was performed by microwave citrate method, and staining using the antibody clone CUB7402 (Abcam; 1:800). Semiquantitative scoring of TG2 levels on whole tissue sections was performed independently and in a blinded manner by a

Published OnlineFirst May 1, 2015; DOI: 10.1158/1541-7786.MCR-14-0466

specialist pathologist (G.J. Thomas) and a further investigator (A.H. Mirnezami). A modified 3-point scoring method was used: (i) low/negative staining (<10% positivity), (ii) focal/patchy staining (10%–50% positivity), (iii) strong diffuse staining (>50% positive). All patients provided informed consent in accordance with the Helsinki protocol, and the study was approved by the regional research ethics committee.

microRNA analysis

Prediction of miRNA targets for TG2 was performed using four target prediction algorithms: TargetScan (http://www.targetscan.org; release 5.1); miRanda (http://www.microrna.org; 2010 release); miR Walk (http://www.umm.uni-heidelberg.de/apps/zmf/mirwalk/); and DIANA—microT (http://diana.cslab.ece.ntua.gr/microT/; v3.0). For quantification of miRNA levels in patient samples, laser-capture microdissection (LCM) was performed on frozen human tissue specimens. Sections were fixed in 75% ethanol, stained with 1% cresyl violet, and dehydrated with ethanol before air drying. Microdissection was performed on the Leica AS microdissection platform, and captured colorectal cancer tissue collected directly into lysis buffer prior to RNA isolation (RNA AQueous MicroPrep Kit; Ambion). Ten randomly selected specimens were analyzed from two clinically defined groups: (i) primary colorectal cancer tumor tissue, (ii) patient-matched liver tissue from colorectal cancer metastasis. The expression of miRNAs was performed using TaqMan assays (Applied Biosystems) according to the manufacturer's instructions, and normalized to U6 expression. Expression of miRNA was calculated relative to the endogenous reference gene U6B using the formula $2^{-\Delta\Delta C}{}_{T}$. miRNA expression in cell lines was obtained from microarray data published previously (25), which is available in the EBI database (http://www.ebi.ac.uk/arrayexpress/experiments/; accession number E-MEXP-3270).

SNP6 array hybridization, data extraction, and analysis

DNA was isolated from cell lines using the Qiagen DNeasy method prior to being purified, amplified, labeled, and hybridized to the Affymetrix SNP6 platform (Affymetrix) as previously described (26). The data were aligned (Build 36.3) and analyzed by two independent researchers using Partek Genomics Suite (Partek Inc.). Copy number alterations (CNA) were defined as a deviation of 50 consecutive probes from a normal value of 2 (±0.3), within a consecutive genomic window of 50 kb. The 270 HapMap Reference baseline (Affymetrix) was used as a control and germline copy number variants were excluded on the basis of the Database of Genomic Variants (http://projects.tcag.ca/variation/). The allele ratio was calculated for each sample using the HapMap Allele Reference baseline (Affymetrix) and in the absence of paired normal DNA; copy number neutral loss of heterozygosity (CNNLOH) was defined as a region greater than 20 Mb, extending to a telomere. We also analyzed copy number data from 437 Colon Adenocarcinoma cases from the Cancer Genome Atlas data COAD dataset (https://tcga-data.nci.nih.gov/tcga/) using the UCSC Cancer Genomics Browser (https://genome-cancer.soe.ucsc.edu/) to identify recurrent regions of copy number gain and loss that include our miRNAs of interest.

TG2 3′-UTR luciferase reporter assay

TG2-3′-UTR wild-type and TG2-3′-UTR mutant vectors were generated by GenScript Inc. A 750 bp region of the TGM2 gene 3′-UTR containing the single predicted miR-19a binding site was synthesized and was subcloned into the pRL-TK plasmid vector (Promega) downstream of the *Renilla*-Luc gene at the *Xba*1 site. Insert orientation was in the same sense as the luciferase reporter in pRL-TK. The mutant vector was generated by changing the sequence TTTGCACA to TTTATTGA. Reporter genes were transfected into SW480/SCC and SW480/miR-19a lines using Fugene 6, and luciferase activity quantified using the Dual-Luciferase reporter system (Promega) to collect the activity of firefly (PGL3 vector control) and *Renilla* (TG2-3′-UTR) measured in the same sample. SW480/SCC and SW480/miR-19a cells were plated at 4,000 cells per well in 100 μL DMEM in a CulturPlate-96 microplate (PerkinElmer). Twenty-four hours after plating, cells were transfected with 30 nmol/L Pre-miRNAs, 10 ng PGL3, and 500 ng of TG2-3′-UTR (wild-type or mutant) vectors per well. Light produced was measured using a plate reader at 2-second intervals and activity was calculated as *Renilla* activity per light unit of firefly activity. 3′-UTR *Renilla* activity was normalized to firefly activity, and results presented as the difference between the wild-type and mutant vectors.

Statistical analysis

Statistically significant differences between experimental conditions were assessed using the Student *t* test, and paired *t* test where appropriate. Alternatively, where multiple comparisons were necessary, ANOVA with the Bonferroni post-hoc test was used. All analyses were performed in GraphPad Prism, and P values of <0.05 were considered statistically significant. All experiments were performed a minimum of three times.

Results

TG2 expression is decreased in SW620 cells compared with SW480 cells

It has been reported previously that differential TG2 levels are observed in the SW model of metastasis, with high levels in the primary colon adenocarcinoma SW480 line, and significantly reduced levels in the patient-matched SW620 lymph-node–derived line (11). We confirmed these observations at protein level by Western blot analysis (Supplementary Fig. S1A), showing considerable reduction of the full-length 79-kb isoform of TG2 in SW620 cells. Decreased protein expression of this full-length transcript in SW620 cells was matched by a decrease in mRNA transcript level (Supplementary Fig. S1B). Interestingly, protein expression of the 55-kD exon-10–truncated splice variant of TG2 (TG2-E10) was actually relatively higher in SW620 cells (Supplementary Fig. S1A). This is in contrast to a decrease in mRNA transcript level (Supplementary Fig. S1B), indicating differential regulation of the splice variants.

Reduced TG2 is associated with increased invasiveness in SW480/SW620 cells

Because TG2 levels were significantly reduced in SW620 cells when compared with SW480, and SW620 cells are more invasive (12, 27), we hypothesized that TG2 may be inversely correlated to invasive potential. In an invasion assay using Matrigel as a substrate, SW620 cells, as expected, displayed increased invasive behavior (Fig. 1A), with counts of invading cells reaching 20,000 compared with 5,500 for SW480 cells. This was not due to significant differences in cell proliferation within the lower chamber as differences were not observed in an MTT proliferation assay (data not shown), nor were any differences accounted for by

Published OnlineFirst May 1, 2015; DOI: 10.1158/1541-7786.MCR-14-0466

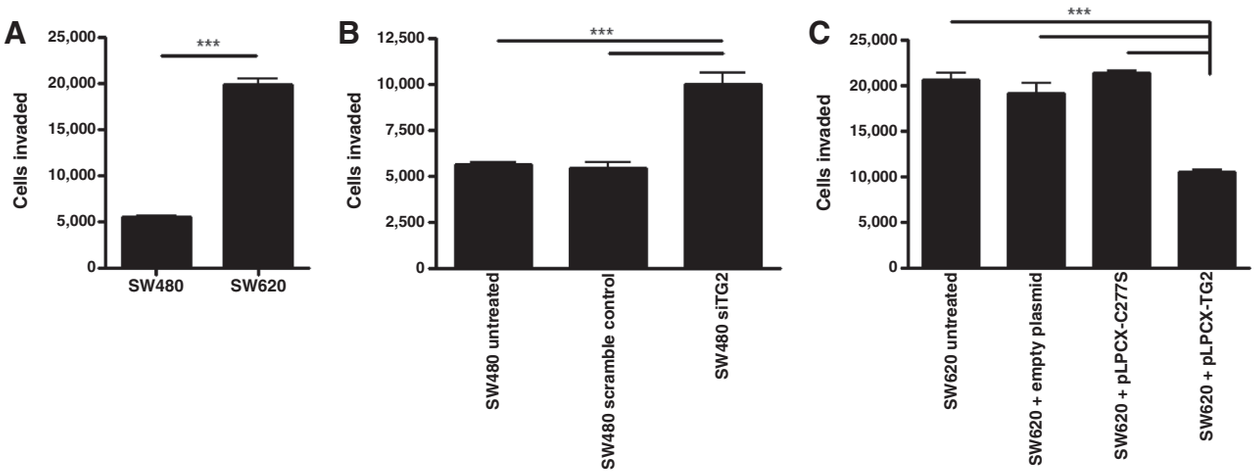

Figure 1.
TG2 is involved in the invasive ability of SW cells. The number of cells invading through Matrigel substrate toward an FCS chemoattractant in 24 hours was compared for SW480 cells and SW620 cells (A), in the presence or absence of TG2 siRNA to knock down TG2 expression, or scrambled siRNA as a control, in SW480 cells (B), and following the transfection of a TG2 expression plasmid or the catalytically inactive expression plasmid C277S into SW620 cells (C). Statistical significance is indicated by the asterisks, ***, $P < 0.0001$.

apoptosis using Annexin V staining (data not shown). When SW480 cells were treated with siRNA to TG2, the cells became significantly more invasive, showing a 100% increase in the number of invading cells when compared with cells either untreated or treated with a scrambled, control siRNA ($P < 0.0001$; Fig. 1B). In contrast, overexpression of TG2 in SW620 cells using a plasmid encoding TG2 significantly decreased the number of invading cells by around 50%, compared with untreated, empty vector, or cells transfected with the cross-linking-deficient TG2 plasmid C277S ($P < 0.0001$; Fig. 1C). Thus, TG2 cross-linking activity appears to restrict invasive behavior of SW cells, whereas loss of TG2 in SW620 cells facilitates invasion.

TG2 activity in SW cells is localized intracellularly

Because TG2 activity decreased invasiveness of SW cells, we wished to define its cellular localization, because cell-surface TG2 may interact directly with the cell-surface and extracellular matrix (ECM) proteins (28, 29), whereas intracellular TG2 has a cell signaling function (24, 30, 31). Imaging of TG2 by immunofluorescent microscopy showed that TG2 protein was expressed throughout the cytoplasm in both SW480 and SW620 cells (Fig. 2A, red). Furthermore, cytoplasmic TG2 was catalytically active as assessed using a fluorescent TG2 substrate (Fig. 2A, green). The staining for protein and activity were colocalized (Fig. 2A, merge). Expression of both TG2 protein and cross-linking activity was higher in SW480 cells compared with SW620 cells (mean CTCF of 33.3×10^5 compared with 18.3×10^5 for protein, 19×10^5 compared with 9.3×10^5 for activity, respectively), consistent with previous data. Significant TG2 was also observed localized to the nucleus (Fig. 2A). By comparing nuclear expression to cytoplasmic expression, we observed that 17%/24% of the cellular TG2 protein/activity was localized to the nucleus of SW480 cells, and 11% of both protein/activity was localized to the nucleus of SW620 cells. The absence of cell-surface TG2 data were confirmed by flow cytometry. Cells stained for cell-surface expression of TG2 showed very limited staining, and no differences were observed between SW480 and SW620 cells (Fig. 2B). In contrast, when cells were permeabilized prior to staining, strong expression of TG2 was observed, with >99% cells expressing TG2, and with considerably stronger staining in SW480 cells compared with SW620 cells.

TG2 activity influences inflammatory profile of SW cells

Because intracellular TG2 is known to drive proinflammatory signaling (9, 23, 30), we also measured IL8 production by SW480 and SW620 cells. IL8 was not detected in SW620 supernatants, but was clearly produced by SW480 cells. Using TG2-specific siRNA, TG2 levels could be reduced from 300 to 100 pg/mL compared with control ($P < 0.05$; Fig. 2C). We next compared the expression of cytokines in the two cell lines, and observed that the production of proinflammatory cytokines by SW480 cells was generally higher when compared with SW620 cells, including IL8 and TNFα (Supplementary Fig. S2A; $P < 0.05$). However, although TG2 siRNA reduced IL8 and TNFα mRNA expression, the differences were not significantly different (Supplementary Fig. S2B), and we could not detect expression of TNFα in cell supernatants (data not shown). Because proinflammatory signaling pathways are also linked to the release of enzymes that can break down tissue, we also investigated whether matrix metalloproteinase (MMP) production was influenced by TG2. As expected, the more invasive SW620 cells expressed higher levels of MMP mRNA, notably significantly higher levels of MMP-7 ($P < 0.05$; Supplementary Fig. S3A). Interestingly, SW620 cells also expressed significantly lower mRNA of one member of this enzyme family, MMP-14 ($P < 0.05$; Supplementary Fig. S3A). However, when we compared MMP mRNA expression in SW480 cells treated with and without siRNA to TG2, no significant changes to MMP mRNA expression were observed (Supplementary Fig. S3B), indicating that TG2-linked invasion was not directly related to enhanced MMP production.

TG2 levels are downregulated in metastatic tumors compared with primary tumors

Because our data in the SW model demonstrated downregulation of TG2 in the metastatic SW620 cell line, and correlation of TG2 levels with tumor invasiveness, we investigated the

Published OnlineFirst May 1, 2015; DOI: 10.1158/1541-7786.MCR-14-0466

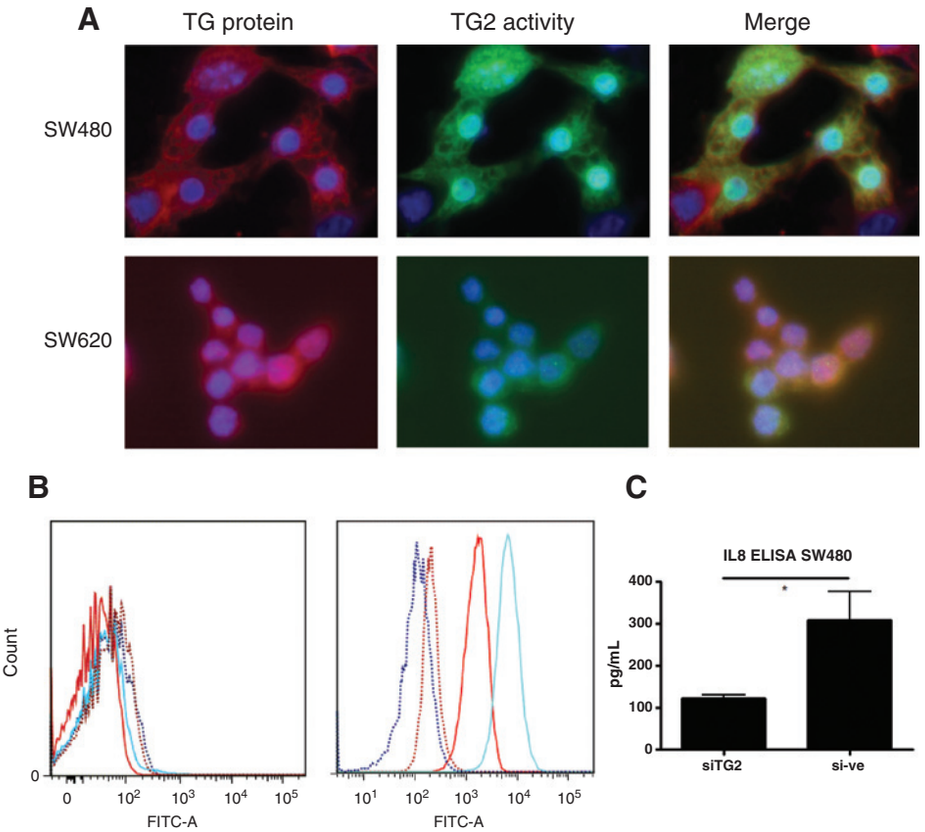

Figure 2.
TG2 is distributed throughout the cell cytoplasm, and is not localized to the cell surface in SW cells. The cellular distribution of TG2 was assessed by measuring the presence of TG2 protein in fixed cells by immunolocalization with the antibody clone 7402 coupled to Alexa Fluor 492–conjugated secondary antibody (A, red stain), and colocalizing protein to TG2 activity visualized using the biotinylated MDC-substrate assay coupled to a FITC-streptavidin secondary antibody (A, green). DAPI counterstaining (blue) indicates the cell nucleus (A). The presence of cell-surface TG2 was also determined by flow cytometry (B), using TG2 staining of whole live cells with the antibody clone 7402 (left), compared with cells permeabilized to assess intracellular levels (right panel). SW480 cells are displayed as blue lines, and SW620 cells as red lines. The dotted lines represent unstained controls. IL8 production by SW480 cells in the presence or absence of siRNA to TG2 was analyzed by ELISA (C). *, $P < 0.05$.

expression of TG2 in human colorectal cancer sections, comparing primary tumors taken from patients grouped according to confirmed lymph node involvement, and from liver metastases. Staining for TG2 was detected in primary tumor sections (Fig. 3A and B), mainly at the invasive front (Fig. 3A), but not in liver metastases (Fig. 3C). Scoring by two independent investigators quantified this differential expression pattern (Fig. 3D), with TG2 expression found to negatively correlate with tumor stage. However, in these sections the most intense staining was detected in the tumor stroma (Fig. 3A–C), with cells surrounding the cancerous cells appearing to produce significant amounts of TG2, both at the primary and metastatic sites. No TG2 staining was observed in normal epithelia (data not shown).

TG2 is a predicted miRNA target

To better understand the differential protein expression of TG2 splice variants in SW cells (Supplementary Fig. S1A), we next examined the mRNA expression of TG2 splice variants by RT-PCR. In SW480 cells, expression of the mRNA for all of the TG2 splice variants assessed was higher in SW480 compared with SW620 cells, at differences ranging from 100- to 2,000-fold ($P < 0.0001$; Supplementary Fig. S1B). The protein and mRNA expression of full-length TG2 therefore appear to correlate, but the protein level of the 55-kD splice variant does not correlate to the mRNA expression of TG2-E10. There is an increasing evidence that miRNAs are intimately involved in the metastatic progression of colon cancer (18, 20, 25, 32). miRNAs bind to the 3′-UTR of their target genes, and the TG2 splice variants are 3′-truncated (15, 33). We therefore examined the possibility that TG2 may be a target for miRNA regulation, and explain why expression of TG2 splice variants is different at mRNA and protein level. Potential miRNA regulators of TG2 were identified by *in silico* analysis of the 3′-UTR using a panel of four target prediction algorithms. These identified only a single miRNA, miR-19a/b, predicted to bind to the 3′-UTR of TG2 across all platforms. Binding of miR-19a/b was predicted to occur at a conserved UUUGCACA sequence at position 1588–1595 of the 3′-UTR (Supplementary Fig. S4A), suggesting miR-19a/b may represent a potential regulatory miRNA for TG2.

miR-19 is upregulated in metastatic tumors compared with primary tumors

The level of miR-19 in sections taken from patients with colorectal cancer was assessed using LCM, in order to isolate epithelial and stromal expression (Supplementary Fig. S4B). miRNA microarray profiling showed that miR-19a/b expression was significantly different in tumor epithelia when compared with normal epithelia ($P < 0.05$; Supplementary Fig. S4C). miR-19a/b expression was not significantly different in tumor stroma compared with normal stroma (Supplementary Fig. S4D). Noticeably, both epithelial and stromal analyses showed several specimens with high expression of miR-19; interestingly, however, these did not correlate to the same patients for epithelial/stromal expression. Our data indicated that differences in TG2 expression were observed between primary tumor specimens and liver metastases.

Published OnlineFirst May 1, 2015; DOI: 10.1158/1541-7786.MCR-14-0466

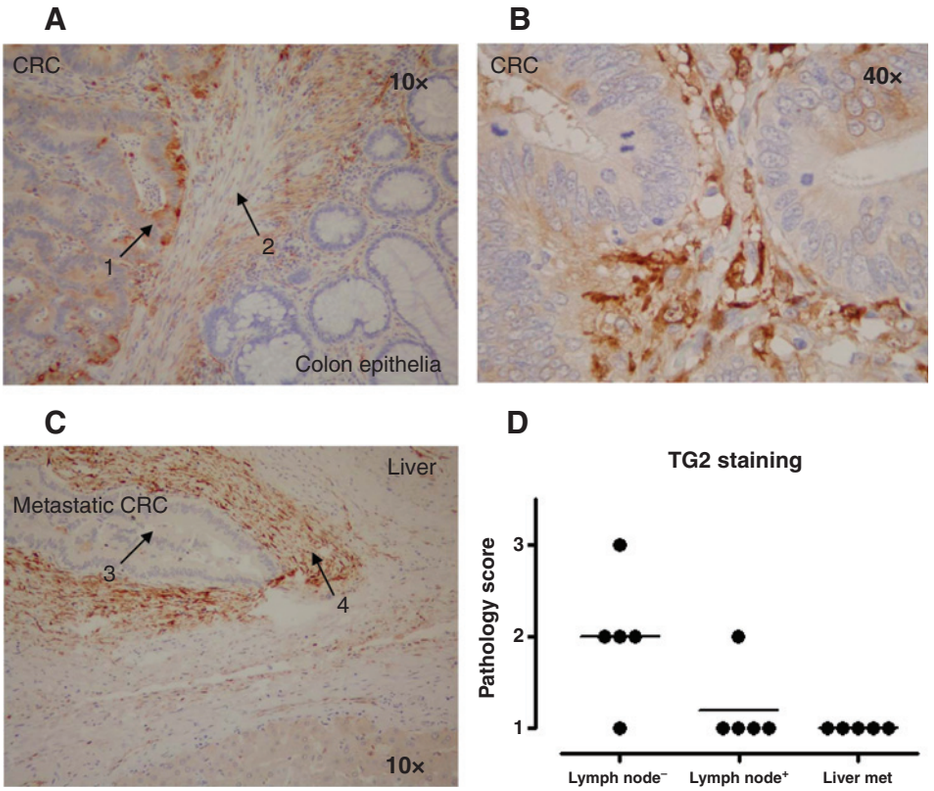

Figure 3.
TG2 is expressed in human colorectal cancer specimens, but lost in liver metastases. TG2 was stained in colorectal cancer tumor sections using antibody clone 7402. A, representative image showing staining in primary colorectal cancers, with arrows indicating tumor (1) and stroma (2). B, TG2 staining at higher magnification in primary colorectal cancer, and C illustrates a representative image of a liver metastasis, with arrows showing tumor cells (3) and stroma (4). In both cases, strong stromal expression of TG2 is observed. As illustrated following scoring by a senior pathologist, TG2 expression is lost in sections taken from liver metastases (D).

We therefore analyzed miR-19a using TaqMan in LCM samples to compare these two groups. miR-19a expression was significantly upregulated in sections taken from liver metastases compared with sections taken from primary tumors (Fig. 4A; $P < 0.01$).

miR-19 is upregulated in SW620 cells compared with SW480 cells, and its genomic locus is amplified in colorectal cancer

To test whether overexpression of miR-19 could be a mechanism for TG2 downregulation, we first established the levels of miR-19a and miR-19b in SW620 cells compared with SW480 cells. microRNA microarray profiling of SW620 and SW480 cells demonstrated a 2.6-fold increase of miR-19a and a 3-fold increase in miR-19b in SW620 cells compared with SW480 cells [normalized values of 274.49 vs. 105.45, and 3082.57 vs. 1026.25 for miR-19a and miR-19b, $P = 0.01$, and <0.0001, respectively (25)], subsequently validated by qPCR analysis, confirming observations from other groups (20, 34). Deregulation of miRNAs has been attributed to genomic copy number changes (35), and miRNAs have been noted to be over-represented in regions of genomic gain in colorectal cancer (36), consequently we next examined whether copy number changes could account for the upregulation of miR-19a and b in the SW cell lines. SW480 and SW620 cells were analyzed using a Genome-Wide Human SNP Array 6.0 with the HapMap 270.422 dataset as reference. miR-19a and miR-19b1 are located on chromosome 13 and both were found to be gained in both cell lines (Fig. 4B). In contrast, miR-19b2 showed normal copy number in both cell lines from its locus on chromosome X (data not shown). To clarify whether the miR-19a/b loci are subject to copy number change in primary human colorectal cancer, we next examined the Cancer Genome Atlas (TCGA) dataset. In the data available from 437 human colorectal cancers, both miR-19a and miR-19b were subject to amplification through recurrent chromosome 13 gains. However, this was due to recurrent gains in chromosome 13, rather than any focal CNAs at the specific miR-19 loci (Fig. 4C). The data therefore indicate that advanced colorectal cancer frequently gains an additional copy of the whole chromosome 13. Further analysis of the TCGA dataset reveals that this amplification in colorectal cancer patients occurs in later stages of disease; no significant differences are observed when comparing patients with stage I, II or III disease, but significant differences ($P < 0.05$) are seen when comparing stage III and IV disease (data not shown).

miR-19 directly targets TG2 and alters the invasive behavior of SW cells

To confirm our *in silico* prediction of miR-19 targeting TG2, we manipulated miR-19a levels in SW480 cells by establishing stable cell lines overexpressing a scrambled plasmid control (SW480/SCC), a miR-19a expression plasmid (SW480/miR-19a), and by transient transfections with molecular miRNA mimics. Downregulation of TG2 was observed by Western blot analysis in SW480 cells manipulated to overexpress miR-19a (Fig. 5A), which was statistically significant when assessed by densitometry ($P < 0.05$). The direct binding of miR-19a to the 3′-UTR of TG2 was assessed using a luciferase reporter assay, which showed a reduction of 3′-UTR activity by almost 50% in the SW480/miR-19a cells ($P < 0.01$; Fig. 5B). To evaluate the functional

Published OnlineFirst May 1, 2015; DOI: 10.1158/1541-7786.MCR-14-0466

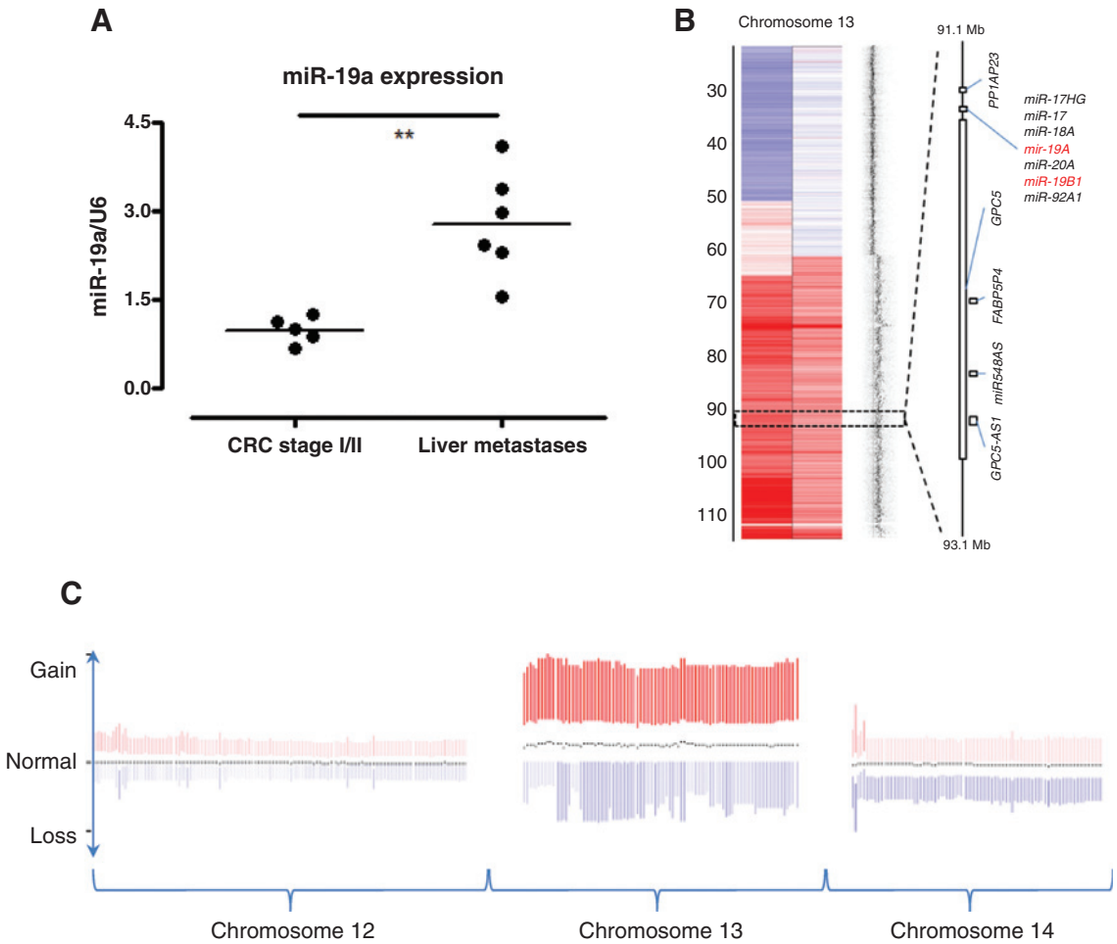

Figure 4.
miR-19a is upregulated in metastatic cells through instability of chromosome 13. The expression of miR-19a was assessed by TaqMan in RNA isolated from sections of primary colorectal cancer tissue compared with liver metastases (A). Copy number heatmap from SNP6 data of chromosome 13 forSW620 and SW480 to the left and right, respectively. Normal copy number, gain, and loss are shown in gray, red, and blue, respectively. Data show duplication/amplification of distal 13q, including the miR-19a and miR-19b1 loci (B). Relative copy number for chromosomes 12, 13, and 14 positioned from left to right from the COAD dataset (C). The mean profile for each chromosome is shown by the black dots, indicating copy number at different points along each chromosome from 437 patients with colorectal cancer. The color intensity is proportional to the deviation from the median, and the shift upward toward red indicates increased chromosome 13 copy number in relation to chromosomes 12 and 14.

consequences of this, invasion assays were performed on these stable cell lines. SW480 cells overexpressing miR-19a showed enhanced invasiveness when compared with control cells (Fig. 5C; $P < 0.01$). Thus, elevating the levels of miR-19a has a similar effect to reducing TG2 using siRNA. To confirm that TG2 was the target for miR-19a in this model, we transfected SW480/19a cells with the TG2 expression plasmid, lacking the 3′-UTR binding site for miR-19a (pLPCX-TG2). Restoring TG2 in this way reduced invasion of SW480/miR-19a cells to a level similar to that observed in 480/SCC cells in a statistically significant manner (Fig. 5C; $P < 0.05$). Finally, IL8 production from the stable SW480 cell lines was assessed by ELISA. Although slightly lower IL8 production was seen from SW480/miR-19a cells compared with SW480/SCC cells, this was not significant (Fig. 5D). However, transfection with the pLPCX-TG2 plasmid significantly increased the production of IL8 ($P < 0.05$), further illustrating the functional effect of TG2 lacking the 3′-UTR miRNA-binding site.

Discussion

There is a widespread body of literature spanning the past two decades illustrating that TG2 is involved with many cellular processes linked to tumor development and progression including chemoresistance, adhesion, migration, invasion and EMT, and TG2 has been found in tumor cells from a variety of origins. The primary role of TG2 is as a protein cross-linking enzyme, linking glutamine and lysine residues, and this can eventually lead to the formation of protein aggregates (37). A wide range of TG2 substrates has been reported, which includes both intra- and extracellular proteins, implying a role for TG2 both inside and outside of the cell. The range of cell behaviors linked to TG2 and sometimes contradictory results in studies of TG2 activity suggest a role that is isoform-, context- and cell-type dependant (14).

It is interesting that we observe an inverse relationship between TG2 and invasion *in vitro* in the SW cell model. This finding

Published OnlineFirst May 1, 2015; DOI: 10.1158/1541-7786.MCR-14-0466

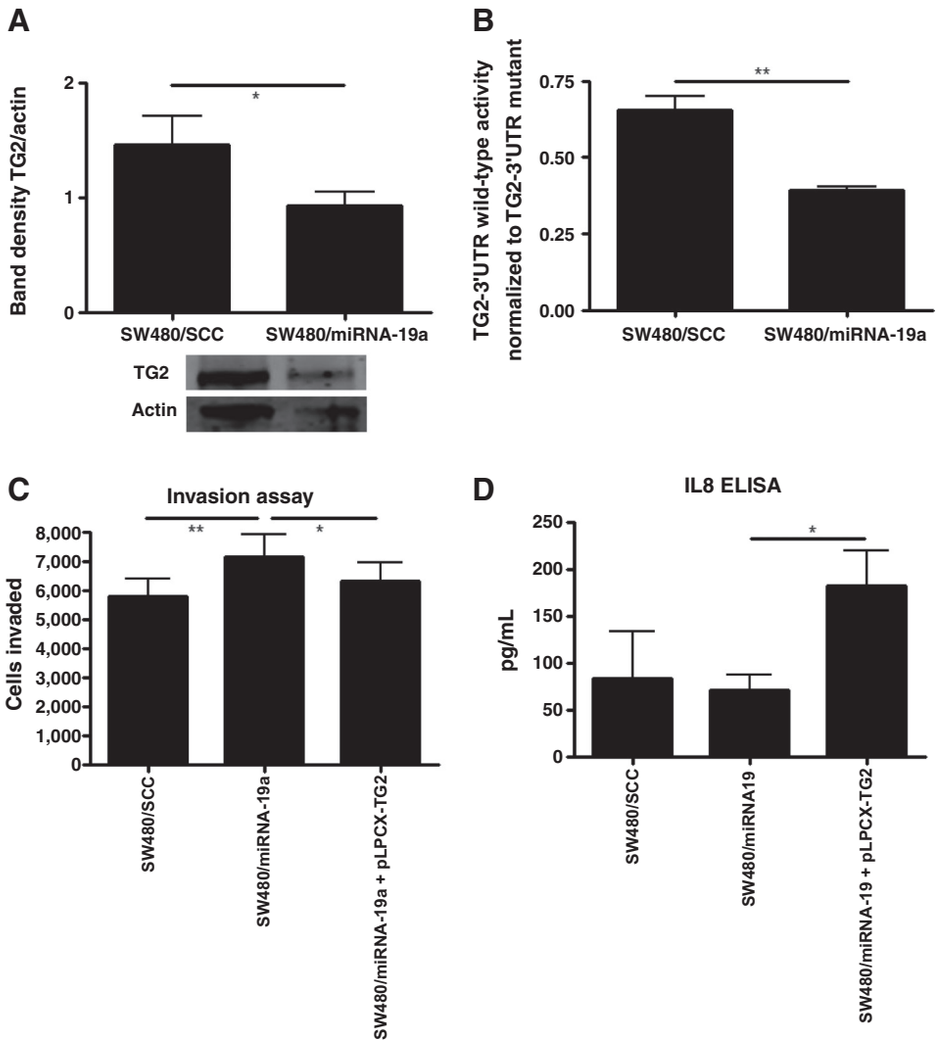

Figure 5.
miR-19 promotes changes in colorectal cancer cell behavior through TG2. The effect of miR-19a overexpression in SW480 cells was assessed following stable transfection with a miR-19a expression plasmid (480/miR-19a), compared with a control plasmid (SCC). Western blotting was performed to observe the effect of miR-19a on TG2 protein levels (A) and quantified by densitometry, and direct targeting of TG2 by miR-19a was assessed using a 3′-UTR luciferase reporter gene (B). The effect of miR-19a overexpression on invasion was assessed in the SW480 stable lines using the Matrigel invasion assay (C). The effects of miR-19a on invasion were established to be through TG2 by cotransfecting the cells with a TG2 expression plasmid lacking the 3′-UTR miRNA binding sequence. The effect of miR-19a on inflammatory signaling was assessed using IL8 ELISA on supernatants from SW480 stable cell lines (D).
*, $P < 0.05$; ** = $P < 0.01$.

supports studies describing a correlation between metastatic potential and TG2 expression in colorectal cancer cells (12), but runs contrary to reports in several other cell models (8, 27, 38, 39). In a similar manner to studies showing that TG2 can function in a pro- or antiapoptotic manner (14), the cell-, isoform-, and context dependence of TG2 makes interpretation of such apparently contradictory results difficult. In an important study, it was demonstrated that the truncated form of TG2 promoted cell death, in contrast to the full-length protein which promoted cell survival (32). Although we observe a downregulation of full-length protein in SW620 cells compared with SW480 cells, we actually observe a small upregulation of the truncated protein (Supplementary Fig. S1). If cell behavior is linked to the balance between TG2 isoforms, this shift could well be critical—it is notable that the smaller form is truncated at the 3′-end, making it likely that miR-19 will not inhibit transcription of the truncated protein. Because this truncation also removes the GTP-binding site that inhibits cross-linking function, this isoform is highly active and may compensate for the miR-19–induced reduction of the full-length protein in the metastatic cell line, maintaining critical functionality such as adhesive and migratory behavior.

Interestingly, in several previous studies where TG2 has been shown to promote invasive behavior, this activity was not dependent on cross-linking activity, and active site mutated TG2 was also able to promote invasion (8, 39). In contrast, when we transfected the active site mutated TG2 into SW620 cells, no effect on cell invasion was observed. Given the clear inhibition of invasive behavior we observe when we transfect active TG2, we conclude that in the SW model system, TG2 inhibits invasive behavior in a cross-linking dependent manner. Because promotion of invasion by TG2 in other model systems is not dependent on cross-linking it likely involves signal transduction mediated by interaction with integrins/FAK at the cell membrane/ECM boundary (8, 27–29, 40). Our observation that SW cells lack cell-surface expression of TG2 supports a role for TG2 in restricting invasion in early-stage colorectal cancer through this separate mechanism. We did not specifically examine secretion of TG2 in this study, but experiments to examine whether TG2 released directly into the matrix would be informative, because modification of ECM by TG2 is known to restrict invasion (41). In early colorectal cancer, it may be the case that cancer progression is driven by cross-linked, stiffened ECM (42), linking TG2 expression to poor prognosis as

Published OnlineFirst May 1, 2015; DOI: 10.1158/1541-7786.MCR-14-0466

proposed by previous reports (13), but at the expense of rapid invasion, a feature that is reversed as the tumor progresses.

Although our data indicated a lack of cell surface expression of TG2, we observed extensive staining in the cytoplasm and nucleus. In these cell compartments, TG2 cross-linking activity is limited under physiologically normal conditions due to high nucleotide and low calcium conditions. However, intracellular cross-linking is known to occur as a consequence of cell stress—for example, activity is upregulated by ROS (23, 43). One of the consequences of this response is the upregulation of proinflammatory signaling pathways such as NF-κβ that has been reported in both inflammatory and tumor cell models (24, 30, 31), and we identified that IL8 secretion from SW480 cells is inhibited by silencing TG2. IL8 is known to play a significant role in colorectal cancer, and has been proposed as a marker of disease progression, but to our knowledge this is the first study linking IL8 to TG2 in colorectal cancer models (44, 45). Because SW620 cells are derived from an advanced-stage, invasive, metastatic tumor, and IL8 secretion was undetectable from these cells, it may be that stress-linked proinflammatory signaling through pathways like NF-κβ promotes progression of early colorectal cancer, whereas inhibition of this signaling in advanced disease promotes evasion of the immune system in advanced colorectal cancer. Further work would to clarify this would be extremely informative.

High TG2 levels inhibited invasive behavior of SW cells, but silencing of TG2 did not significantly alter MMP expression (Supplementary Fig. S3B), although MMP expression tended to be higher in SW620 cells. This may be a consequence of the experimental system; culturing cells in plates—as we did in the present study when analyzing MMP gene expression—induces significantly different responses in tumor cells when compared with the 3D environment cells experience *in vivo*, or within the Matrigel layer of the invasion assay (46, 47). Actin is reported to be an intracellular TG2 substrate (48), so it is also feasible that intracellular TG2 could play a role in colorectal cancer cell invasion in the cytoskeletal remodeling involved during cell mobility and invasion. Further experiments to examine TG2 secretion, MMP expression, and cytoskeletal changes by SW cells in a 3D model will be extremely informative.

The downregulation of TG2 in metastatic SW620 cells and in sections taken from liver metastases illustrates the context dependence of using TG2 as either a marker of disease or as a therapeutic target in colorectal cancer. The negative relationship between TG2 expression and invasive potential has been reported previously in the SW model (12), and the inverse relationship between TG2 and metastasis observed in other studies (49–51). It will therefore be interesting to examine whether this biphasic model of TG2 involvement in cancer progression is a general phenomenon, as it would have significant implications for the targeting of TG2 therapeutically. Our observation of significant TG2 expression in the stroma of both primary and metastatic colorectal cancer, despite downregulation of TG2 in metastatic cells, suggests that the majority of TG2 is produced as a defensive response rather than by the tumor (41, 52, 53). Further clarification of the cellular source of TG2 in colorectal cancer is important, as the differential impact of TG2 activity in cancer cells and in the surrounding tissue complicates the use of TG2 as a therapeutic target. Identifying pathways that specifically regulate TG2 expressed in cancer cells may therefore offer a promising alternative approach.

Examining the role of miRNAs in regulating TG2 was a consequence of our data showing differential expression of two splice variants of TG2 at transcript and protein level; indeed, over the course of the study TG2 protein levels were observed to vary significantly. Examining putative miRNA binding sites revealed that TG2 is a predicted target for miR-19, which has two closely related members miR-19a and miR-19b within the miRNA17-92 cluster. This adds to previous studies identifying regulatory roles for miR-1285, miR-181a, and miR-218 in regulating TG2 (54, 55), and because TG2 plays an important role in inflammatory disease (22, 24), multiple miRNA pathways may therefore have an important role in regulating innate immune responses as well as cancer cell behavior linked to TG2 activity. It is interesting that we did not see a significant change in IL8 in SW480/miR-19a cells compared with SW480/SCC control cells. This would be expected given that we observed that IL8 production is inhibited by silencing TG2 in SW480 cells, TG2 is suppressed by miR-19, and we also observe that transfection of the TG2 plasmid into SW480/miR-19a cells upregulates IL8. This could be the consequence of the multiple pathways that converge on NF-κB in cancer cells, for example NF-κB activation can be inhibited by blocking K-Ras activity in SW620 cells (56). However, these data may also simply represent technical differences in manipulating TG2 using siRNA—which is highly efficient in our model—compared with manipulating TG2 using miR-19, which alters expression by less than 50% (Fig. 5A).

Multiple studies have demonstrated that miR-19 is upregulated in colorectal cancer patients, notably at the invasive front of the tumor, and also in SW620 cells when compared with SW480 cells (25, 32, 34). (32, 34), strongly implicating these miRNAs in disease progression. We focused on miR-19a, demonstrating upregulation in sections taken from liver metastases when compared with primary colorectal cancer sections, and in metastatic SW620 cells compared with primary SW480 cells. Overexpressing miR-19a led to a reduction in TG2 expression in SW480 cells, with consequent increased invasive behavior. We therefore propose that the miR-19–TG2 axis can be added to the growing list of miRNA-regulated pathways that are linked to metastasis. Moreover, we identified that both in the SW cell model and in patients with colorectal cancer, overexpression of miR-19a/b is linked to chromosomal instability on chromosome 13, at the locus encoding a series of miRNAs, including miR-19a and miR-b1. Amplification of chromosome 13 is observed frequently in colorectal cancer, despite encoding relatively few genes linked to oncogenic pathways (57), and these observations may provide a mechanistic link between colorectal cancer and instability at this locus, via miRNAs and TG2.

Identifying miRNA regulation of TG2 in colorectal cancer cells may provide a more targeted pathway to therapeutic intervention, given the presence of TG2 in both tumor and stroma. Further work is required to establish the precise mechanisms by which TG2 acts to influence cell invasion, and how invasion, inflammation, and metastasis interact to drive the disease process. If TG2 is indeed a stress response, the role of ROS and calcium may be critical as they promote TG2 activity. We were not able to alter TG2 expression using ROS inhibitors, and defective calcium signaling is an established feature of colorectal cancer (58). Continuing to investigate a pathway linking stress, inflammatory signaling and invasion has the potential to provide useful insights into the mechanisms driving an increasing burden on the world's health.

Disclosure of Potential Conflicts of Interest

No potential conflicts of interest were disclosed.

Authors' Contributions

Conception and design: D. Cellura, S. Quaratino, A.H. Mirnezami, N.J. Peake
Development of methodology: D. Cellura, J.C. Strefford, G.J. Thomas, A.H. Mirnezami, N.J. Peake
Acquisition of data (provided animals, acquired and managed patients, provided facilities, etc.): D. Cellura, K. Pickard, H. Parker, G.J. Thomas, A.H. Mirnezami
Analysis and interpretation of data (e.g., statistical analysis, biostatistics, computational analysis): D. Cellura, K. Pickard, S. Quaratino, H. Parker, J.C. Strefford, R. Mitter, A.H. Mirnezami, N.J. Peake
Writing, review, and/or revision of the manuscript: D. Cellura, K. Pickard, S. Quaratino, J.C. Strefford, A.H. Mirnezami, N.J. Peake
Administrative, technical, or material support (i.e., reporting or organizing data, constructing databases): D. Cellura, K. Pickard, A.H. Mirnezami, N.J. Peake
Study supervision: S. Quaratino, A.H. Mirnezami, N.J. Peake
Other (funding support): A.H. Mirnezami

Grant Support

This study was supported by Cancer Research UK and the Royal College of Surgeons of England and Wessex Medical Research.

The costs of publication of this article were defrayed in part by the payment of page charges. This article must therefore be hereby marked *advertisement* in accordance with 18 U.S.C. Section 1734 solely to indicate this fact.

Received August 19, 2014; revised February 17, 2015; accepted April 15, 2015; published OnlineFirst May 1, 2015.

References

1. Center MM, Jemal A, Smith RA, Ward E. Worldwide variations in colorectal cancer. CA Cancer J Clin 2009;59:366–78.
2. Weitz J, Koch M, Debus J, Hohler T, Galle PR, Buchler MW. Colorectal cancer. Lancet 2005;365:153–65.
3. Soreide K, Berg M, Skudal BS, Nedreboe BS. Advances in the understanding and treatment of colorectal cancer. Discov Med 2011;12:393–404.
4. Li B, Cerione RA, Antonyak M. Tissue transglutaminase and its role in human cancer progression. Adv Enzymol Relat Areas Mol Biol 2011;78:247–93.
5. Eckert RL, Kaartinen MT, Nurminskaya M, Belkin AM, Colak G, Johnson GV, et al. Transglutaminase regulation of cell function. Physiol Rev 2014;94:383–417.
6. Mehta K, Fok J, Miller FR, Koul D, Sahin AA. Prognostic significance of tissue transglutaminase in drug resistant and metastatic breast cancer. Clin Cancer Res 2004;10:8068–76.
7. Sun Y, Mi W, Cai J, Ying W, Liu F, Lu H, et al. Quantitative proteomic signature of liver cancer cells: tissue transglutaminase 2 could be a novel protein candidate of human hepatocellular carcinoma. J Proteome Res 2008;7:3847–59.
8. Verma A, Wang H, Manavathi B, Fok JY, Mann AP, Kumar R, et al. Increased expression of tissue transglutaminase in pancreatic ductal adenocarcinoma and its implications in drug resistance and metastasis. Cancer Res 2006;66:10525–33.
9. Verma A, Guha S, Diagaradjane P, Kunnumakkara AB, Sanguino AM, Lopez-Berestein G, et al. Therapeutic significance of elevated tissue transglutaminase expression in pancreatic cancer. Clin Cancer Res 2008;14:2476–83.
10. Lentini A, Abbruzzese A, Provenzano B, Tabolacci C, Beninati S. Transglutaminases: key regulators of cancer metastasis. Amino Acids 2013;44:25–32.
11. Fukuda K. Induction of tissue transglutaminase expression by propionate and n-butyrate in colon cancer cell lines. J Nutr Biochem 1999;10:397–404.
12. Zirvi KA, Keogh JP, Slomiany A, Slomiany BL. Transglutaminase activity in human colorectal carcinomas of differing metastatic potential. Cancer Lett 1991;60:85–92.
13. Miyoshi N, Ishii H, Mimori K, Tanaka F, Hitora T, Tei M, et al. TGM2 is a novel marker for prognosis and therapeutic target in colorectal cancer. Ann Surg Oncol 2010;17:967–72.
14. Chhabra A, Verma A, Mehta K. Tissue transglutaminase promotes or suppresses tumors depending on cell context. Anticancer Res 2009;29:1909–19.
15. Antonyak MA, Jansen JM, Miller AM, Ly TK, Endo M, Cerione RA. Two isoforms of tissue transglutaminase mediate opposing cellular fates. Proc Natl Acad Sci U S A 2006;103:18609–14.
16. Hu W, Coller J. What comes first: translational repression or mRNA degradation? The deepening mystery of microRNA function. Cell Res 2012;22:1322–4.
17. Schetter AJ, Harris CC. Alterations of microRNAs contribute to colon carcinogenesis. Semin Oncol 2011;38:734–42.
18. Schetter AJ, Okayama H, Harris CC. The role of microRNAs in colorectal cancer. Cancer J 2012;18:244–52.
19. Chang KH, Miller N, Kheirelseid EA, Lemetre C, Ball GR, Smith MJ, et al. MicroRNA signature analysis in colorectal cancer: identification of expression profiles in stage II tumors associated with aggressive disease. Int J Colorectal Dis 2011;26:1415–22.
20. de Krijger I, Mekenkamp LJ, Punt CJ, Nagtegaal ID. MicroRNAs in colorectal cancer metastasis. J Pathol 2011;224:438–47.
21. Mirnezami AH, Pickard K, Zhang L, Primrose JN, Packham G. MicroRNAs: key players in carcinogenesis and novel therapeutic targets. Eur J Surg Oncol 2009;35:339–47.
22. Luciani A, Villella VR, Vasaturo A, Giardino I, Raia V, Pettoello-Mantovani M, et al. SUMOylation of tissue transglutaminase as link between oxidative stress and inflammation. J Immunol 2009;183:2775–84.
23. Zhang J, Lesort M, Guttmann RP, Johnson GV. Modulation of the *in situ* activity of tissue transglutaminase by calcium and GTP. J Biol Chem 1998;273:2288–95.
24. Maiuri L, Luciani A, Giardino I, Raia V, Villella VR, D'Apolito M, et al. Tissue transglutaminase activation modulates inflammation in cystic fibrosis via PPARgamma down-regulation. J Immunol 2008;180:7697–705.
25. Zhang L, Pickard K, Jenei V, Bullock MD, Bruce A, Mitter R, et al. miR-153 supports colorectal cancer progression via pleiotropic effects that enhance invasion and chemotherapeutic resistance. Cancer Res 2013;73:6435–47.
26. Parker H, Rose-Zerilli MJ, Parker A, Chaplin T, Wade R, Gardiner A, et al. 13q deletion anatomy and disease progression in patients with chronic lymphocytic leukemia. Leukemia 2011;25:489–97.
27. Kim HR, Wheeler MA, Wilson CM, Iida J, Eng D, Simpson MA, et al. Hyaluronan facilitates invasion of colon carcinoma cells *in vitro* via interaction with CD44. Cancer Res 2004;64:4569–76.
28. Priglinger SG, Alge CS, Neubauer AS, Kristin N, Hirneiss C, Eibl K, et al. TGF-beta2-induced cell surface tissue transglutaminase increases adhesion and migration of RPE cells on fibronectin through the gelatin-binding domain. Invest Ophthalmol Vis Sci 2004;45:955–63.
29. Mangala LS, Fok JY, Zorrilla-Calancha IR, Verma A, Mehta K. Tissue transglutaminase expression promotes cell attachment, invasion and survival in breast cancer cells. Oncogene 2007;26:2459–70.
30. Verma A, Guha S, Wang H, Fok JY, Koul D, Abbruzzese J, et al. Tissue transglutaminase regulates focal adhesion kinase/AKT activation by modulating PTEN expression in pancreatic cancer cells. Clin Cancer Res 2008;14:1997–2005.
31. Mann AP, Verma A, Sethi G, Manavathi B, Wang H, Fok JY, et al. Overexpression of tissue transglutaminase leads to constitutive activation of nuclear factor-kappaB in cancer cells: delineation of a novel pathway. Cancer Res 2006;66:8788–95.
32. Kahlert C, Klupp F, Brand K, Lasitschka F, Diederichs S, Kirchberg J, et al. Invasion front-specific expression and prognostic significance of microRNA in colorectal liver metastases. Cancer Sci 2011;102:1799–807.
33. Lai TS, Liu Y, Li W, Greenberg CS. Identification of two GTP-independent alternatively spliced forms of tissue transglutaminase in human leukocytes, vascular smooth muscle, and endothelial cells. FASEB J 2007;21:4131–43.
34. Arndt GM, Dossey L, Cullen LM, Lai A, Druker R, Eisbacher M, et al. Characterization of global microRNA expression reveals oncogenic potential of miR-145 in metastatic colorectal cancer. BMC Cancer 2009;9:374.

35. Calin GA, Sevignani C, Dumitru CD, Hyslop T, Noch E, Yendamuri S, et al. Human microRNA genes are frequently located at fragile sites and genomic regions involved in cancers. Proc Natl Acad Sci U S A 2004;101:2999–3004.
36. Lamy P, Andersen CL, Dyrskjot L, Torring N, Orntoft T, Wiuf C. Are microRNAs located in genomic regions associated with cancer? Br J Cancer 2006;95:1415–8.
37. Luciani A, Villella VR, Esposito S, Brunetti-Pierri N, Medina D, Settembre C, et al. Defective CFTR induces aggresome formation and lung inflammation in cystic fibrosis through ROS-mediated autophagy inhibition. Nat Cell Biol 2010;12:863–75.
38. Kumar A, Xu J, Brady S, Gao H, Yu D, Reuben J, et al. Tissue transglutaminase promotes drug resistance and invasion by inducing mesenchymal transition in mammary epithelial cells. PLoS One 2010;5:e13390.
39. Hwang JY, Mangala LS, Fok JY, Lin YG, Merritt WM, Spannuth WA, et al. Clinical and biological significance of tissue transglutaminase in ovarian carcinoma. Cancer Res 2008;68:5849–58.
40. Herman JF, Mangala LS, Mehta K. Implications of increased tissue transglutaminase (TG2) expression in drug-resistant breast cancer (MCF-7) cells. Oncogene 2006;25:3049–58.
41. Mangala LS, Arun B, Sahin AA, Mehta K. Tissue transglutaminase-induced alterations in extracellular matrix inhibit tumor invasion. Mol Cancer 2005;4:33.
42. Levental KR, Yu H, Kass L, Lakins JN, Egeblad M, Erler JT, et al. Matrix crosslinking forces tumor progression by enhancing integrin signaling. Cell 2009;139:891–906.
43. Luciani A, Villella VR, Vasaturo A, Giardino I, Pettoello-Mantovani M, Guido S, et al. Lysosomal accumulation of gliadin p31-43 peptide induces oxidative stress and tissue transglutaminase-mediated PPARgamma downregulation in intestinal epithelial cells and coeliac mucosa. Gut 2010;59:311–9.
44. Bunger S, Haug U, Kelly FM, Klempt-Giessing K, Cartwright A, Posorski N, et al. Toward standardized high-throughput serum diagnostics: multiplex-protein array identifies IL-8 and VEGF as serum markers for colon cancer. J Biomol Screen 2011;16:1018–26.
45. Lee YS, Choi I, Ning Y, Kim NY, Khatchadourian V, Yang D, et al. Interleukin-8 and its receptor CXCR2 in the tumour microenvironment promote colon cancer growth, progression and metastasis. Br J Cancer 2012;106:1833–41.
46. Baker EL, Lu J, Yu D, Bonnecaze RT, Zaman MH. Cancer cell stiffness: integrated roles of three-dimensional matrix stiffness and transforming potential. Biophys J 2010;99:2048–57.
47. Baker EL, Bonnecaze RT, Zaman MH. Extracellular matrix stiffness and architecture govern intracellular rheology in cancer. Biophys J 2009;97:1013–21.
48. Nemes Z Jr, Adany R, Balazs M, Boross P, Fesus L. Identification of cytoplasmic actin as an abundant glutaminyl substrate for tissue transglutaminase in HL-60 and U937 cells undergoing apoptosis. J Biol Chem 1997;272:20577–83.
49. Barnes RN, Bungay PJ, Elliott BM, Walton PL, Griffin M. Alterations in the distribution and activity of transglutaminase during tumour growth and metastasis. Carcinogenesis 1985;6:459–63.
50. Knight CR, Rees RC, Griffin M. Apoptosis: a potential role for cytosolic transglutaminase and its importance in tumour progression. Biochim Biophys Acta 1991;1096:312–8.
51. Hager H, Jensen PH, Hamilton-Dutoit S, Neilsen MS, Birckbichler P, Gliemann J. Expression of tissue transglutaminase in human bladder carcinoma. J Pathol 1997;183:398–403.
52. Jones RA, Kotsakis P, Johnson TS, Chau DY, Ali S, Melino G, et al. Matrix changes induced by transglutaminase 2 lead to inhibition of angiogenesis and tumor growth. Cell Death Differ 2006;13:1442–53.
53. Haroon ZA, Lai TS, Hettasch JM, Lindberg RA, Dewhirst MW, Greenberg CS. Tissue transglutaminase is expressed as a host response to tumor invasion and inhibits tumor growth. Lab Invest 1999;79:1679–86.
54. Hidaka H, Seki N, Yoshino H, Yamasaki T, Yamada Y, Nohata N, et al. Tumor suppressive microRNA-1285 regulates novel molecular targets: aberrant expression and functional significance in renal cell carcinoma. Oncotarget 2012;3:44–57.
55. Eom S, Kim Y, Kim M, Park D, Lee H, Lee YS, et al. Transglutaminase II/microRNA-218/-181a loop regulates positive feedback relationship between allergic inflammation and tumor metastasis. J Biol Chem 2014;289:29483–505.
56. Lin G, Tang Z, Ye YB, Chen Q. NF-kappaB activity is downregulated by KRAS knockdown in SW620 cells via the RAS-ERK-IkappaBalpha pathway. Oncol Rep 2012;27:1527–34.
57. Neklason DW, Tuohy TM, Stevens J, Otterud B, Baird L, Kerber RA, et al. Colorectal adenomas and cancer link to chromosome 13q22.1-13q31.3 in a large family with excess colorectal cancer. J Med Genet 2010;47:692–9.
58. Saidak Z, Mentaverri R, Brown EM. The role of the calcium-sensing receptor in the development and progression of cancer. Endocr Rev 2009;30:178–95.

Published OnlineFirst May 1, 2015; DOI: 10.1158/1541-7786.MCR-14-0466

Molecular Cancer Research

miR-19–Mediated Inhibition of Transglutaminase-2 Leads to Enhanced Invasion and Metastasis in Colorectal Cancer

D. Cellura, K. Pickard, S. Quaratino, et al.

Mol Cancer Res 2015;13:1095-1105. Published OnlineFirst May 1, 2015.

Supplementary Figure 1

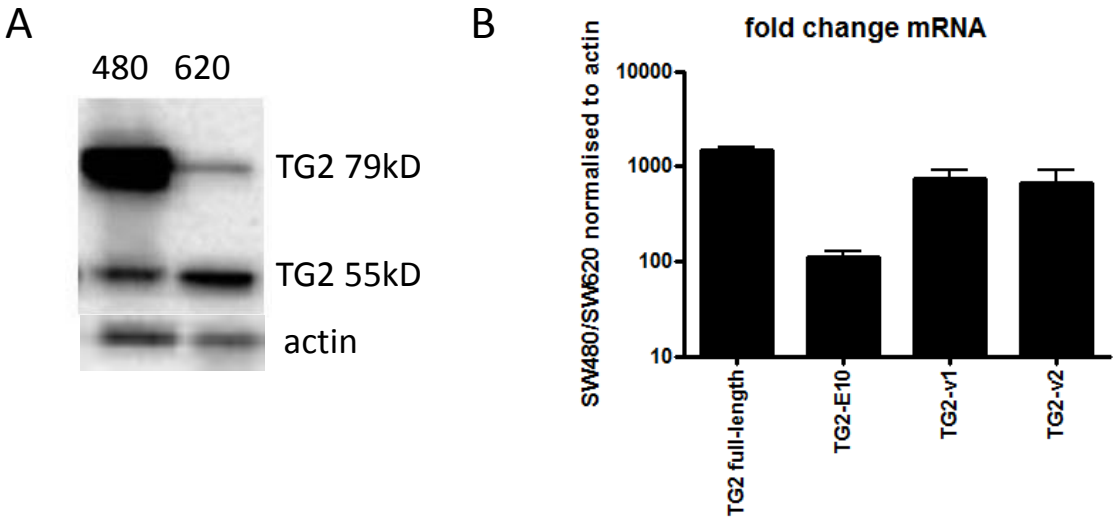

Supplementary Figure 2

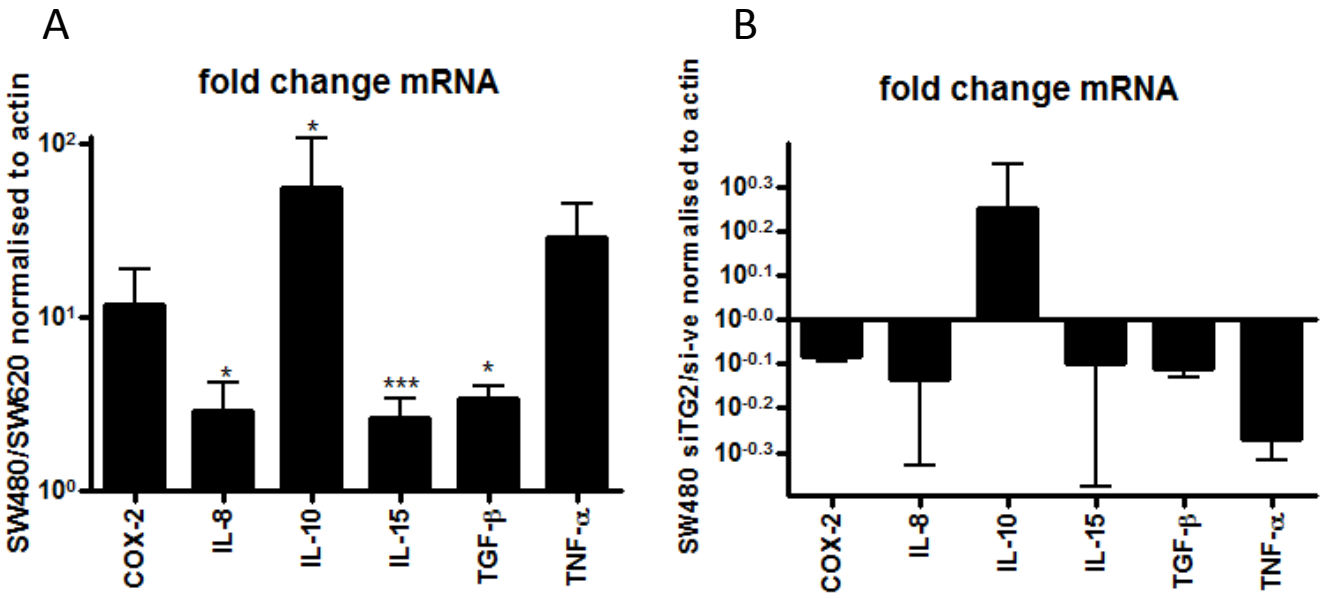

Supplementary Figure 3

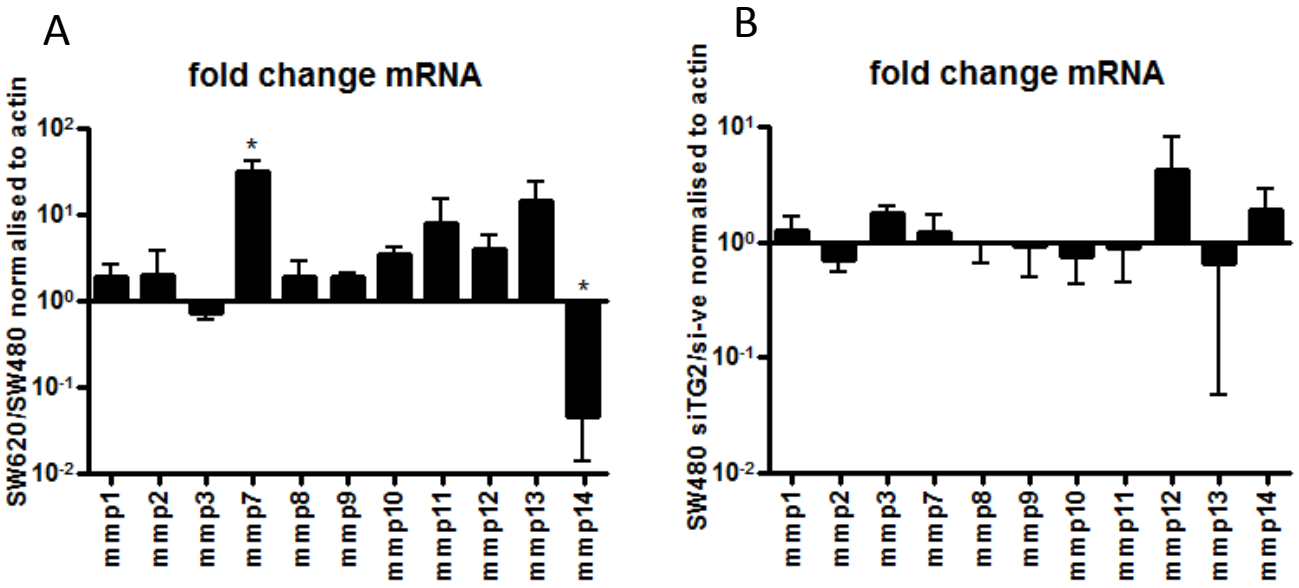

Supplementary Figure 4

A

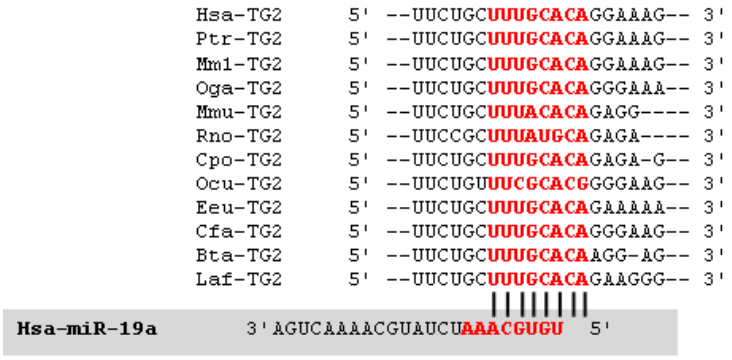

B

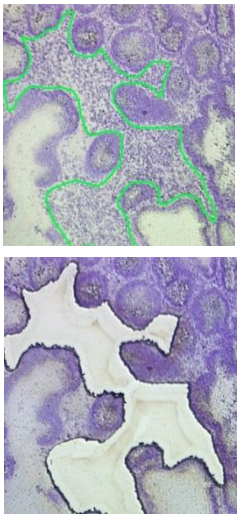

C

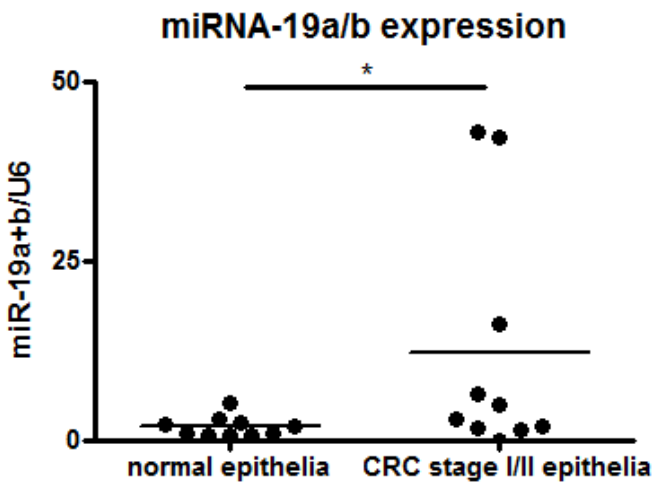

D

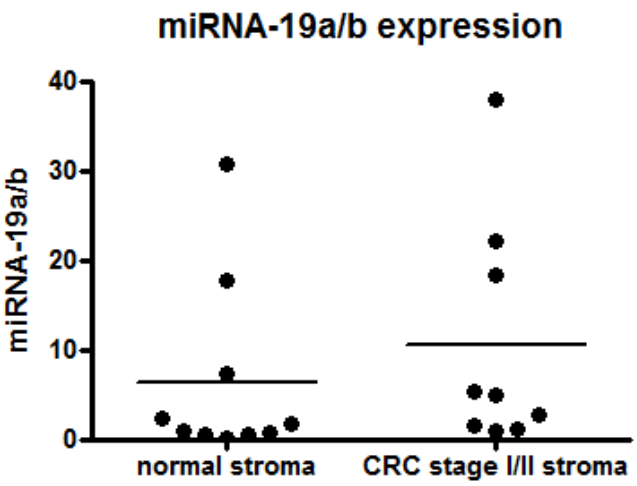

SUPPLEMENTARY MATERIAL

Supplementary materials & methods.

Quantification of cytokine gene expression was performed using RT-PCR. After RNA isolation and cDNA synthesis, PCR was performed using Promega GoTaq reagents using standard conditions of 3 min denature (94°C), 25 cycles of 30 sec (94°C), 30 sec (60°C) and 1 min (72°C), followed by final extension for 10 min (72°C). PCR products were resolved on 1% agarose, bands quantified using densitometry (ImageJ), and values normalised to β-actin. Quantification of MMP gene expression was performed by real-time qRT-PCR on the same cDNA samples using Promega GoTaq Sybr Green reagents, quantified from a standard curve generated from serial dilutions of a control cDNA, and normalised to β-actin. Array-based comparative genomic hybridisation was used to look for copy number changes of miRNA chromosomal loci as previously described (Zhang et al., 2013).

Supplementary table 1: primer sequences used for PCR.

Gene	***sense***	***Antisense***
IL-1β	CCCTAAACAGATGAAGTGCTCCTT	GGGATCTACACTCTCCAGCTGTAG
IL-6	CCTTCTCCACAAGCGCCTTCGGTCC	CTAGATTCTTTGCCTTTTTCTGCAGG
IL-8	CTCTCTTGGCAGCCTTCCTGATT	AACTTCTCCACAACCCTCTGCAC
IL-10	AGCTCAGCACTGCTCTGTTG	GCATTCTTCACCTGCTGCTCCAC
IL-15	GGATTTACCGTGGCTTTGAGT	TTCCTCCAGTTCCTCACATTCT
IL-33	CAAGCTGGGAAATAAGGTGT	ACTTATGGAGCTCCACAGAG
IFN-γ	AATGCAGGTCATTCAGATG	TTGGACATTCAAGTCAGTT
TNF-α	GGATGTTCGTCCTCCTCACAGGGCAATG	GGCCCAGGCAGTCAGATCATCTTC
COX-2	TTCAAATGAGATTGTGGAAAAAT	AGATCATCTCTGCCTGAGTATCTT
β-ACTIN	ATGACCCAGATCATGTTTGAGACC	GAGCAATGATCTTGATCTTCATTG
MMP1	GGAGGGGATGCTCATTTTGATG	CATCGTGTTGCAGCTCATGAAC
MMP2	AGATCTGCAAACAGGACATTGTATT	TTCTTCTTCAAGGACCGGTTCATTT
MMP3	CCTGCTTTGTCCTTTGATGC	TTTTGGCGCAAATCCCTCAG
MMP7	TCTTTGGCCTACCTATAACT	AATAATGCAGAAGCCCAGAT
MMP8	TGGACCCAATGGAATCCTTGC	GAAACATGGACCAACACCTCC
MMP9	CAACATCACCTATTGGATCC	CGGTGATTGACGACGCCTTT
MMP10	CTGCCATTGAGAAAGCTCTGA	TCTCCAGGCTGTATGAAGGAGA
MMP11	AAGACTCACCGAGAAGGGGAT	AGGTGGCAGCCCATGAATTTG
MMP12	TTGTTCCTCACTGCTGTTCAC	TCTCTGCTGATGACATACGTG
MMP13	TTGTTGCTGCGCATGAGTTCG	CCTGGAGCACTCATGTTTCCT
MMP14	GATGTTTGTCTTCAAGGAGCG	AAGTGATGGATGGATACCCAA
TG2	TGAACAAACTGGCCGAGAAG	ACGCTCTTCTCAGAGAAAGGC
TG2-E10	TGAACAAACTGGCCGAGAAG	AGGGCTTTACCAGAGAAAGGC
TG2-v1	GATCCGGATCCTTGGGGAG	TGCTCCCTTGTGGAGGTGCA
TG2-v2	GATCCGGATCCTTGGGGAG	GCCACTGGTGTGGAGGTGCA

Supplementary figure 1: Differences in TG2 expression between SW480 and SW620 cells.

TG2 levels in SW480 and SW620 cells were assessed by Western blot to assess protein expression (A), and by RT-PCR for the expression of mRNA for full-length TG2, and of the truncated splice variants (B). Expression of mRNA is displayed as the ratio SW480/SW620 after normalising to β-actin. All mRNA transcripts were expressed at a higher level in SW480 cells compared to SW620 cells at a statistically significant level, $p < 0.0001$.

Supplementary figure 2: Pro-inflammatory cytokine expression in SW480/SW620 cells.

The expression of cytokines and pro-inflammatory mediators were assessed in SW480 and SW620 cells by RT-PCR and quantified by densitometry. No mRNA was detected for IL-1β, IL-6, IL-33 or IFN-γ. Values were normalised to β-actin levels, then plotted as SW480 vs SW620 ratio (A), and SW480 siTG2/si-ve control ratio (B). * = $p < 0.05$, *** = $p < 0.0001$.

Supplementary figure 3: MMP expression in SW480/SW620 cells.

MMP expression was assessed by qRT-PCR, normalised to β-actin levels, then plotted as SW480 vs SW620 ratio (A), and SW480 siTG2/si-ve control ratio (B). * = $p < 0.05$.

Supplementary figure 4: regulation of TG2 by overexpression of miRNA-19 in SW480/SW620 cells.

TG2 is a target for miRNA-19a binding, and this 3'UTR binding sequence is phylogenetically conserved (A). Isolation of miRNA-19a expression from tumour cells and the surrounding stroma was performed by LCM (B), and compared between normal and tumour epithelia (C), and between normal and tumour stroma (D). * = $p < 0.05$.